Hydrofoil Static Pressure Acquisition at High Reynolds Number

Joshua M. Hamel

M.S.E Degree Thesis
University of Michigan
December 2001

AD NUMBER	DATE 17 JUNE 2002	DTIC ACCESSION NOTICE
1. REPORT IDENTIFYING INFORMATION		REQU
A. ORIGINATING AGENCY NAVAL POSTGRADUATE SCHOOL,MONTEREY,CA 93943		1. Put y on re 2. Comp 3. Attacl maile 4. Use u infon 5. Do not for 6
B. REPORT TITLE AND/OR NUMBER HYDROFOIL STATIC PRESSURE ACQUISITION AT HIGH REYNOLDS NUMBER		
C. MONITOR REPORT NUMBER BY JOSHUA M. HAMEL, UNIV OF MICHIGAN		
D. PREPARED UNDER CONTRACT NUMBER n62271-97-G-0062		
2. DISTRIBUTION STATEMENT APPROVED FOR PUBLIC RELEASE; DISTRIBUTION UNLIMITED		DTIC: 1. Assign 2. Return

20020710 025

DTIC Form 50 DEC 91 PREVIOUS EDITIONS ARE OBSOLETE

Acknowledgments

I would like to thank the following individuals for their support in my contributions to the Hifoil project and in my pursuit of a Master's Degree in Mechanical Engineering from the University of Michigan:

Dwayne A. Bourgoyne, PhD Candidate and Hifoil Project Leader,
Steven L. Ceccio, PhD, Project Advisor,
David R. Dowling, PhD, Co-Project Advisor,
Carolyn Judge, PhD,
Mike Cutbirth, PhD, LCC Staff,
Mike Deebel, LCC Staff,
Steve and Peggy Hamel, my parents
and all my friends and family that helped me hold on to my life outside of this project.

Table of Contents

Abstract

From 1999 through 2001 the University of Michigan carried out an experimental study of the high Reynolds number turbulent flow over a hydrofoil. The high Reynolds number foil, or Hifoil project was carried out in three phases at the U.S. Navy's William B. Morgan Large Cavitation Channel (LCC), the world's largest variable pressure recirculating water tunnel. Several standard flow measurements were made over the course of this project, including surface static pressure field measurements. Static pressure was measured through the use of surface static pressure taps drilled into the foil model at various chordwise and spanwise locations. Pressure data was collected by a custom designed and built static pressure acquisition system, which could automate the process if so desired. The foil model was a modified NACA 16 shape with a chord of 7 feet and a span of 10 ft. The baseline foil was tested at 0, -1 and +1 degrees angle of attack measure relative to the foil's flat pressure side. Additional data was collected on the foil with a modified trailing edge shape again at 0 degrees angle of attack. Data was collected at flow speeds ranging from 1.5 to 18.3 m/s and at temperatures ranging from 22 to 40 °C (70 to 104 °F), resulting in a chord based Reynolds number range of 3 to 60 million. The Reynolds number range extends from the existing model scale up to full scale for some naval applications. Data is presented here in the form of normalized nondimensional pressure as a function of chordwise location represented in percentage of chord at all the various geometric and flow speed test conditions. In addition a numeric integration of the pressure curves was performed to calculate the pressure lift generated by the foil at the various test conditions. This data is also presented in the form of lift coefficient as a function of foil configuration and Reynolds number. The pressure data presented shows the expected increase in lift with increased angle of attack and little to no Reynolds number dependence.

Nomenclature

C	foil chord
C_P	nondimensional pressure coefficient $\frac{P_w - P_\infty}{\frac{1}{2}\rho U^2}$
C_L	lift coefficient $\frac{L}{\frac{1}{2}\rho U^2 A}$
C_D	drag coefficient $\frac{D}{\frac{1}{2}\rho U^2 A}$
Re_C	chord based Reynolds number $\frac{U c}{\upsilon}$
ρ	fluid density
P	fluid pressure
U	fluid velocity
υ	kinematic viscosity
x/C	nondimensional chordwise position, measured aft from the leading edge
y/C	nondimensional thickness position, measured up from the pressure side

Abbreviations

ADC	Analog to Digital Conversion
AOA	Angle of Attack
CFD	Computational Fluid Dynamics
Hifoil	High Reynolds Number Foil
LDV	Laser Doppler Velocimetry
LCC	William B. Morgan Large Cavitation Channel
NAVSEA	Naval Surface Warfare Center, Carderock Division
NACA	National Advisory Committee for Aeronautics
NPT	National Pipe Taper
PIV	Particle Imaging Velocimetry
TE	Trailing Edge of the foil

List of Figures

Introduction

From the fall of 1999 through the summer of 2001 an experiment was conducted by the University of Michigan to investigate the turbulent flow over a large hydrofoil shape relevant to the U.S Navy. The experiments were performed at a range of Reynolds numbers that reached full scale for some actual naval applications. All experiments associated with this project were conducted at the U.S. Navy's William B. Morgan Large Cavitation Channel (WBM-LCC), the world's largest variable pressure recirculating water tunnel. The High Reynolds Number Foil, or Hifoil project was carried out for a variety of reasons. One important goal of the experiment was to collect, under controlled experimental settings, a high Reynolds number hydrofoil data set for the U.S. Navy which could bridge the gap between the existing model scale data and the full scale.

The data set produced by the Hifoil project will be used in part to prove that what is understood about this type of a flow field at lower Reynolds numbers actually does scale up to higher Reynolds numbers in a predictable manner. As a result, it was important for the data collected during this project to be of the kind appropriate for use in validating scaling laws and computational models that were developed based on the existing model scale data. The Navy obviously knows a great deal about the flow over various foil shapes on the model scale, however there is very little data concerning this type of a flow over foil shapes at the full scale due to the costs and complications associated with collecting high Reynolds number data. Because the Hifoil project will be able to achieve essentially full scale chordwise Reynolds numbers, one of the major purposes of the project was to provide information that can be readily used by the Navy in Reynolds number scaling studies.

To this end, several relatively simple measurements were made during the Hifoil project in order to compare the flow field to that of similar experiments conducted at lower Reynolds numbers. Among these were trailing edge velocity measurements, foil acceleration levels and both dynamic and static surface pressure measurements. The foil surface pressure gradients measured over the course of the experiment were of particular importance. Surface pressure gradients are used to help understand various aspects of a flow field, such as the amount of lift generated. Static pressure is a simple but critical measurement that must be made in any foil experiment. As a result there is a vast amount of preexisting static pressure data from various different foil shapes at various Reynolds numbers. This fact made the static pressure data one of the critical data sets collected during the Hifoil project because it offers a direct comparison to data taken during virtually every other foil experiment done in the recent past. To see recent applications of static pressure data see Astolfi [1], Niewald [7,8], Wood [10] and Zandieh [11].

In order to measure the static pressure during the Hifoil project, several issues had to be addressed. Essentially all static pressure measurements made in recent memory were made using small surface pressure tap holes drilled orthogonal to the surface of the experimental model. The same method was implemented for the Hifoil project. However the number, size and location of the pressure taps to be used had to be determined while giving careful consideration to any errors or disturbances that the taps may be introducing into both the pressure measurements and the flow field in general. Next, the sensors to be used had to be selected carefully while considering the full range of pressures that the foil was likely to experience over the course of the experiment. Lastly, a pressure acquisition system had to be designed and implemented which could measure the fluid pressure in the various taps accurately and in a reasonable amount of

time. The time required to make each measurement on the Hifoil project was always an important factor due to the high operating costs of the experimental facility.

A great deal of work has been done concerning the process of measuring static pressure in a flow with wall pressure taps. The work of Franklin and Wallace [6], Ducruet [4,5] and Zogg [12], among others has provided a set of guidelines to be observed when measuring static pressure with wall taps. First, the taps must be drilled in the surface of the model orthogonal to the flow. Second, the taps must have as clean and sharp of edges as possible. The tap itself should be a clean and flat hole in the surface of the model with no rounding of its edges or distortions in the surface of the model upstream or downstream of the tap. Any of these problems will create undesired errors in the pressure measurements. However, all the pressure tap work done has shown that errors in the pressure measurements are unavoidable because the presence of the pressure tap on the model will alter the flow over the tap slightly no matter how well it has been machined into the surface of the model. Benedict compiled data from various pressure tap studies and created a correlation for this unavoidable static pressure tap hole error. [3] This correlation is function of hole diameter, flow speed, wall shear stress, fluid viscosity and fluid density. It was developed using the data from four different pressure tap studies, including Franklin and Wallace's data. As a result this correlation can be taken to be fairly accurate, assuming the static pressure taps are properly machines as earlier described. This pressure tap theory was observed in the designing of the static pressure acquisition system for the Hifoil project, in the selection of the transducers and other components used on the project, in the machining of the pressure taps into the foil and in the calculation of the uncertainty associated with the static pressure measurements made over the course of the project.

Throughout the Hifoil project surface pressure measurements were made at various chordwise locations on both the suction and pressure side of the foil. These measurements were repeated at various speeds and for various angles of attack. Based on these pressure measurements pressure lift was then calculated at all the various conditions in order to get a complete picture of the effect, if any, that high Reynolds number has on lift. Errors arose in the measurements due to various sources such as transducer error, calibration offset errors and static pressure tap hole errors. However, all these sources of error were anticipated, quantified in some reasonable manner and then either reported or corrected for within the data.

Experimental Procedure

Project Overview

The Hifoil project was conducted in a series of three phases at the WBM-LCC over the course of two years. A series of experiments were conducted on a modified NACA 16 foil. The modifications made to the base NACA 16 foil included a flat pressure side to simplify the construction of the model and an increased knuckle on the trailing edge in order to prevent the foil from producing excessive pressure induced noise, a phenomenon known as singing. These modifications were made based on recommendations from the Naval Surface Warfare Center, Carderock Division (NAVSEA), who developed the foil design for the University of Michigan. The foil model used for the project had a chord of 7 ft and a span of 10 ft. The foil was cast from a naval grade nickel-aluminum bronze and machined to a nominal surface roughness of 25 μin. See figure 1 for a diagram of the foil cross-section and figure 2 for a close up of the trailing edge. Several different measurements were made on the foil over the course of the experiment. These included: laser doppler velocimety (LDV) average velocity measurements made both onboard the foil and externally, particle imaging velocimety (PIV) instantaneous velocity measurements of the trailing edge flow, foil vibration levels made at various locations in the foil using onboard mounted accelerometers, dynamic pressure fluctuation measurements made at the trailing edge of the foil using flush mounted dynamic pressure transducers and surface static pressure measurement made using a number of static pressure taps and differential diaphragm pressure transducers. See figure 3 for an overview of the locations of the various onboard instrumentation mounted in the foil.

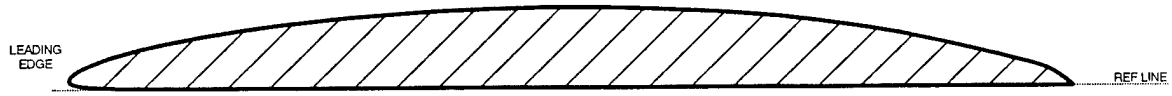

Figure 1: Cross-Section view of baseline Hifoil

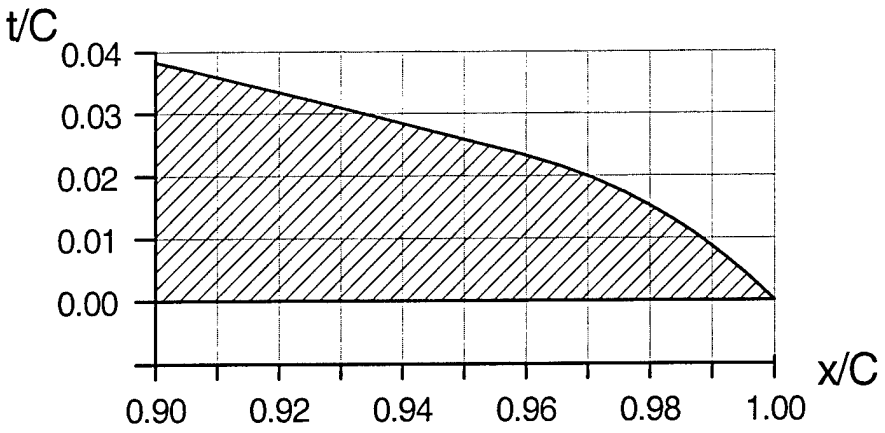

Figure 2: Detail of baseline trailing edge

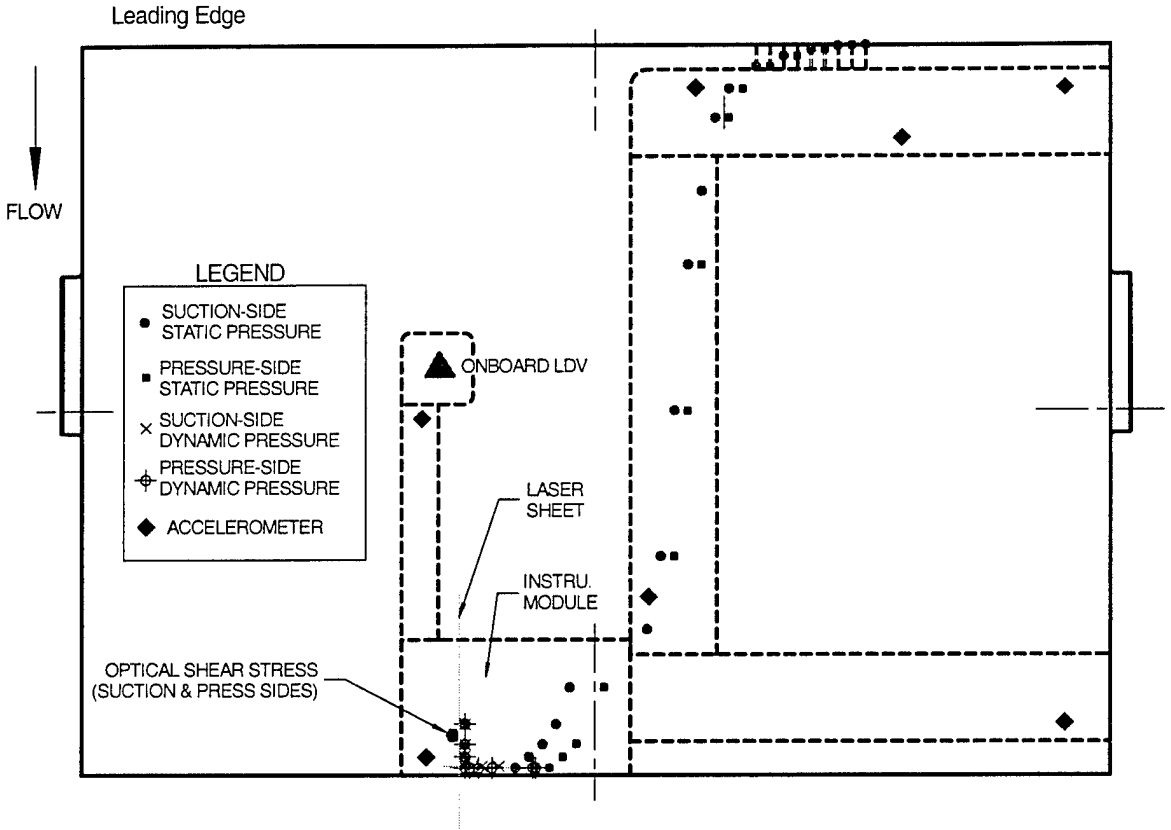

Figure 3: Foil instrumentation overview

Over the course of the project these measurements were made on the baseline foil at flow speeds ranging from 0.25 m/s through 18.3 m/s. The various measurement were repeated on the baseline foil at angles of attack of 0 degrees, -1 degrees and +1 degrees, measured relative to the flat pressure side of foil. Additionally, a modification was made to the trailing edge of the baseline foil and another series of measurement were made at 0 degrees angle of attack at flow speeds ranging again from 0.25 m/s though 18.3 m/s. See figure 4 for a diagram of the modified trailing edge relative to the baseline foil. The modification is represented in the drawing by the alternate hatch pattern seen at the trailing edge. The modification consisted of a piece of brass that had the baseline foil shape machined into its underside and the new trailing edge shape machined into its outer surface. The modification stretched the entire span of the foil and was attached with bolts and faired into the original trailing edge with bonding compound.

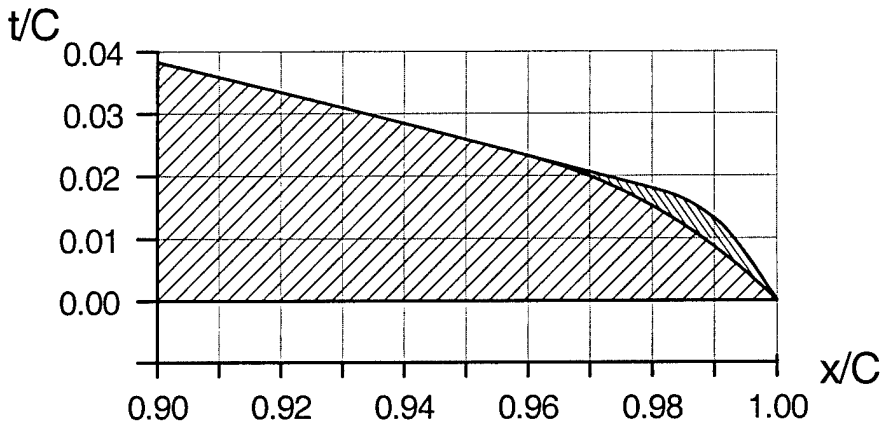

Figure 4: Detail of trailing edge modification

The Hifoil project was conducted in three phases. Phase one, conducted in October of 1999 was concerned mainly with the average flow field at the trailing edge of the foil. All

measurements taken during this phase were made using and external two-component LDV system, owned and operated by the LCC staff. Phase two took place in February and March of 2001 and it was during this phase that the majority of the measurements were made including PIV at the trailing edge, foil vibration, onboard LDV measurements of the boundary layer at the mid-chord, trailing edge pressure fluctuations and surface static pressure measurements. It was also during this phase that the angle of attack study was performed. Phase three was conducted during August of 2001 and was concerned with making low speed measurements on the baseline foil and then repeating several of the measurements made during phase two on the foil with the modified trailing edge.

Experimental Facility

All three phases were conducted at the WBM-LCC in Memphis, Tennessee. The LCC is a variable pressure recirculating water tunnel with can flow water from 0.25 m/s up to 18.3 m/s through at 43 ft long test section with a 10 ft by 10 ft square cross-section. The pressure in the test section can be varied 0.5 to 60 psia, in order to control the onset of cavitation in the test section. The LCC pump is powered by 10,440 kW motor. Given these statistics, a foil chord of 7ft and a channel water temperature range of 70 to 104 ^{o}F, the chord based Reynolds number possible during this experiment ranged from 1 to 60 million, using the definition:

$$\mathrm{Re}_C = \frac{Uc}{\upsilon} \quad (1)$$

Where U is the free stream fluid velocity, c is the chord length of the foil and υ is the kinematic viscosity of the water, which is a function of water temperature. Figure 5 is a schematic of the LCC and figure 6 is diagram of the foil model mounted in the test section of the LCC.

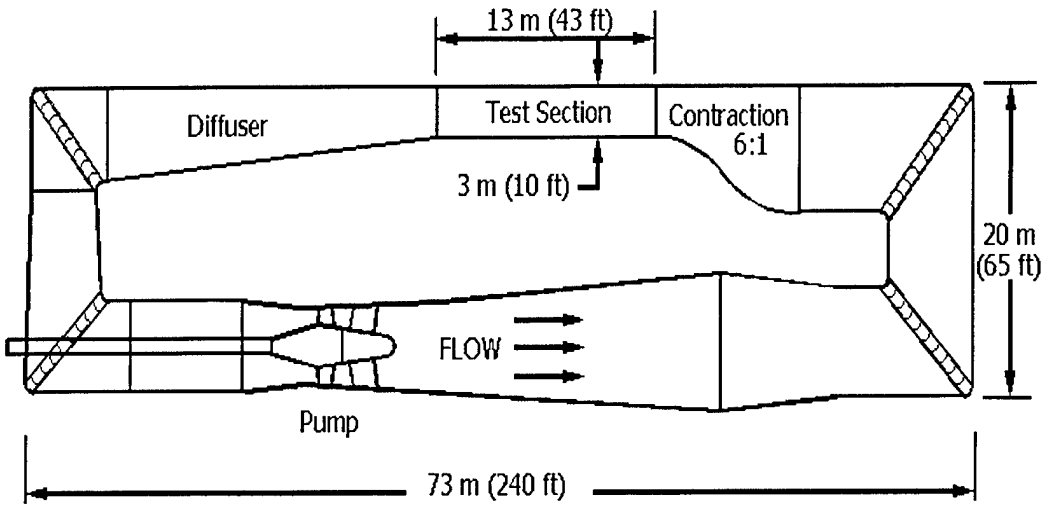

Figure 5: Diagram of the LCC

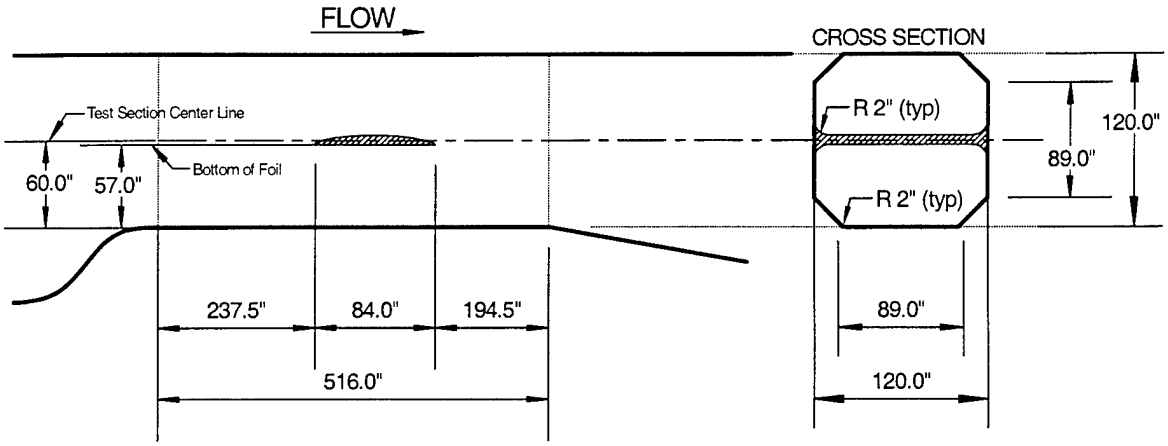

Figure 6: Drawing of the Hifoil mounted in the LCC test section

Pressure Acquisition System Hardware

In order to measure the static pressure gradients on the foil it was necessary to design and implement and entire static pressure acquisition system. This systems consisted of the following parts: the pressure taps themselves, the tubing system that brings the fluid out of the test section

of the channel to where its pressure can be measured, a manifold system that makes it possible to valve between the different pressure tap lines and bleed any air out of the lines, the transducers used to make the pressure measurements and finally the computer system which records the readings from the transducers and controls the system.

The pressure taps are the most important aspect of this system. There are three important considerations to be made in deciding how to measure static pressure with pressure taps. First, the number of taps to be used is critical. The surface static pressure field on the foil is obviously a continuous function of chordwise position. However, it is impossible to measure the pressure continuously because this would take an infinite number of pressure taps. Therefore it is important to decide how many taps will adequately capture the trends of the pressure field while minimizing the number of taps that have to drilled into the model in an effort to minimize machining costs. In preparation for the Hifoil project a simple calculation was made by NAVSEA using a two-dimensional representation of the foil in the LCC test section to approximate the probable pressure field on the surface of the foil. This calculation was done using simplified boundary conditions and a two-dimensional panel method integral solver. From the calculation it was determined that 30 taps would be required to accurately capture the shape of the pressure field. A larger percentage of the taps had to be located near to the nose and the trailing edge of the foil, where the pressure gradients were anticipated to be the largest. Having more taps in these areas will make it easier to spatially resolve these larger gradients. Figure 7 shows the results of the computation made by NAVSEA presented as the negative of the nondimensional pressure coefficient, C_p versus chordwise position in percent of chord (x/C). The convention is to plot $-C_P$ in order to place the suction side data curve above the pressure side curve in pressure coefficient plots in order to mirror the actual geometry of the foil. Figure 7

also show the x/C location of each of the 30 taps, while table 1 shows the numeric x/C location of each tap. The dots on the foil cross-section in figure 7 indicate the location of the pressure taps. The formula used for computing C_P is as follows:

$$C_p = \frac{P_w - P_\infty}{\frac{1}{2}\rho U_\infty^{\ 2}} \quad (2)$$

Where P_w is the measured wall pressure, P_∞ is the free stream pressure, ρ is the fluid density and U_∞ is the free stream velocity. As can be seen from this equation, the pressure coefficient is a nondimensional way to represent the measured wall pressure as a differential from the free stream pressure.

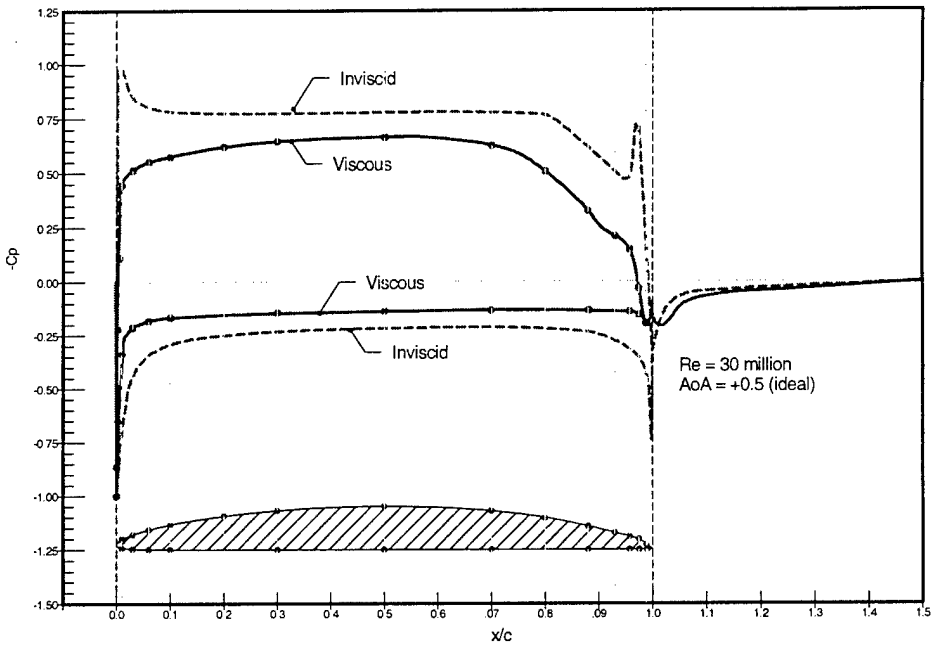

Figure 7: NAVSEA predicted pressure distributions and pressure tap x/C location

It was also important to carefully determine the spanwise location of each tap in addition to the chordwise location. As previously stated, putting a pressure tap in a model to measure the

static pressure will disturb the flow in that spanwise location. Therefore, no piece of instrumentation can lie downstream of any static pressure tap without the upstream pressure tap producing uncertainty in the downstream measurements. This made it necessary to place each of the static pressure taps in a slightly different spanwise location so as not to corrupt any other measurements. Refer back to figure 3 to see the spanwise location of each pressure tap in a planform view.

Lastly the size of each pressure tap was an important factor to consider. The correlation provided by Benedict suggests that the smaller the tap size the better. [3] Smaller pressure taps disturb the surrounding flow less and result in smaller hole error values. However, experience in the LCC has found that pressure taps less than one sixteenth of an inch in diameter tend to clog with the random debris that exists in the water used in the LCC. For this reason, it was decided that the majority of the pressure taps in the foil should be one sixteenth of an inch in diameter to avoid clogging. However, near the leading edge of the foil the high radius of curvature of the nose required a slightly smaller size tap diameter in order to reduce error. A one sixteenth inch diameter tap size near the nose of the foil would create a large defect in the surface of the foil and it was speculated that taps of this size would most likely disturb the flow too much at the leading edge of the foil. For this reason is was determined that it would be better to have smaller taps near the nose and risk having them get clogged over the course of the experiment in order to reduce the possibility of corrupting any other measurements to be made over the course of the project. Table 1 also shows the diameter of each of the thirty foil static pressure taps.

Suction Side Taps

Tap	x/C	Diameter (in)
1	0.000	0.0313
2	0.001	0.0313
3	0.004	0.0313
4	0.010	0.0313
5	0.030	0.0313
6	0.060	0.0625
7	0.100	0.0625
8	0.200	0.0625
9	0.300	0.0625
10	0.500	0.0625
11	0.700	0.0625
12	0.800	0.0625
13	0.880	0.0625
14	0.930	0.0625
15	0.958	0.0625
16	0.975	0.0625
17	0.988	0.0625

Pressure Side Taps

Tap	x/C	Diameter (in)
18	0.985	0.0625
19	0.975	0.0625
20	0.958	0.0625
21	0.880	0.0625
22	0.700	0.0625
23	0.500	0.0625
24	0.300	0.0625
25	0.100	0.0625
26	0.060	0.0625
27	0.030	0.0313
28	0.010	0.0313
29	0.004	0.0313
30	0.001	0.0313

Table 1: x/C location and hole size of foil pressure taps

With the size and location of each of the taps determined, the next challenge was to devise a method for actually measuring fluid pressure at each tap. Within the foil, the opposite side of each pressure tap was machined to a female sixteenth inch national pipe taper (NPT) thread. A special adapter fitting was used to mate the NPT thread to an o-ring tube fitting. This made it possible to use eighth inch outer diameter flexible nylon 11 tubing to connect to each of the taps. Eighth inch outer diameter tubing was chosen to minimize the amount of space occupied by static pressure tubing within the foil. Outside of the test section of the water tunnel each of the thirty tubes coming from the pressure taps was then connected to a custom built common manifold.

The manifold was designed with two main purposes in mind. First, it had to be capable of bleeding the air out of each of the pressure tap lines and/or capable of pushing pressurized water out of each of the pressure tap lines in an effort to clear all the air and debris from each of

the pressure lines. This was necessary because the presence of bubbles or other debris in the pressure tap lines could have corrupted the pressure measurements. Bubbles in the fluid lines could cause the surface pressures to be inaccurately transmitted down the line to the pressure transducers. The common manifold also needed to be able to isolate each pressure tap lines individually in order to make it possible to measure the pressure in each individual line independently. There are basically two ways to do accomplish this function. Either each line can have its own dedicated sensor or one sensor can be used, but it must then be possible to isolate each pressure line from the sensor with valves. The first method was not cost effective both in terms of number of transducers that would be required for the thirty foil pressure taps, nor in terms of the time it would take to calibrate thirty different transducers before any data could be collected. For this reason the second method was chosen. As a result the common manifold was designed and built with the capability to valve on or off each of the pressure lines independently. The process of isolating each fluid line with valves could be done by hand with mechanical Swagelok compression fitting ball valves. Three way valves were used to direct the fluid pressure in one of two directions, either to a common bleed manifold which could be sealed off or opened to atmospheric pressure, or to the transducer manifold.

The transducer manifold consisted of a Scanivalve solenoid driven rotary valve. This device was capable of taking forty-eight input fluid lines and opening up those input lines to a single output line one at a time. This device could be controlled with digital computer logic, making it possible to computer control the pressure measurement process. Information about the Scanivalve can be found in appendix B.

The Scanivalve system was used to make it possible to automatically isolate an individual pressure line, a necessary capability when attempting to measure static pressure on several

pressure taps with a single pressure transducer. The Scanivalve option was chosen because it was more cost effective than building two separate manifolds and an individual solenoid driven ball valve for each pressure tap line, a system that would have cost approximately $400 per pressure tap and required a entire control circuit for each valve. The complete Scanivalve system cost only $2000 total and could support up to forty-eight pressure taps. However, the Scanivalve device proved to have limited reliability. When it was operational the Scanivalve worked very well, but it did tend to break down, get clogged with debris due to its small size and have electronic control problems from time to time.

The Scanivalve system uses a custom 0.063 inch outer diameter tubing in all of its fittings in order to facilitate the geometric constraints of the system. Custom 0.063 inch to quarter inch outer diameter Swagelok fittings were purchased in order to incorporate the Scanivalve into the pressure acquisition system. Swagelok quarter inch outer diameter tube fittings were used for all the other the plumbing applications in the static pressure manifold. Swagelok compression fittings were chosen for their excellent quality and reliability. Brass fittings were chosen based on cost. This choice was justified because brass is an acceptable material for use in low-pressure water applications. Quarter inch outer diameter tubing was chosen due to the greater inner diameter when compared to the eighth inch tubing used inside the foil. The greater inner diameter made it easier to push out trapped bubbles and debris. This dimension also made it less likely that any bubble that might be trapped in the tubing would be large enough to entirely block the tube, a situation that could create errors in the pressure measurements. A special reduction union tube fitting was used to step up each of the eighth inch outer diameter tubes coming out of the foil to the quarter inch outer diameter tubing used in the manifold.

Appendix C shows a schematic of the pressure acquisition manifold plumbing system. The system could support up to forty-eight pressure taps to match the forty-eight inputs into the Scanivalve. It was designed to be flexible in the number of inputs used to support other later experiments that would perhaps use a different number of pressure taps than the Hifoil project. The manifold, valves, Scanivalve, all electronic circuits and transducers were all mounted on a self-contained stand built from Unistrut framing material, sheet metal and plywood. Figure 8 shows a photograph of the pressure acquisition stand.

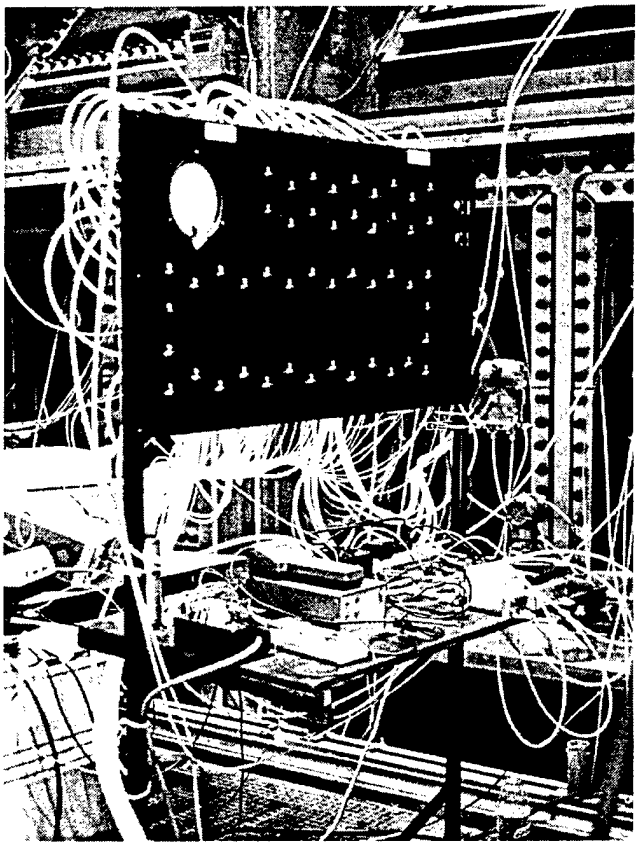

Figure 8: Photograph of static pressure acquisition system (D. Bourgoyne)

For the second phase of the Hifoil project all forty-eight inputs were used, including the thirty taps on the model and an additional eighteen wall taps to record the wall pressures inside the LCC test section at various places upstream and downstream of the foil. These pressures were recorded to provide boundary condition information for the Hifoil project data set. During phase three pressure data was taken on only the thirty foil taps. The LCC staff collected the wall pressure data using an LCC designed and operated static pressure acquisition system. Wall pressure data will not be addressed in this document.

To actually measure the pressures in each tap, a differential pressure measurement approach was used. In the case of the Hifoil project, the free stream pressure was taken to be the pressure measured at a channel wall pressure tap that lied approximated 2 chord lengths upstream of the foil in the LCC test section. The data for all static pressure taps was taken as a differential from the pressure measured at this upstream wall tap using one of several differential pressure instruments employed over the course of the experiment. In other words, each transducer had two inputs that it measured a pressure differential between. One input into the transducers came from the output of the Scanivalve used in the pressure acquisition manifold while the other input came from the upstream reference tap.

Before selecting any transducers for the Hifoil project, a preliminary uncertainty analysis was done to take into account the range of error expected in the measurements. The uncertainties included in the calculations included the transducer's manufacturer stated uncertainty, analog to digital quantization error due to the data acquisition computer limitations and the expected static pressure hole error in the measurement. Each separate transducer considered had a slightly different stated uncertainty associated with it as reported by the manufacturer. This uncertainty is reported in a certain percentage of the full scale operating

range of the transducer. This error source was usually the largest contribution to the total predicted error for any given measurement. The quantization error in any measurement was a function of the analog to digital converter (ADC) used to convert the analog voltage output from the transducer into the digital signal that is stored by the computer. This uncertainty is a function of the resolution of ADC and the full scale range of voltages output by the transducer. The data acquisition computer system will be discussed in detail later in this document, however it was found that the quantization error in any measurement was orders of magnitude less than the other elemental sources of error, and was thus essentially not a factor in the total uncertainty of any measurement. The only other expected source of error in the static pressure measurements was static pressure tap hole error. Based on the previous experimental data discussed earlier and Benedict's findings, hole error is known to be a bias error that is a function of hole size and shape, flow speed and fluid properties. [3] Using the known empirical relations, an estimation of static pressure hole error was included in the preliminary uncertainty analysis. A sample worksheet of this preliminary calculation is contained in table 2.

U (m/s)		**18.3**	**12**	**6**	**3**
Transducer Full Scale		-Rosemount 3051CD			
Error Types-					
hole (+/- psi)		0.1457	0.0501	0.0076	0.0004
transducer (+/- psi)		0.0555	0.0555	0.0555	0.0555
-error (mfg)	0.00075				
-FS (psi)	74				
A/D (+/- psi)		0.0156	0.0156	0.0156	0.0156
-Efsr (V)	8				
-QE (+/- V)	0.001953				
Total (+/- psi)		**0.1566**	**0.0763**	**0.0581**	**0.0576**

Table 2: Sample calculation of expected uncertainty in pressure measurements

Based on this type of a rough calculation, two acceptable candidate transducers were selected due to their specifications and ability to measure differential pressure in water. The two models included the Setra P230 differential pressure transducer and the Rosemount 3051CD differential pressure instrument. Both models were eventually purchased and used at some point over the course of the project. The Setra devices were originally selected due to their more reasonable cost. However the Rosemount instruments, though more expensive, proved to be much better measurement devices. Appendix D contains pictures and general specifications for both instruments.

Selecting a single pressure transducer for adequately measuring the foil static pressure over the entire range of flow speeds of the test proved to be impractical. The largest pressure differential seen by the foil was almost 25 psid, which is the stagnation pressure at 18.3 m/s, while at 0.25 m/s pressure differentials were as small as tenths of a psi. There are no commercially available differential pressure instruments made which can accurately span this entire range. This made it necessary to use a number of transducers, each sized for a certain range of pressures and intended for use at a specific set of flow speeds. For phase two the anticipated test conditions were 3, 6, 12 and 18.3 m/s, thus the anticipated pressure range was 0.1-25 psid. To accommodate this range, two Setra transducers were purchased, one with a +/- 10 psid range for the smaller pressure differentials and a +/- 50 psid ranged transducer for the higher differentials. A solenoid driven ball valve was used to isolate the lower ranged transducer from the line pressure when the line pressure was higher than the transducer's safe operating range. This was accomplished by closing the valve after each measurement, testing the line pressure in the new tap line with the larger ranged transducer and then deciding if the pressure differential in the line was low enough to not damage the lower ranged transducer. If the

pressure level was safe, the isolating valve was opened and data was recorded for that tap on both transducers, while if the pressure was too high, the transducer was kept isolated and data was record only on the larger transducer. This process was achieved entirely by computer programming and control and is discussed later in the document.

A single Rosemount transducer was also purchased for phase two in case the accuracy of the Setra transducers proved to be unacceptable. This transducer had a max range of +/- 36 psid. The Setra transducers cost approximately one third of the Rosemount device and thus were a better option from a cost perspective. However, the Rosemount transducers were known to be reliable and accurate devices and so one was purchased as a backup. As could have been predicted, the Setra devices were less than ideal and as a result the vast majority of the phase two static pressure data was taken on the single Rosemount device. For phase three an additional Rosemount instrument with a max operating range of +/- 1 psid was purchased to more accurately measure the static pressure differentials at the lower flow speed test conditions in the phase three test plan. Efforts were also made to devise a process of re-ranging and recalibrating the Rosemount transducers to reduce their full scale operating ranges and the resulting measurement uncertainty. The Rosemount device has the capability to scale down its operating range using a special computer control device sold by Rosemount, Inc. This allows a user to set the range of the transducer to whatever is needed for a specific measurement. The computer device then adjusts the transducer's internal calibration and gain level to accommodate the desired range. For instance, if the expected pressures at a given condition predicted pressures ranging from –5 up to 12 psid at a given flow speed, the +/- 36 psid Rosemount transducer could have its range spooled down to +/- 13 psid, making the full scale operating range 26 psid, which would thus reduce the uncertainty in the measurements made at that test condition. This process

was used throughout phase three, and table 3 shows the range that each transducer was set to for each flow speed in phase three test plan. The ranges were selected to minimize the error in the measurements at each test condition. This approach was employed in an effort to improve the uncertainty in the measurements made during phase three over those made during phase two when the transducer ranges were the same throughout the test, especially at the low speeds where the pressure differentials are very small.

	Transducer Limits (psi)		
U (m/s)	Range	1	2
<1	A	3.61	0.09
1.5	B	3.61	0.36
3	C	3.61	0.90
6	C	3.61	0.90
12	E	25.25	0.90
18.3	E	25.25	0.90

Table 3: Phase three transducer ranges as a function of flow speed

Data Acquisition Computer System and Software

The entire pressure acquisition system was controlled by a Windows 2000 based personal computer running National Instruments' Labview software. A National Instruments PCI-6071E series data acquisition board was used to interface between the computer and the hardware in the pressure acquisition system. The PCI-6071E board contains a 12 bit ADC, 32 differential analog inputs and up to 8 digital input/output (I/O) channels for computer control of various processes. The static pressure system used two analog inputs to record data from the two transducers, and 6 digital channels. The digital channels were used to control the position of the Scanivalve, the isolation valve for the lower range pressure transducer and to read the position of the Scanivalve using an encoder built into the Scanivalve by the manufacturer.

Control and data acquisition programs were written for the static pressure system in the Labview language. Labview is a National Instruments product that works very well when used

with National Instruments hardware. Labview is a computer programming language with a graphical interface that makes is very easy to control mechanical processes, acquire data from sensors, perform limited data processing, view data in near real time and save data to files. There were three major programs developed for the Hifoil project: a data acquisition program, a transducer calibration program and a data-sampling program.

The first program controlled the acquisition process of the static pressure data. This program was developed to take a single set of data for a given test condition when prompted to do so by the user. For a given test condition, when given a specific number of pressure taps to take data from, the program was designed to automatically select the appropriate pressure tap, take a time series of data, find the mean and standard deviation of that time series, record that data point and then adjust the hardware and Scanivalve for the next tap in order to repeat the process. The program produces a data file that contains the average differential pressure and the standard deviation of the time series as measured on both of the transducers, for each desired pressure tap as specified at the beginning of the run by the user.

Over the course of the Hifoil project, three separate derivations of this program were developed. In the original program the computer completely controlled the data acquisition process. The user simply input the flow conditions, the sampling rate, number of samples desired in each time series and the number of taps on which to take data. The computer than automatically took a time series of data on each channel sequentially, found the mean of each time series and saved a data file to the computer's hard drive that contained the input flow data and the acquired mean differential pressure data. The first derivation of this program was developed to allow the user to check the position of the Scanivalve before allowing the computer to take data on that channel. Due to reliability issues with the Scanivalve it became important to

be able to let the computer take data and advance the Scanivalve to the next channel, but then allow the user to verify that the Scanivalve position had actually changed to the correct new position before allowing the computer to proceed with the data acquisition process. The third derivation of the program was written to allow data to be taken in the event that the Scanivalve was inoperable. In this event the Scanivalve was capped off and the transducer manifold was connected to the common bleed manifold. Then the mechanical ball valves were set so that all of the pressure tap lines except for one were fed to the blocked off Scanivalve. The pressure in the manifold was thus able to equalize to the pressure in the single line that was fed into the manifold and the manifold pressure could then measured. The program that controlled this data acquisition system simply took and recorded data, as there was no control involved in this process. The program would take the data on a channel and indicate to the user that it was done. The user would then close the valve of the completed channel and open the valve of the next channel manually. At this point the manifold would come to the pressure of the new channel and the user would then tell the computer to take the next data point. The net result of this program was a data file identical to the data files produced by the original program, however this program required much more active participation by the user. These three programs were written to allow for a variety of failures that could occur in the static pressure acquisition system.

The second program developed for the Hifoil project was a transducer calibration program. This was written to allow the user to calibrate each of the transducers independently using a pressure standard. Both types of transducers stated to have linear calibrations within their full scale operating range. As a result, these calibrations were experimentally verified based on the linear assumption to check and record the slope and zero offset for all transducers on every day that they were to be used to take data. This linear calibration process was based on

eleven data points, 5 with the known pressure applied to one side of the differential pressure instrument, five with a known pressure applied to the opposite side of the transducer and one zero point where both sides of the transducer were simply left open to atmospheric pressure, thus resulting in a zero pressure differential. The program allowed the user to input the applied pressure at one of the eleven points. The computer would then measure and record the average voltage output of the transducer over a specified period of time, usually 3 seconds. After all eleven points are recorded, the program then calculated the slope and intercept of the calibration and saved the raw data to the computer's hard drive.

The last program written was a simple routine that plotted the real time pressure in a selected line as a function of time. This program allowed the user to select a specific pressure tap and then see the pressure in that line as measured by each of the transducers. This program allowed the user to see if the pressure was relatively stable in time and to see how the calibration on the two transducers compared for a given pressure.

The programs used during the Hifoil project were designed to make data acquisition easier and less time intensive for the experimentalist, however the ability to computer control some aspects of the system was slightly limited by hardware. Specifically, the Scanivalve was limited in how it could move between its forty-eight inputs. The forty-eight inputs of the Scanivalve are set up in a circular pattern. The Scanivalve system is set up to index the valve from one input to the next input sequentially along the radius of the circle every time the Scanivalve controller sees a digital logic high pulse of approximately five volts as produced by a computer digital output signal. One of the inputs was randomly selected by the manufacturer to be the number one, or 'home' input, and the rest are numbered in radial order from the number one input. The result of this is that it is a relatively easy process to go from input one to two or

three, etc. However, it is difficult to go between inputs that are not in sequential order or close to each other in number order. It was found that the most efficient method was to step through the inputs sequentially because this required the least amount of pulses to be issued to the Scanivalve controller by the computer. As a result the program was set up to record data from the pressure taps in a sequential manner. The user could select to take data on less than the total number of taps, but had to set the Scanivalve up to start on a specific channel manually. For the purpose of the Hifoil project, the thirty pressure taps on the foil were set up as inputs one through thirty on the Scanivalve. In other words, when running automatically, the Scanivalve stepped through the inputs connected to foil taps first. To facilitate this methodology, each pressure tap was assigned a number from one to forty-eight, and it was this number that was used by the computer program to associate with a specific pressure tap. For example, if the user desired to look at the data on the suction side of the foil at the mid-chord, he would have to set the Scanivalve manually to input 10, the number of the mid-chord tap, and then start the data acquisition program. Because of these constraints, the data acquisition system was limited to taking data on specified number of taps sequentially with the only variables being number of taps and starting tap. The graphical code and user interface screens for each of the programs discussed can be found in appendix E.

Data Regression Techniques

Calculating and plotting the nondimensional pressure coefficient data was a relatively simple task. The voltages output by the transducer were converted to pressures using the corresponding calibration data for the specific transducers and ranges used to collect each specific data set by the data acquisition program as the data set was being recorded. As a result

each data file contained mean pressure differential information as a function of both instrument used and pressure tap. The standard deviation of the time series record at each tap was also saved in each data file again as a function of transducer and pressure tap. Lastly, the flow speed and water temperature for each test condition were also recorded in the file with the pressure data. Using this data and equations 1 and 2, the Reynolds number, pressure coefficient and the resulting statistical uncertainty of the pressure coefficient value for each data point could be calculated. Then, the C_p data for each tap could be plotted as a function of x/C location on the foil. Separate C_p curves were created for each different test condition.

Each set of C_p data was corrected using a zero-flow data point taken each test day. To take this data, the flow in LCC was brought to 0 m/s and a regular static pressure data run was made. Ideally, the differential pressure on each tap at zero-flow should be zero, however this was never the case. The zero-flow condition was taken at some point during each testing day to record the inevitable offsets that were present in the system due to drifting in the calibration offsets of the transducers or from any slight discrepancies in the physical system due environmental conditions such as possible debris in the lines or temperature changes.

The zero-flow data was also used to see if there was a possible clog or problem with any of the taps or inputs into the Scanivalve. If the zero-flow data suggested a problem with a tap, that problem could be investigated before any inaccurate data was taken on that tap.

Uncertainty in the pressure measurements was calculated in terms of a nondimensional offset from the C_p value. This uncertainty has both a precision and bias component. The statistical component comes from the standard deviation of the data time series as calculated by the pressure acquisition program. The bias component is the results of the static pressure tap hole error in the measurement. To compute this component of the uncertainty the static pressure

hole error associated with each and every pressure measurement was calculated using Benedict's correlation. [3] The standard deviation error and the pressure tap hole error were combined using the root sum squares method and reported as the total uncertainty associated with each corresponding C_p value.

In addition to calculating the pressure coefficient at each tap measure for every test condition, the pressure lift coefficient, C_L, and the pressure drag coefficient, C_D, for each test condition were also calculated. Each set of data recorded was nominally comprised of the pressure measured at each of the thirty taps for a single given trailing edge configuration, angle of attack, flow speed and water temperature. Based on this data, each C_p curve has an associated chordwise Reynolds number, angle of attack and trailing edge configuration. This pressure curve can then be integrated to get the lift and drag coefficients, as integrating C_p over x/C gives C_L and integrating C_P over y/C yields C_D. This drag coefficient is not very useful, as pressure drag is typically a very small component of the total drag on a foil. As a result the C_D values are not reported in this document. The calculations used to determine these values were carried out using the Matlab programming language, and can be found in appendix F. In order to integrate the C_P curves, a simple spline function in Matlab was used to interpolate the C_P values at x/C and y/C values between the known data points. Then using a Matlab trapezoid rule numerical integrator, the C_P curves were integrated to yield corresponding lift and drag values for each data set at a specific test condition.

The uncertainty in these integrated quantities was determined by splining and integrating the error bars associated with the C_P curves. An overstated integral value and understated integral value were calculated for each C_P curve. The difference between these two integral quantities was then found, and this value is reported as the uncertainty in the corresponding lift

quantity. This method is simple, but it does produce a basic idea of the uncertainty associated with the calculated lift values reported in this document. These calculations can also be seen in the Matlab code enclosed in appendix F.

Results

The static pressure data collected during the Hifoil project is presented here in form of negative C_P as a function of x/C location on the foil. In general, light colored data points indicate low flow speeds, while darker colored data points represent higher speed flows. As a convention, the four configurations of the foil tested during the Hifoil project are differentiated between in these plots by different shaped markers. Square markers (■) indicate data taken on the baseline foil at 0 degrees angle of attack, gradients (▼) indicate –1 degrees angle of attack data on the baseline foil, deltas (▲) represent data taken at +1 degrees angle of attack on the baseline foil and diamonds (♦) indicate data taken at 0 degrees angle of attack with the modified trailing edge.

The Hifoil project covered flow speeds from 0.25 to 18.3 m/s. However, due to limitations in the transducers and hardware used in the static pressure system, below 1.5 m/s the pressure head in the system was too small to produce repeatable static pressure data. For this reason the static pressure data presented here covers flow speeds from 1.5 to 18.3 m/s and temperatures from 75 to 103 °F, resulting in a Reynolds number range of 3.9 to 57 million. See the following table for exact Re_C ranges for each test speed for which static pressure data is presented.

	Re_C		
U (m/s)	Average	Max	Min
1.5	4.2E+06	4.3E+06	3.9E+06
3	8.5E+06	9.3E+06	7.7E+06
6	1.7E+07	1.8E+07	1.5E+07
12	3.3E+07	3.8E+07	3.0E+07
18.3	5.1E+07	5.7E+07	4.8E+07

Table 4: Re_C ranges for static pressure data at each test speed

The first plot shown here contains all data taken at 0 degrees AOA on the foil with its original trailing edge. As can be seen in this plot, the curves for most of the test conditions

collapse within experimental uncertainty, suggesting little to no Reynolds number dependence in the static pressure data. However, there are a few curves that are obviously offset from the bulk of the data. These curves are the data taken at 1.5 and 3 m/s, and were collected on the same day of the test using two separate calibrations. All three 1.5 m/s data sets overlay with each other and all four of the 3 m/s data also collapse on each other. Additionally there exists static pressure data at 3 m/s taken during phase two which does collapses with the curves from the other flow speeds. This 3 m/s data is not presented here due to its relatively high associated uncertainty, however it clearly suggests that the 3 m/s data should overlay with the other flow speeds. This suggests that a constant offset error existed in the static pressure system on the day that these 1.5 and 3 m/s data sets were collected.

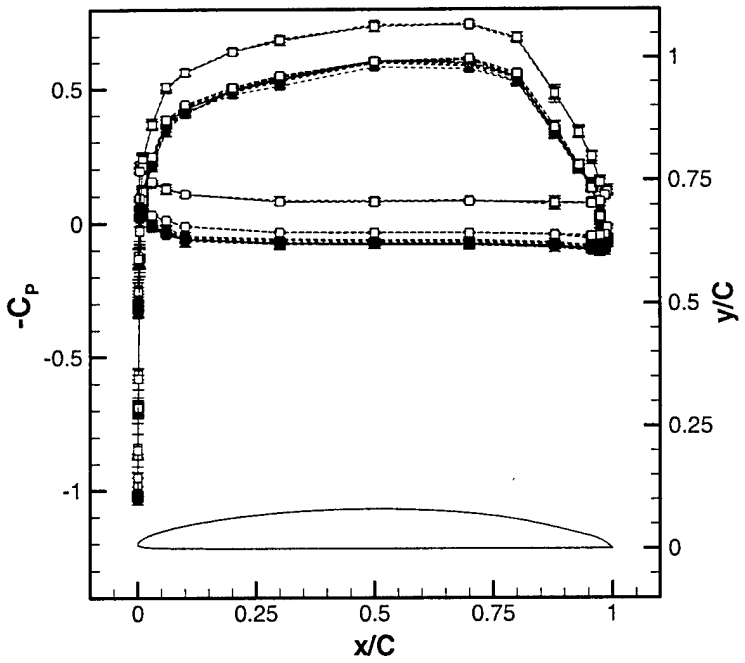

Figure 9: Original trailing edge configuration at 0 degrees AOA, all data, uncorrected

Due to the constant and repeatable nature of this offset error and the fact that the errors all occurred on the same day, this offset is most likely the result of an error made in calibration. As a result this error was corrected using the following method. A 12 m/s data run that collapsed with the majority of the other data sets was selected as an arbitrary baseline data set. Then, the offset of each C_P data point in the questionable curves from the baseline C_P curve was calculated at each corresponding x/C location. The individual offsets at each of the 30 chordwise locations were then averaged together for each of the seven data sets. Each of these resulting single average offsets was then applied as a constant correction to each of the corresponding questionable data sets. The next figure presents the results of this correction method as plotted against the remaining, uncorrected curves.

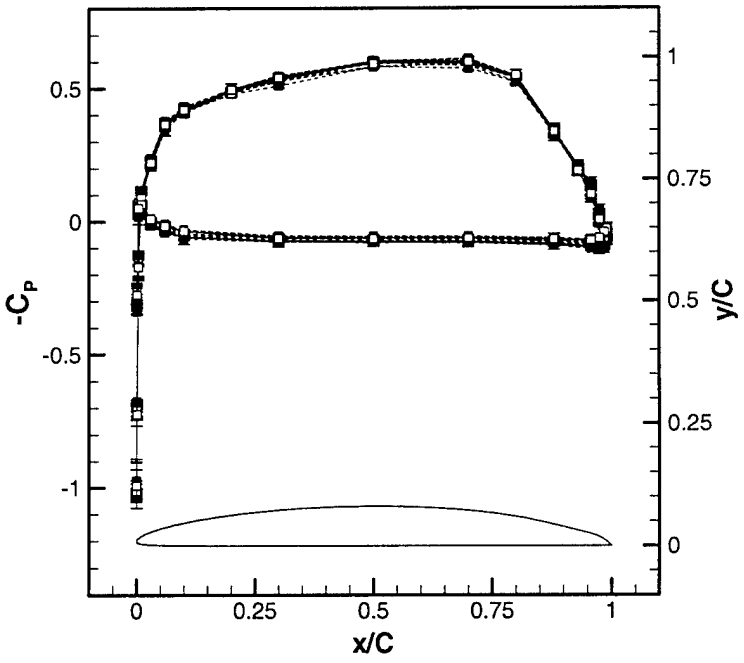

Figure 10: Original trailing edge configuration at 0 degrees AOA, all data, corrected

As can be seen by the agreement in this plot, the offsets have now been eliminated and the 1.5 and 3 m/s data collapses with the rest of the data sets at this foil configuration within experimental uncertainty.

The next four plots presented show the data collected for the original trailing edge shape at –1 and +1 degree AOA. This data was all taken during the angle of attack study done during phase two, and as a result it has some differences from the other data presented in this document. First, the lowest test speed in phase two was 3 m/s, so no data exists for –1 and +1 degrees AOA at 1.5 m/s. Second, the transducers used in phase two had greater uncertainties associated with them and as a result the uncertainty in the C_P values from phase two, especially at the lower test speeds, are substantially higher than those seen in the phase three data. The following figures show first, all the data collected during the angle of attack study for a specific geometry, and then the same data plotted again, this time without the 3 m/s results. This is done to show two things. First, that the 3 m/s data, despite its large uncertainty, does collapse with the data taken at higher flow speeds, and second, that when the data taken with the incorrectly ranged transducers is not considered, the remaining data has a very low associated uncertainty. This evidence suggests that while the uncertainty in the 3 m/s data is high, the true error in these data sets is more than likely only a fraction of the stated maximum uncertainty.

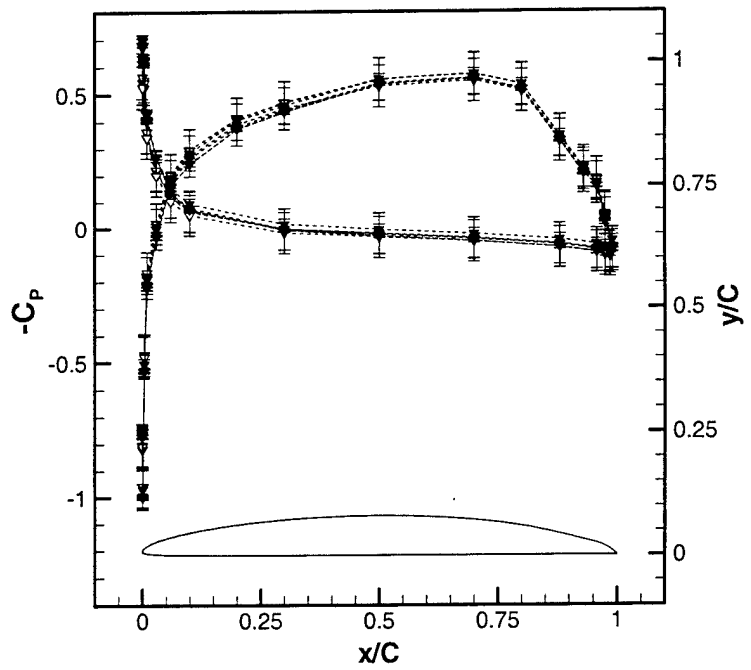

Figure 11: Original trailing edge configuration at -1 degrees AOA, all data

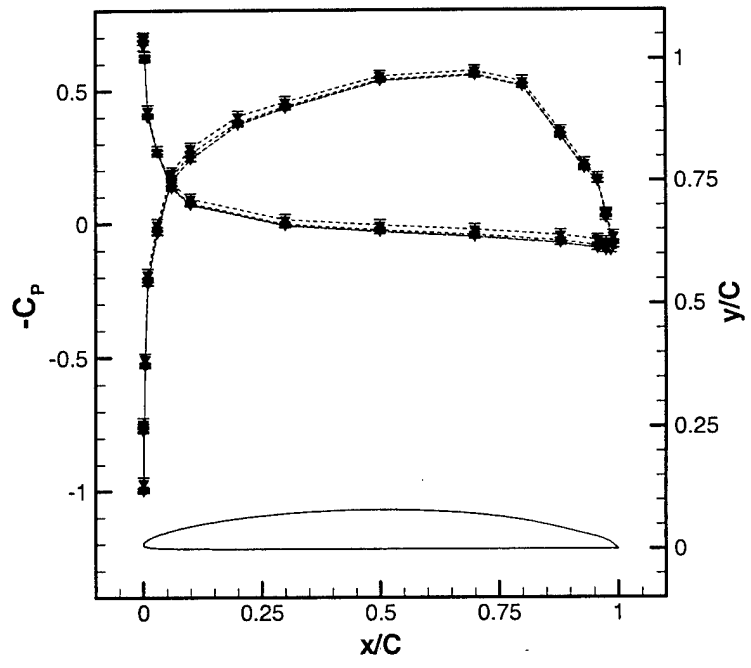

Figure 12: Original trailing edge configuration at -1 degrees AOA, without 3 m/s data

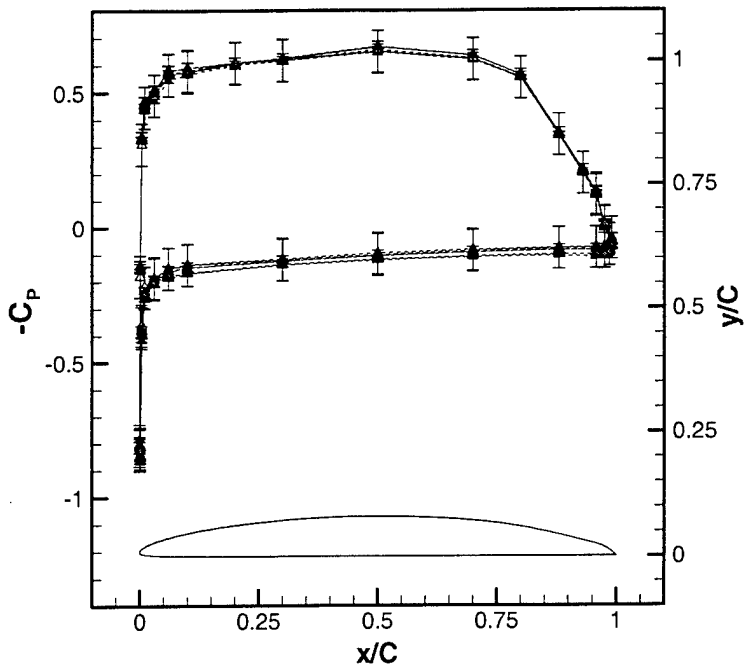

Figure 13: Original trailing edge configuration at +1 degrees AOA, all data

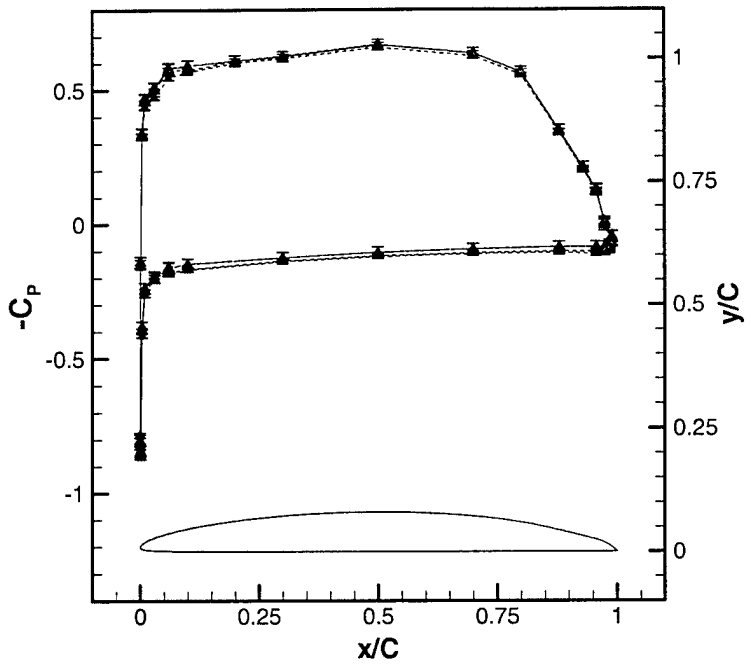

Figure 14: Original trailing edge configuration at +1 degrees AOA, without 3 m/s data

The next plot presented shows the data collected at 0 degrees AOA on the foil with the modified trailing edge. The data curves for this configuration closely resemble the 0 degrees AOA data on the original foil. Further comparisons between these two geometries will be made later in this document.

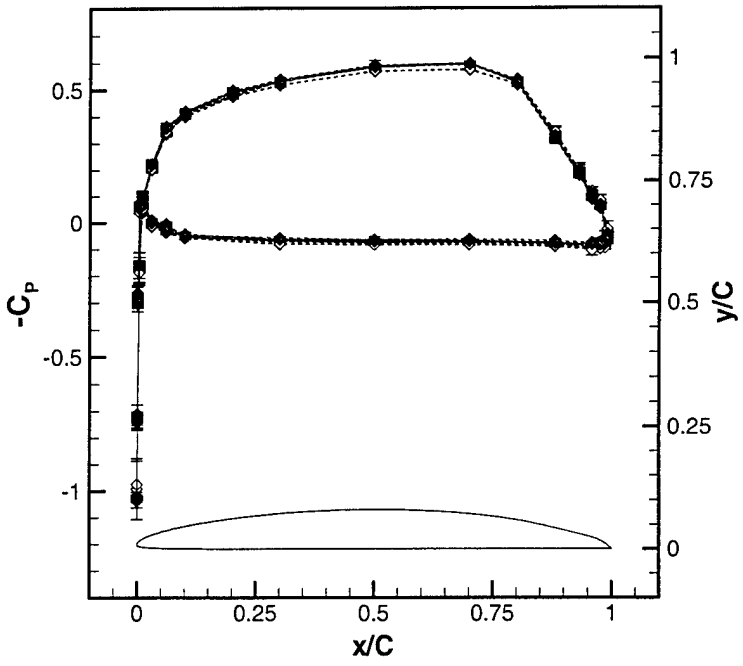

Figure 15: Modified trailing edge configuration at 0 degrees AOA, all data

The next three plots show how the actual data collected compares with the pressure curves predicted by the preliminary NAVSEA computations. They are included to simply prove that the static pressure measurement made during the Hifoil project produced results close to what was predicted by the simple preliminary calculations. Further computational fluid dynamics (CFD) will be done by various groups in the near future to more accurately model and study the data collected by the Hifoil project. The plots presented here show the actual data for the original foil shape at 0, -1 and +1 degrees angle of attack. The 3 m/s data has been excluded

from the –1 and +1 plots to remove the large error bars and thus make the results the plot shows clearer.

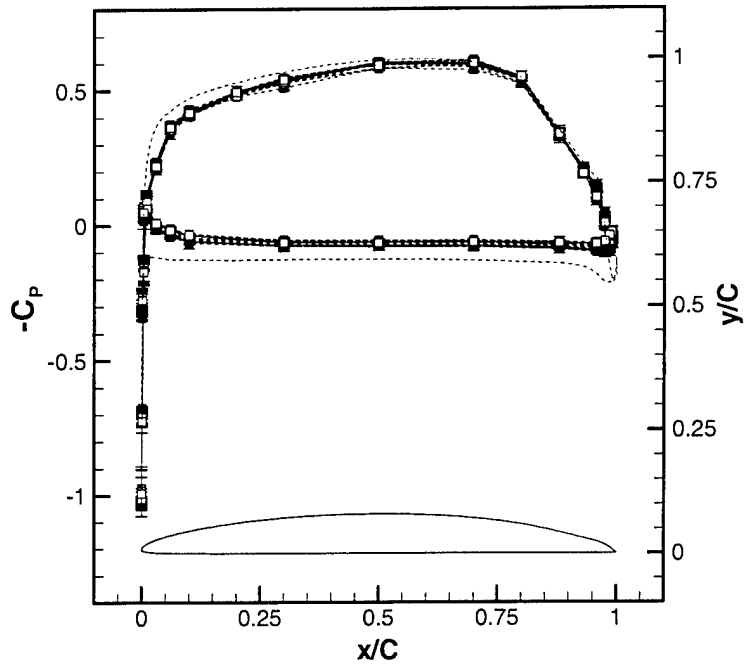

Figure 16: Original TE, 0 degrees AOA, corrected data vs NAVSEA prediction

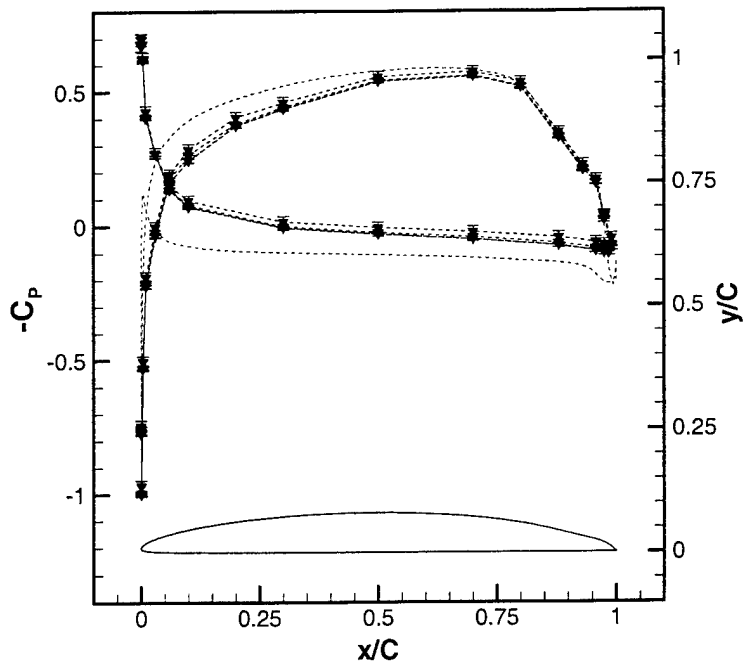

Figure 17: Original TE, -1 degrees AOA data vs NAVSEA prediction

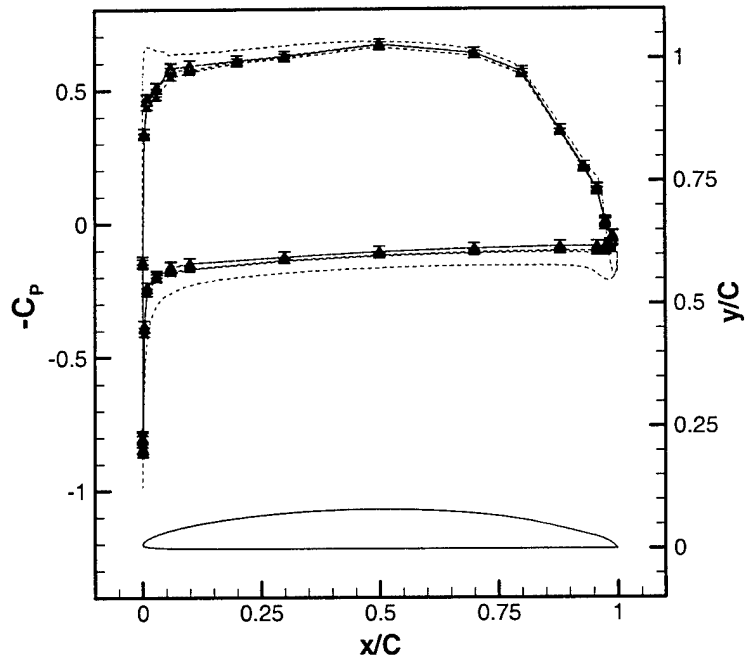

Figure 18: Original TE, +1 degrees AOA data vs NAVSEA prediction

The next two figures present data from the baseline foil at various angles of attack. The data is presented at both high and low flow speeds to show that the shape of the curves at both extremes of the velocity range studied are similar. These plots show the obvious result; that the pressure differentials between the suction and pressure sides of the foil increase with angle of attack.

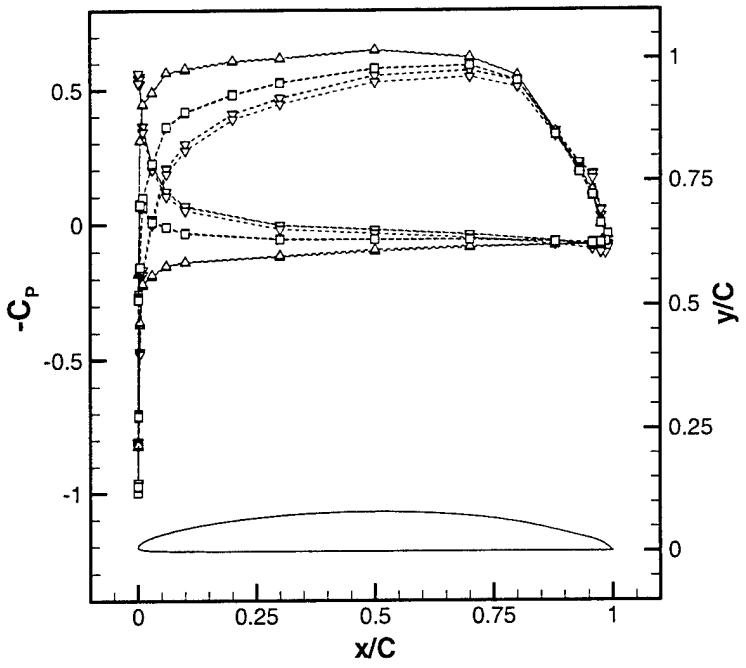

Figure 19: Original TE, All angles of attack at 3 m/s

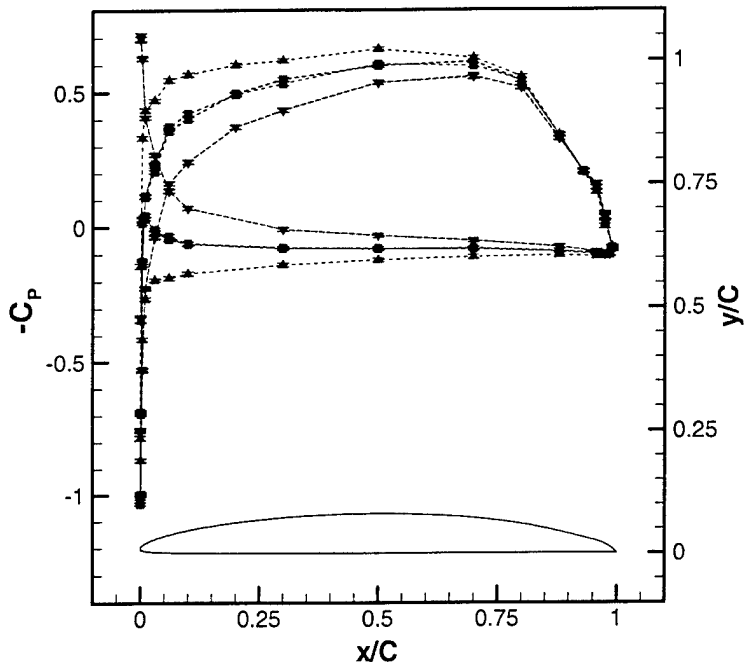

Figure 20: Original TE, All angles of attack at 18.3 m/s

The next four figures show the effect that the trailing edge modification had on the static pressure distributions. Data from the two trailing edge configurations is compared at 1.5 and 18.3 m/s in order to see the effect of different flow speeds on the trailing edge comparison. First all the data is presented, and then a close up view of the trailing edge data is presented. This is done because the most appreciable deviation between the compared data sets occurs near the trailing edge, as might be expected. However, based on the following plots no obvious trends in the data can be seen as a result of the trailing edge modification. The only change seen in the data is a greater scatter in the data points at the trailing edge; a result that is more likely due to the changes made to the geometry of the pressure taps themselves than to the changes in the flow field caused by the new trailing edge geometry. Based on the data in these plots, no generalizations can be made about the effect of changing the trailing edge shape. However, it

should be pointed out that the modification to the trailing edge of the foil was very small and perhaps the resulting changes to the static pressure field were too small to be accurately measured by the pressure transducers used in this project. On the close up views of the data at the trailing edge of the foil, data points taken on the original foil are linked with a dashed line, while modified trailing edge data is represented by a solid line to make any differences between the two configurations easier to see.

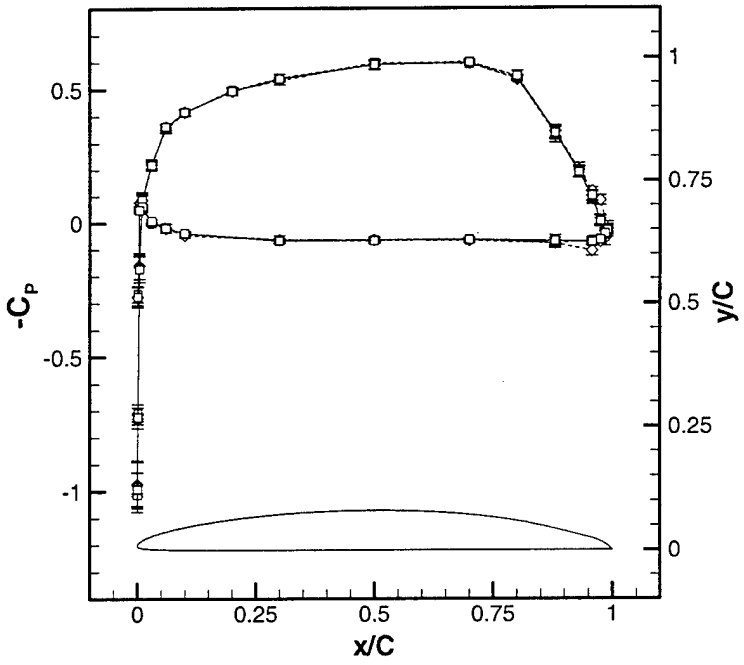

Figure 21: 0 degrees AOA, original vs modified trailing edge data at 1.5 m/s

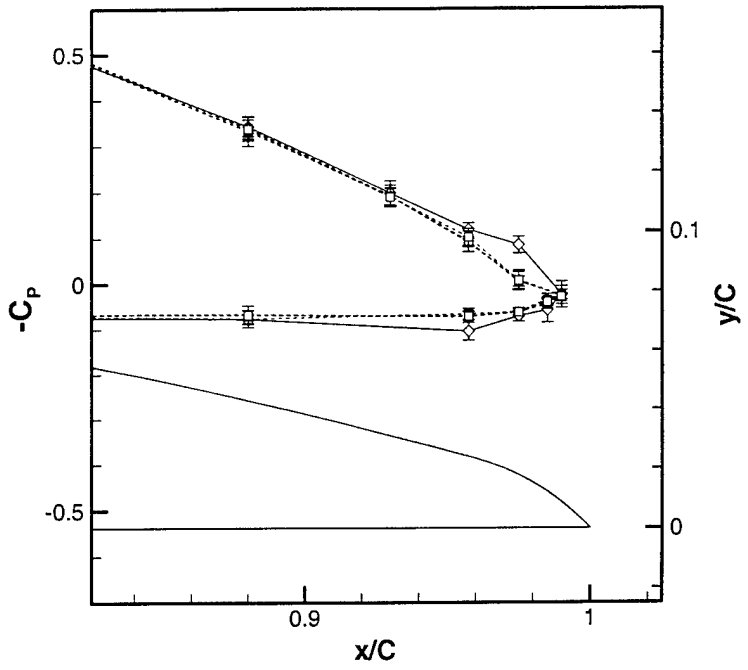

Figure 22: Close up of the trailing edge data in the previous figure

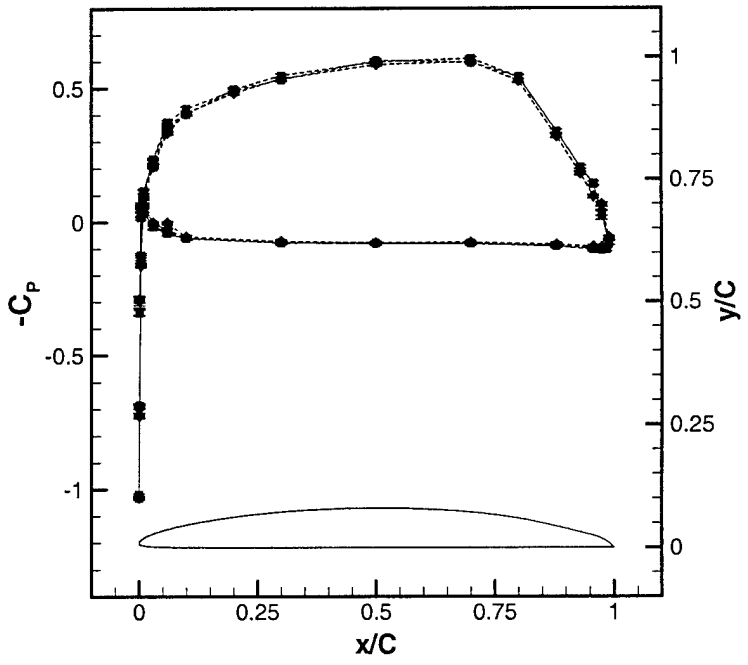

Figure 23: 0 degrees AOA, original vs modified trailing edge data at 18.3 m/s

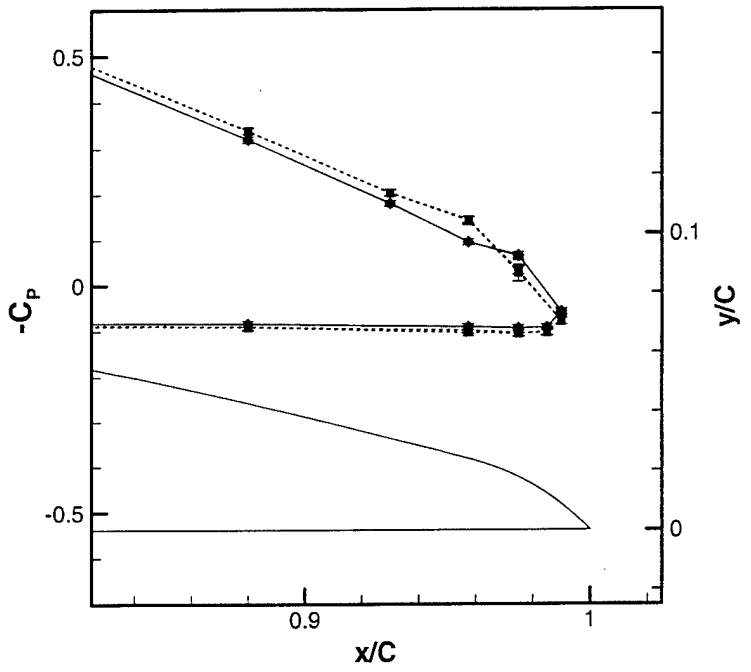

Figure 24: Close up of the trailing edge data in the previous figure

The following figure shows the results of the lift calculations made by integrating the C_P curves. The four lines on this plot are linear best fits of the C_L for each of four test geometries in the Hifoil project. The large error bars seen at the low Reynolds number are the result of the large uncertainty in the 3 m/s C_P data curves at –1 and +1 degrees AOA discussed earlier. This plot shows that there is a slight increase in lift with Reynolds number at 0 and +1 degrees AOA on the original foil. It also show a slight decrease in C_L with Reynolds number for the –1 degree AOA configuration. However, both of these slight trends fall entirely within the error bars of the calculated lift values and cannot be argued with any degree of certainty. The C_L for the foil with the modified trailing edge shows essentially no Reynolds number dependence.

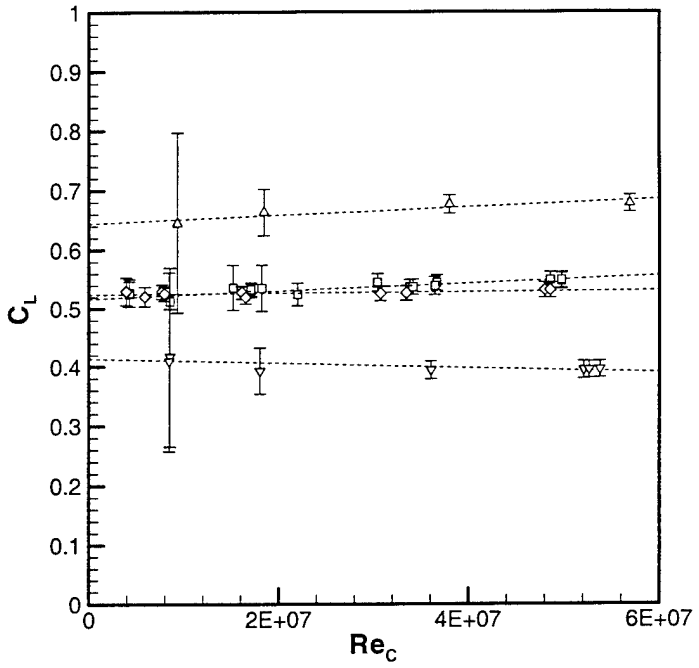

Figure 25: Calculated lift coefficient vs Reynolds number for all configurations

The calculated uncertainty levels in the Hifoil static pressure data are reported below in table 5 and figure 26. Table 5 shows both the maximum and minimum uncertainties found in the complete data set, both in the nondimensional C_P form and also as a differential pressure value in psid. Figure 26 shows both the maximum C_P and maximum pressure uncertainty levels as a function of Re_C. This figure shows that the maximum C_P uncertainty comes from the low Reynolds number data, most likely from the –1 and +1 degrees angle of attack data taken during phase two with the inaccurately ranged transducers. The figure also shows that in terms of pressure the greatest uncertainty lies at the highest Reynolds numbers, but that this high dimensional uncertainty converts to a relative small nondimensional value when normalized by flow speed. However, the maximum uncertainty reported in table 5 may be misleading. At 0 degrees AOA all static pressure curves collapse within a maximum scatter of 0.03 on the C_P plot.

This claim is also supported by the bulk of the C_P uncertainty data reported in figure 26 lying below a value of 0.04. This would suggest that an uncertainty of 0.03 to 0.04 is more indicative of the true error in the static pressure measurements.

	+/- C_P	+/- psi
Max	0.1143	0.4435
Min	0.0093	0.0082

Table 5:Maximum and minimum uncertainties in the Hifoil static pressure data

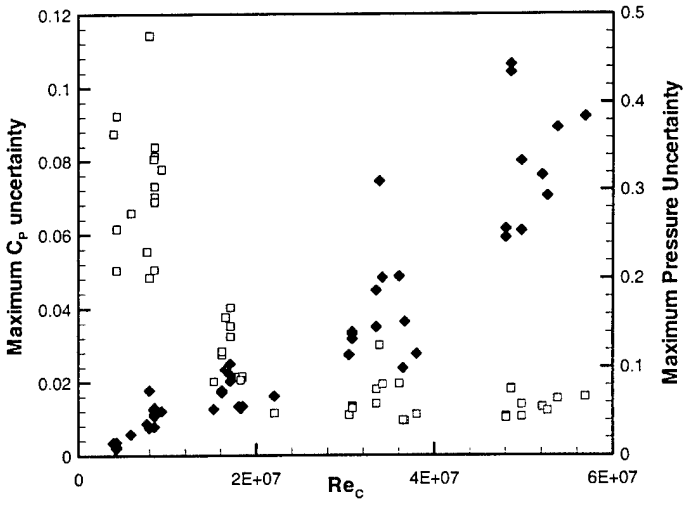

Figure 26: Maximum uncertainty values as a function of Reynolds number

Additional static pressure data plots from the Hifoil project can be found in appendix A.

Conclusions

The static pressure data collected during the Hifoil project proved to be of good quality. The data agreed reasonably well with the preliminary pressure data prediction as calculated by NAVSEA, which proved that the measurements made were at the very least on the right order of magnitude. The collapse of the data taken at various Re_C values suggests that the surface pressures were measured well and that the measurement and calibration techniques were reasonably repeatable. Errant data was corrected when possible with techniques such as using zero-flow data or data taken on other test days at similar flow conditions to correct offset errors. Uncertainty levels were high for some data sets, but on the whole the uncertainty associated with the measurements made was acceptable when the optimal pressure instrument for a corresponding flow condition was used.

No significant Reynolds number dependence exists in the static pressure data collected over the Reynolds number range of the Hifoil project. This is supported by the collapse of the C_P curves taken at various Reynolds numbers and the very slight trends in the calculated lift coefficients. Additionally, the data presented shows the expected increase in lift with increase in angle of attack. Lastly, no appreciable dependence in the pressure data was observed as a result of the change in trailing edge geometry.

Based on the data collected, the static pressure system designed for the Hifoil project functioned well and produced an accurate and useful high Reynolds number static pressure data set, fulfilling one of the major goals of the Hifoil project for the U.S. Navy.

References

[1] Armentrout, E.C. and J.C. Kicks. "Pressure Instrumentation for Gas Turbine Engines- a Review of Measurement Technology." *Journal of Engineering for Power*, **101**, 1979, pp 373.

[2] Astolfi, J.A. et al. "An Experimental Investigation of Cavitation Inception and Development on a Two Dimensional Eppler Hydrofoil." *Journal of Fluids Engineering*, **122**, 2000, pp 164.

[3] Benedict, Robert P. Fundamentals of Temperature, Pressure, and Flow Measurements. John Wiley and Sons, New York, 1984, pp 340-349.

[4] Ducruet, C. and A. Dyment. "The Pressure-Hole Problem." *Journal of Fluid Mechanics*, **142**, 1984, pp 251.

[5] Ducruet, C. "A Method for Correcting Wall Pressure Measurements in Subsonic Compressible Flow." *Journal of Fluids Engineering*, **113**, 1991, pp 256.

[6] Franklin, R.E. and J.M. Wallace. "Absolute Measurements of Static-Hole Error Using Flush Transducer." *Journal of Fluid Mechanics*, **42**, 1970, pp 33.

[7] Niewald, P.W. and S.L. Parker. "Wind-Tunnel Techniques to Successfully Predict F/A-18 In-Flight Lift and Drag." *Journal of Aircraft*, **37**, 2000, pp 9.

[8] Niewald, P.W. and S.L. Parker. "Flight-Test Techniques Employed to Successfully Verify F/A-18 In-Flight Lift and Drag." *Journal of Aircraft*, **37**, 2000, pp 194.

[9] Spaid, Frank W. "High Reynolds Number, Multielement Airfoil Flowfield Measurements." *Journal of Aircraft*, **37**, 2000, pp 499.

[10] Wood, D.H. and R.V. Westphal. "Measurements of the Flow Around a Lifting-Wing/Body Junction." *AIAA Journal*, **30**, 1991, pp 6.

[11] Zandieh, Ali and J. Gordon Leishman. "Boundary Layer and Pressure Measurements on a Cylinder with Unsteady Circulation Control." *AIAA Journal*, **31**, 1993, pp 1769.

[12] Zogg, H. and H. Thomann. "Errors in Static Pressure Measurements Due to Protruding Pressure Taps." *Journal of Fluid Mechanics*, **54**, 1972, pp 489.

Appendix A: Additional Data Plots

Contained in this appendix are additional annotated plots of the static pressure data taken during the Hifoil project. Individual plots at each test condition for which static pressure data was taken are presented here.

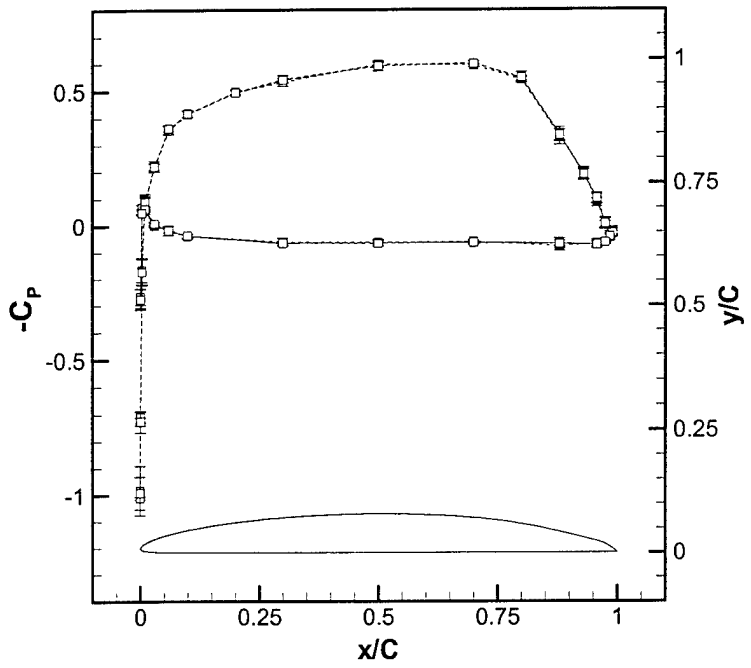

Figure 1: Original trailing edge, O degrees AOA, 1.5 m/s

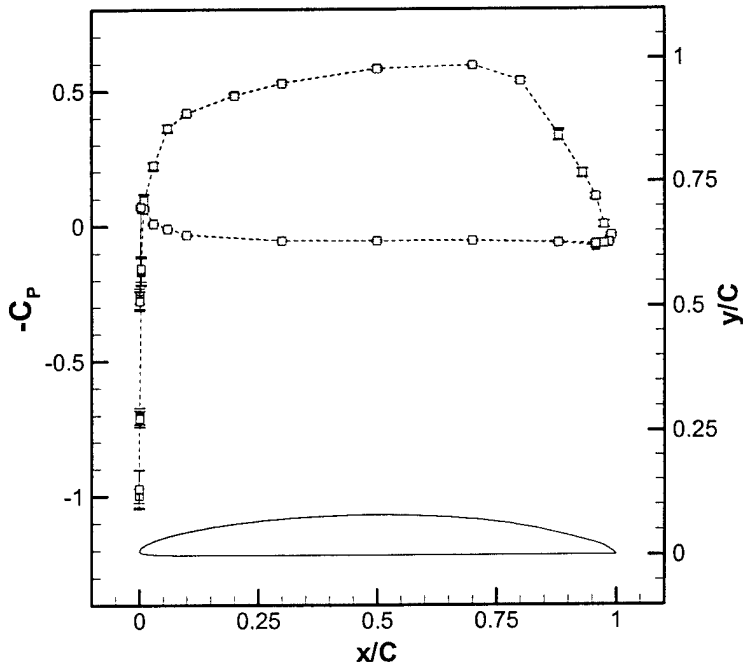

Figure 2: Original trailing edge, O degrees AOA, 3 m/s

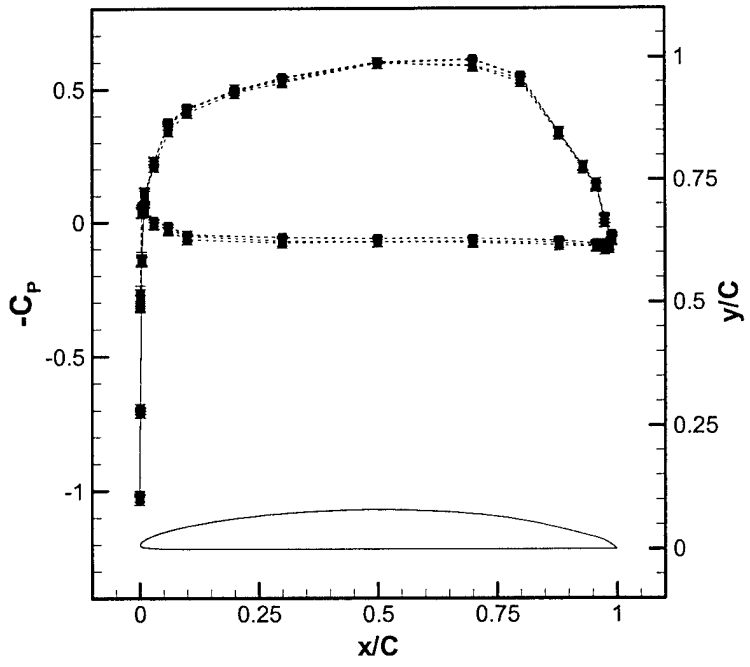

Figure 3: Original trailing edge, O degrees AOA, 6 m/s

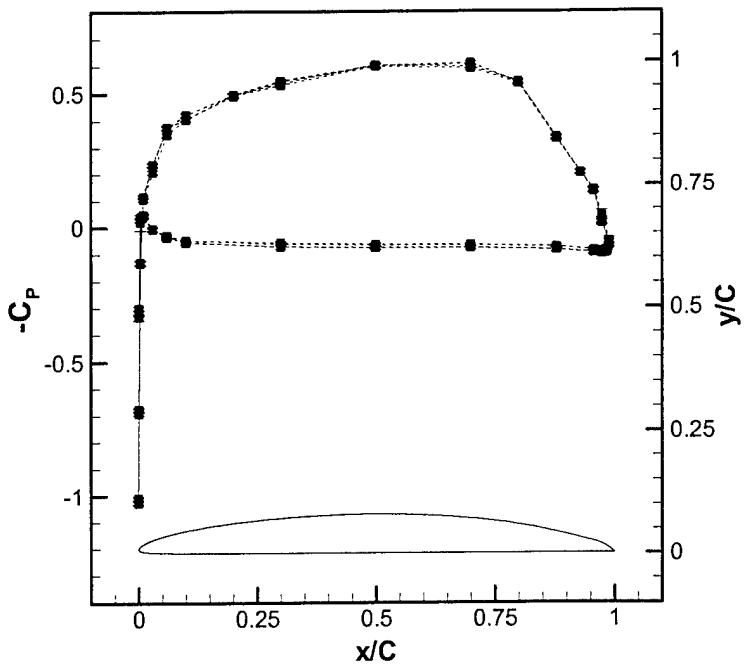

Figure 4: Original trailing edge, O degrees AOA, 12 m/s

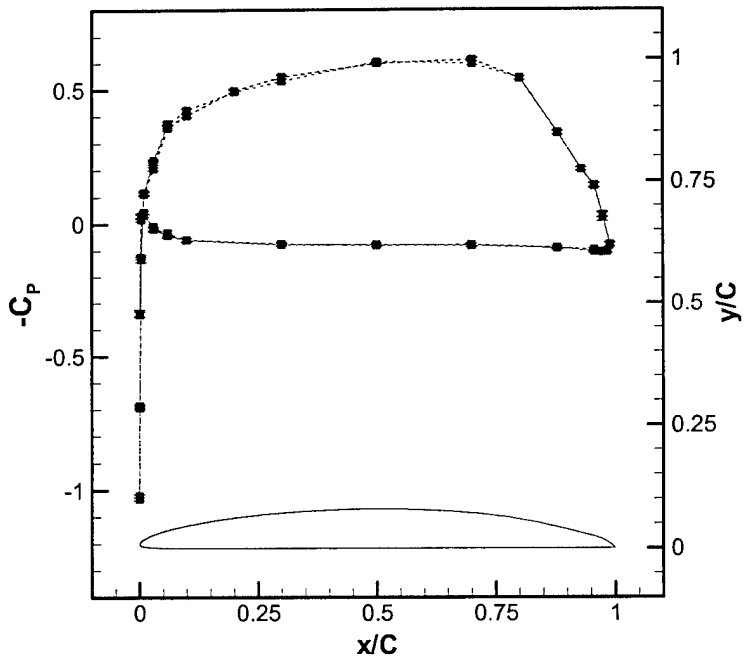

Figure 5: Original trailing edge, O degrees AOA, 18.3 m/s

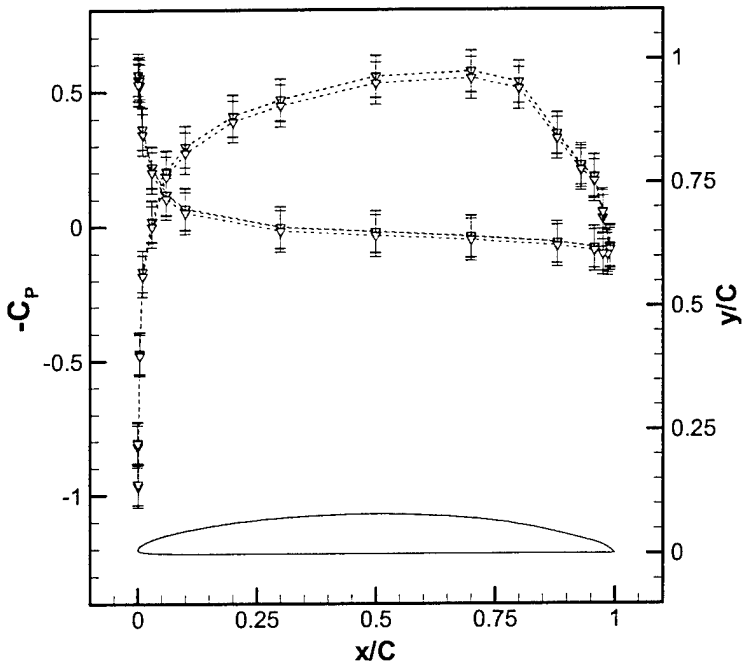

Figure 6: Original trailing edge, -1 degrees AOA, 3 m/s

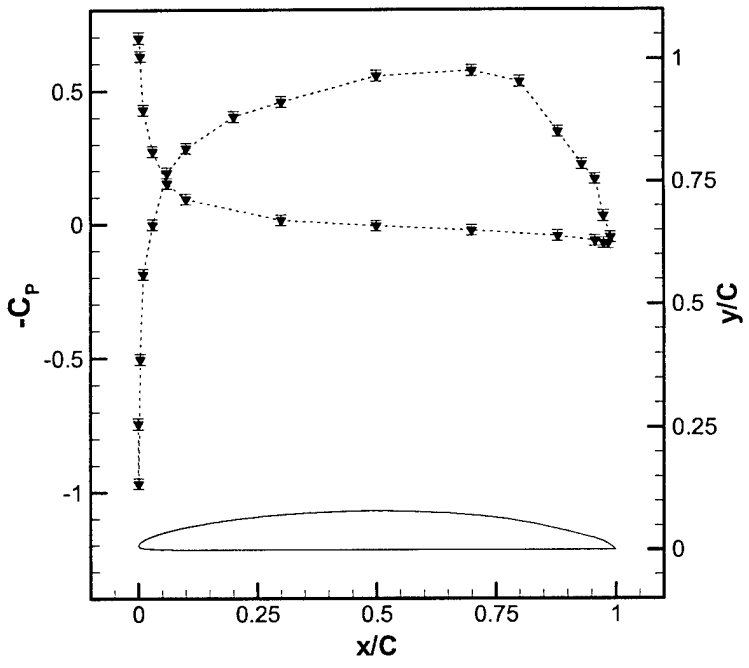

Figure 7: Original trailing edge, -1 degrees AOA, 6 m/s

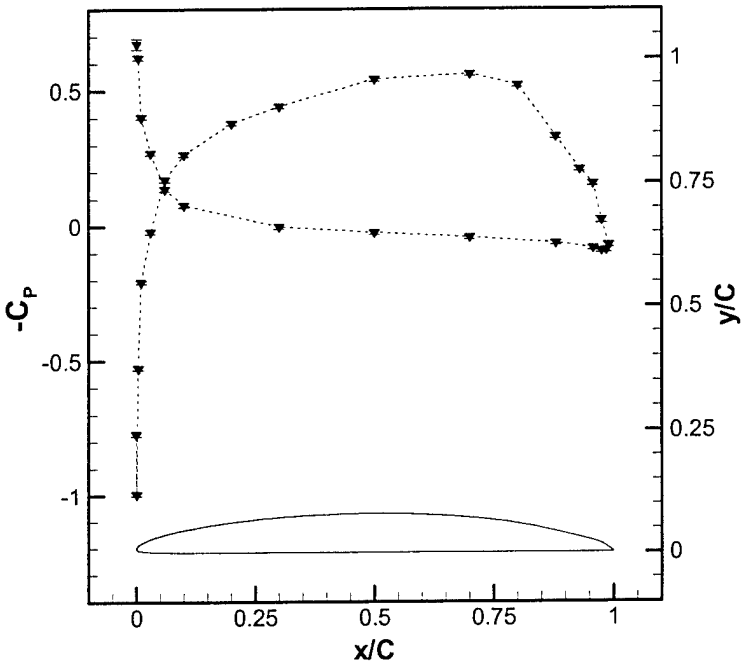

Figure 8: Original trailing edge, -1 degrees AOA, 12 m/s

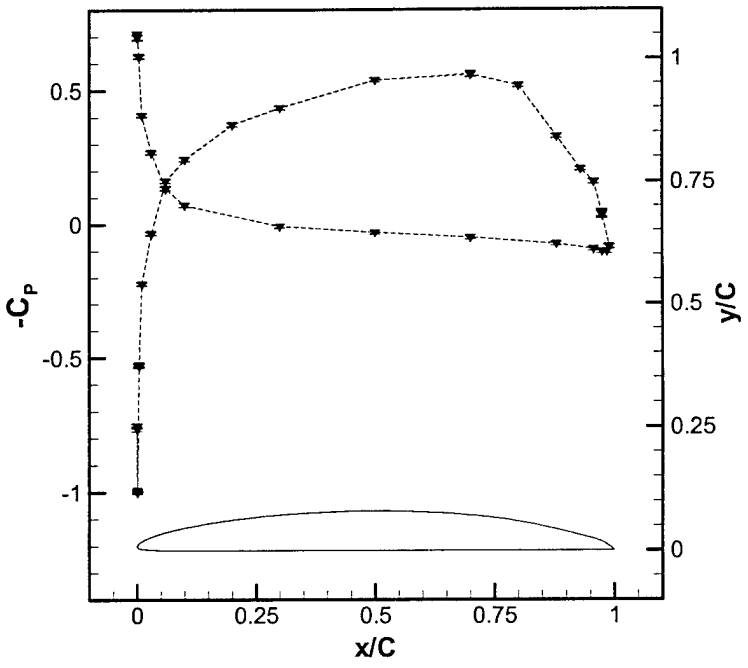

Figure 9: Original trailing edge, -1 degrees AOA, 18.3 m/s

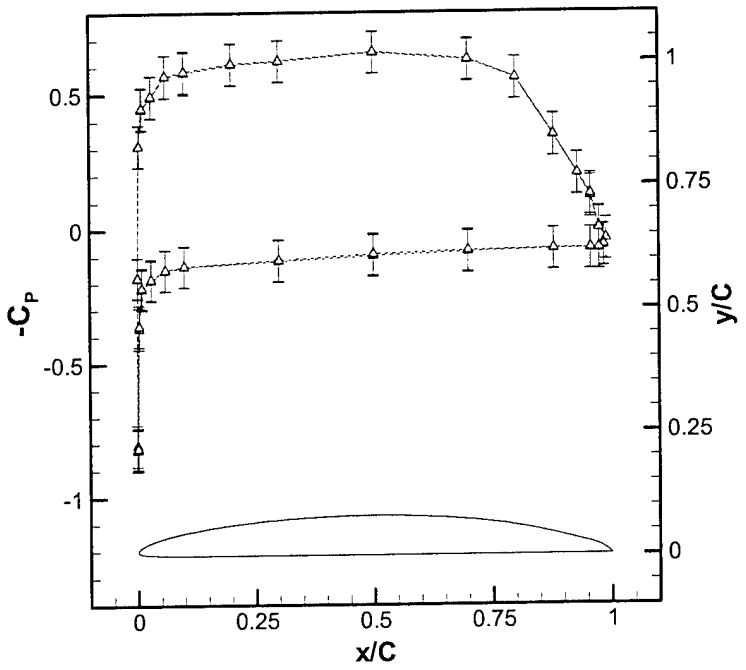

Figure 10: Original trailing edge, +1 degrees AOA, 3 m/s

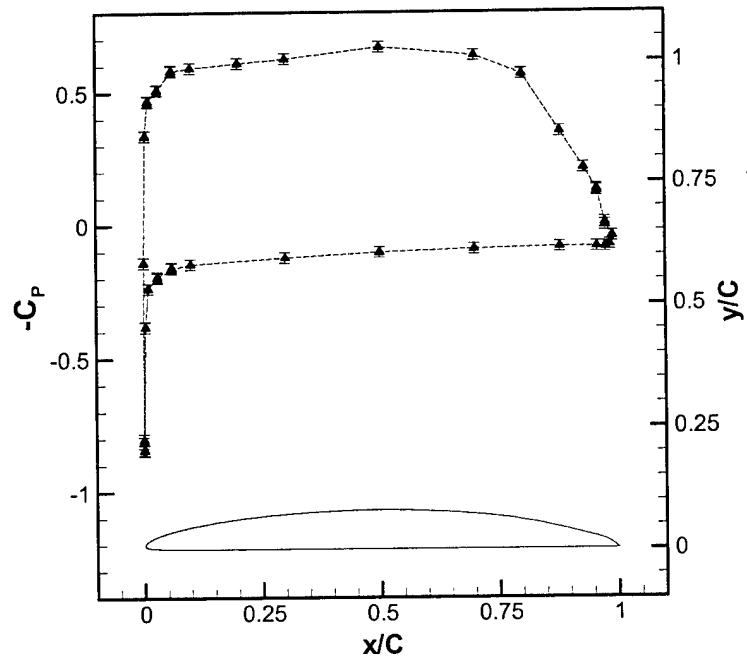

Figure 11: Original trailing edge, +1 degrees AOA, 6 m/s

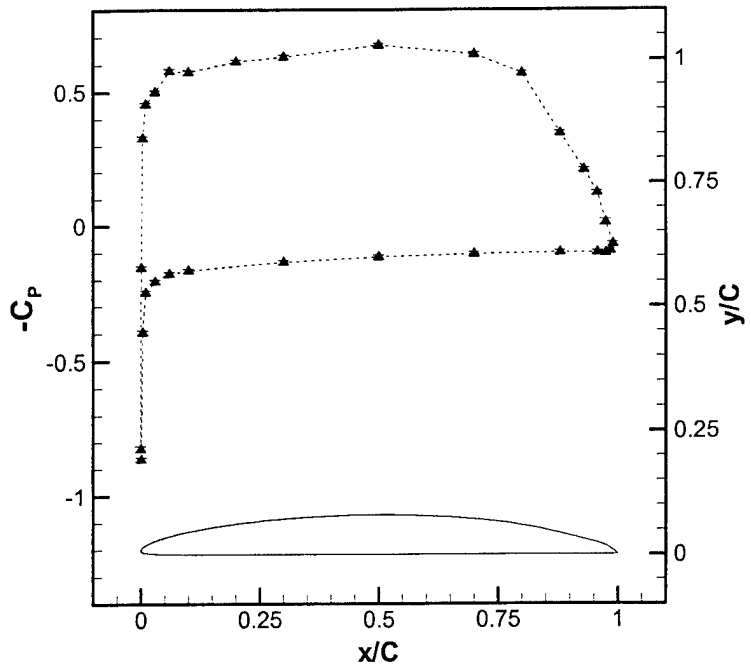

Figure 12: Original trailing edge, +1 degrees AOA, 12 m/s

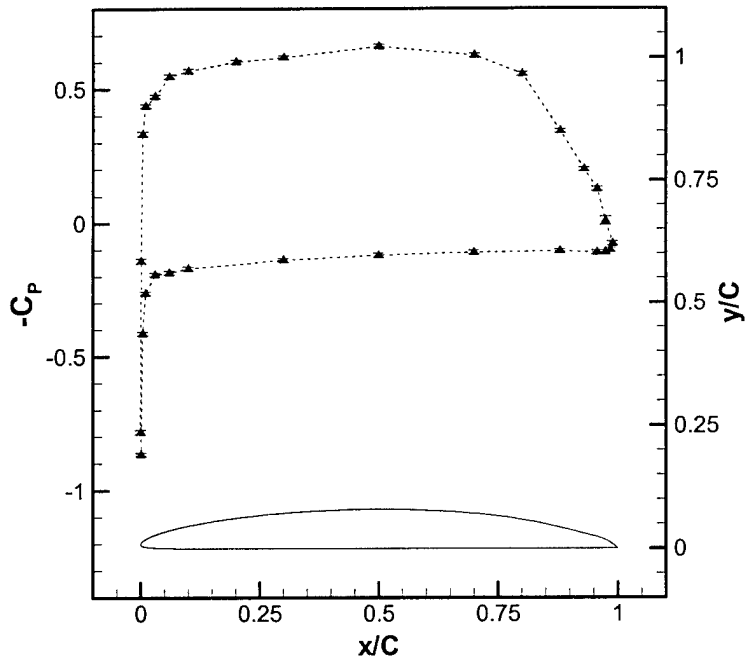

Figure 13: Original trailing edge, +1 degrees AOA, 18.3 m/s

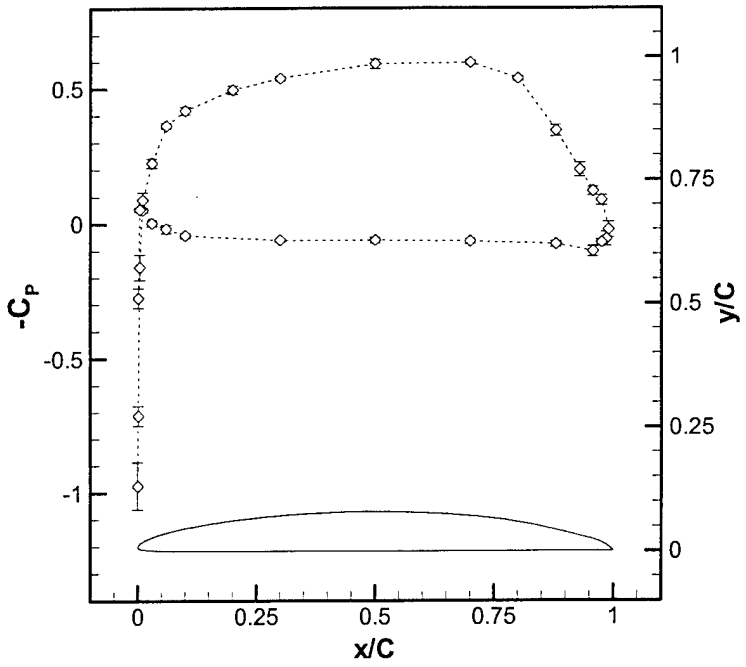

Figure 14: Modified trailing edge, 0 degrees AOA, 1.5 m/s

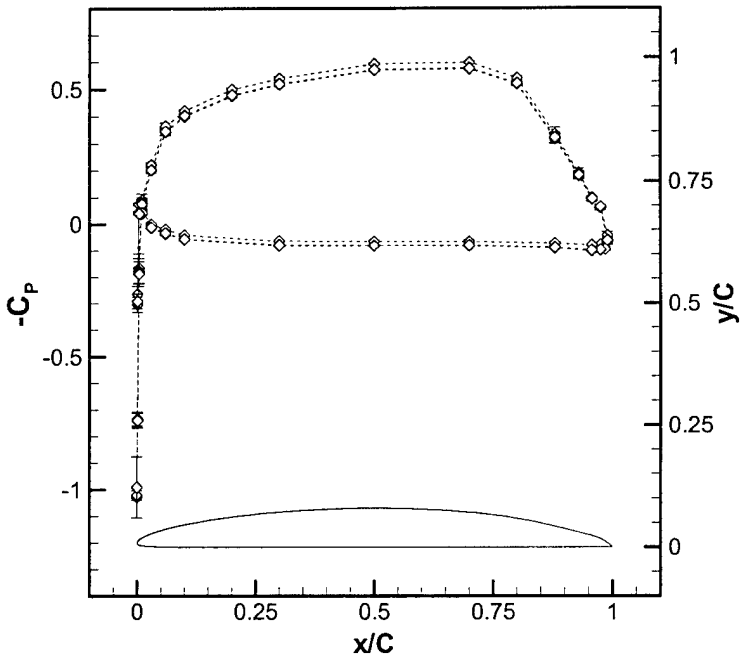

Figure 15: Modified trailing edge, 0 degrees AOA, 3 m/s

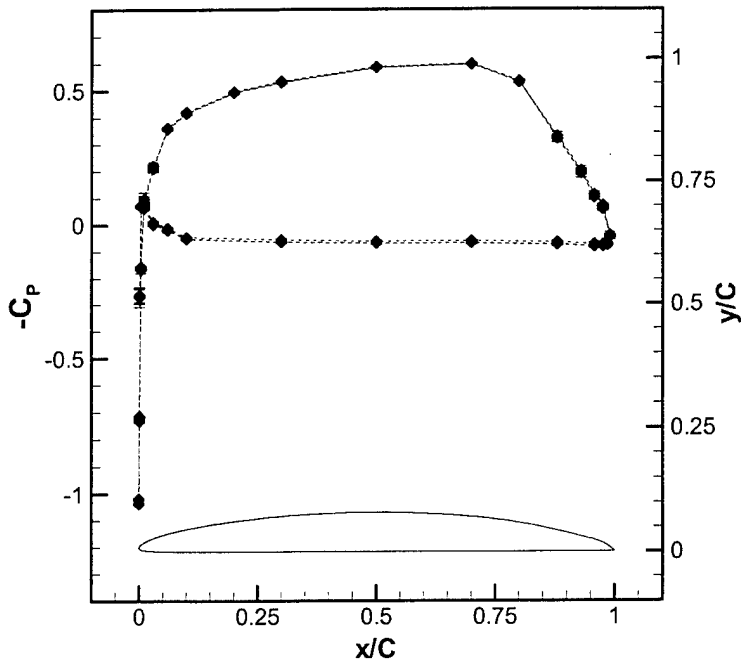

Figure 16: Modified trailing edge, 0 degrees AOA, 6 m/s

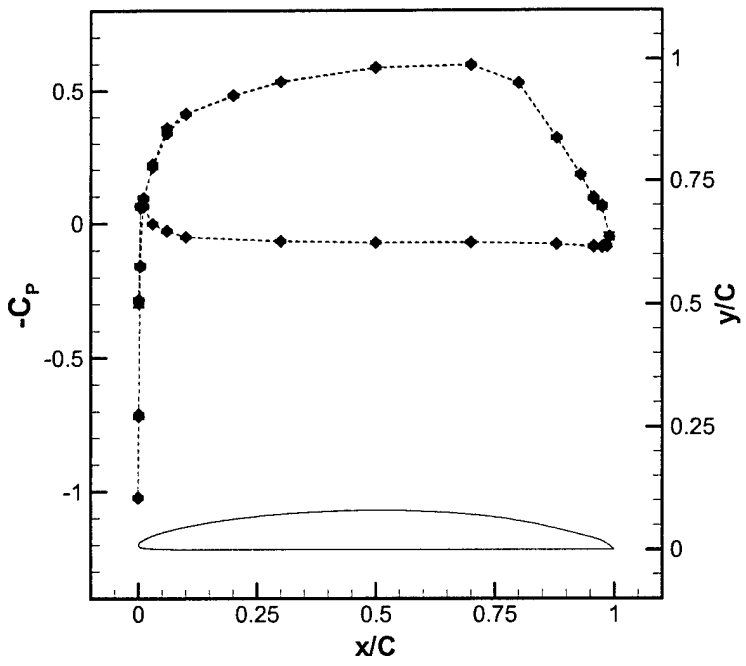

Figure 17: Modified trailing edge, 0 degrees AOA, 12 m/s

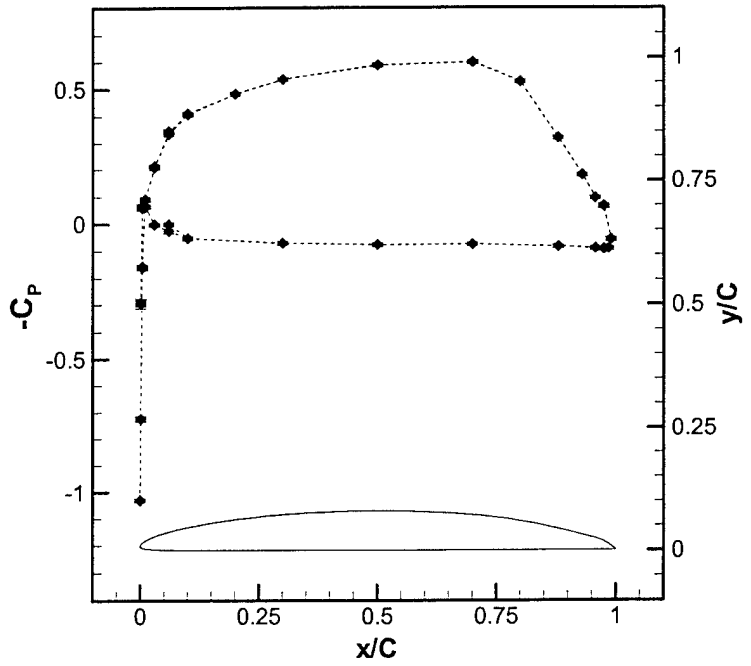

Figure 18: Modified trailing edge, 0 degrees AOA, 18.3 m/s

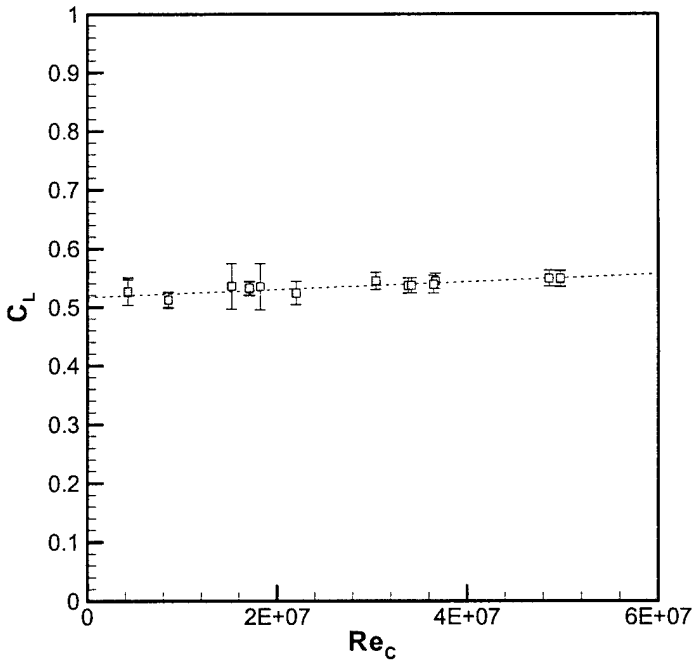

Figure 19: Original trailing edge, 0 degrees AOA, Lift vs Reynolds number

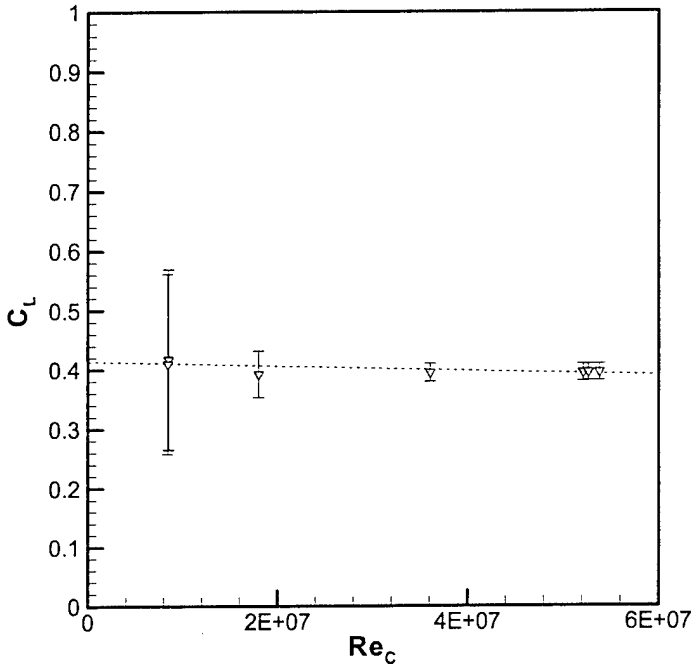

Figure 20: Original trailing edge, -1 degrees AOA, Lift vs Reynolds number

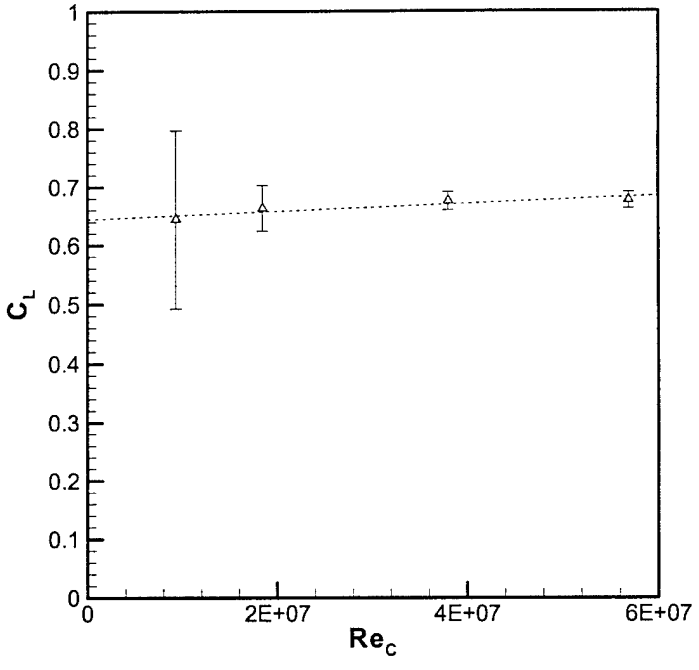

Figure 21: Original trailing edge, +1 degrees AOA, Lift vs Reynolds number

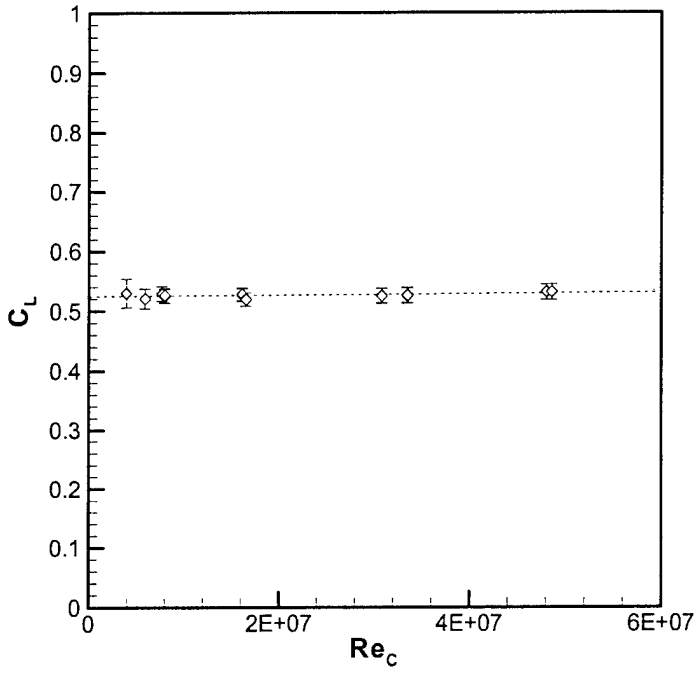

Figure 22: Modified trailing edge, 0 degrees AOA, Lift vs Reynolds number

Appendix B: Scanivalve Information

Below is an annotated image of the J-Type Scanivalve used on the Hifoil project. This picture comes from the Scanivalve Corporation website and briefly describes how the device works.

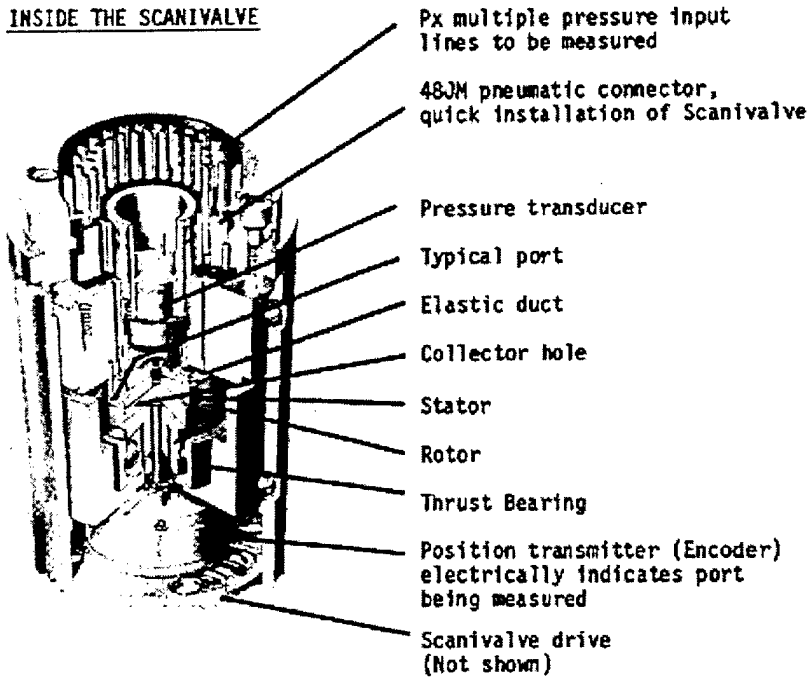

The next image is a schematic of the solenoid driver that powers the J-Type Scanivalve. Below the image is technical information about the drive unit.

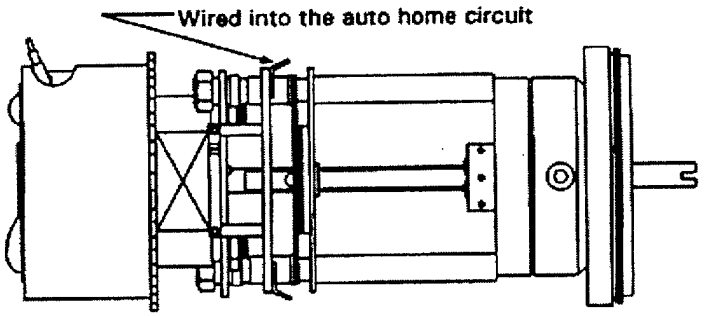

This stepper drive consists of a 12 step, size 4 Ledex solenoid driving a 4-1 gear reducer. This combination makes 48 steps per revolution. It auto homes 48 steps in two seconds. Both wafer switches rotate at solenoid rpm.

This drive requires 30 milliseconds for spring return. Use Scanivalve Model CTLR2/S2-S6, which is a solid state pulse length feed back driving circuit for providing 24Vdc to operate the solenoid drive.
ScanCo# JS4-48----------48 steps/revolution, wired for auto home

SPECIFICATIONS

Duty Cycle: 1/4 at 24 Vdc or 44 seconds "on" period.

Resistance: Available with 8.03 ohm coil for operation at 24 Vdc.

Switch Decks: One auto home wafer. Wafer switches have solid silver contacts (lubricate with light grease.)

Temperature: -60 degrees C to 125 degrees C, can be operated up to 175 degrees C (at solenoid not ambient)

(From www.scanivalve.com)

Appendix C: Experimental Setup Schematics

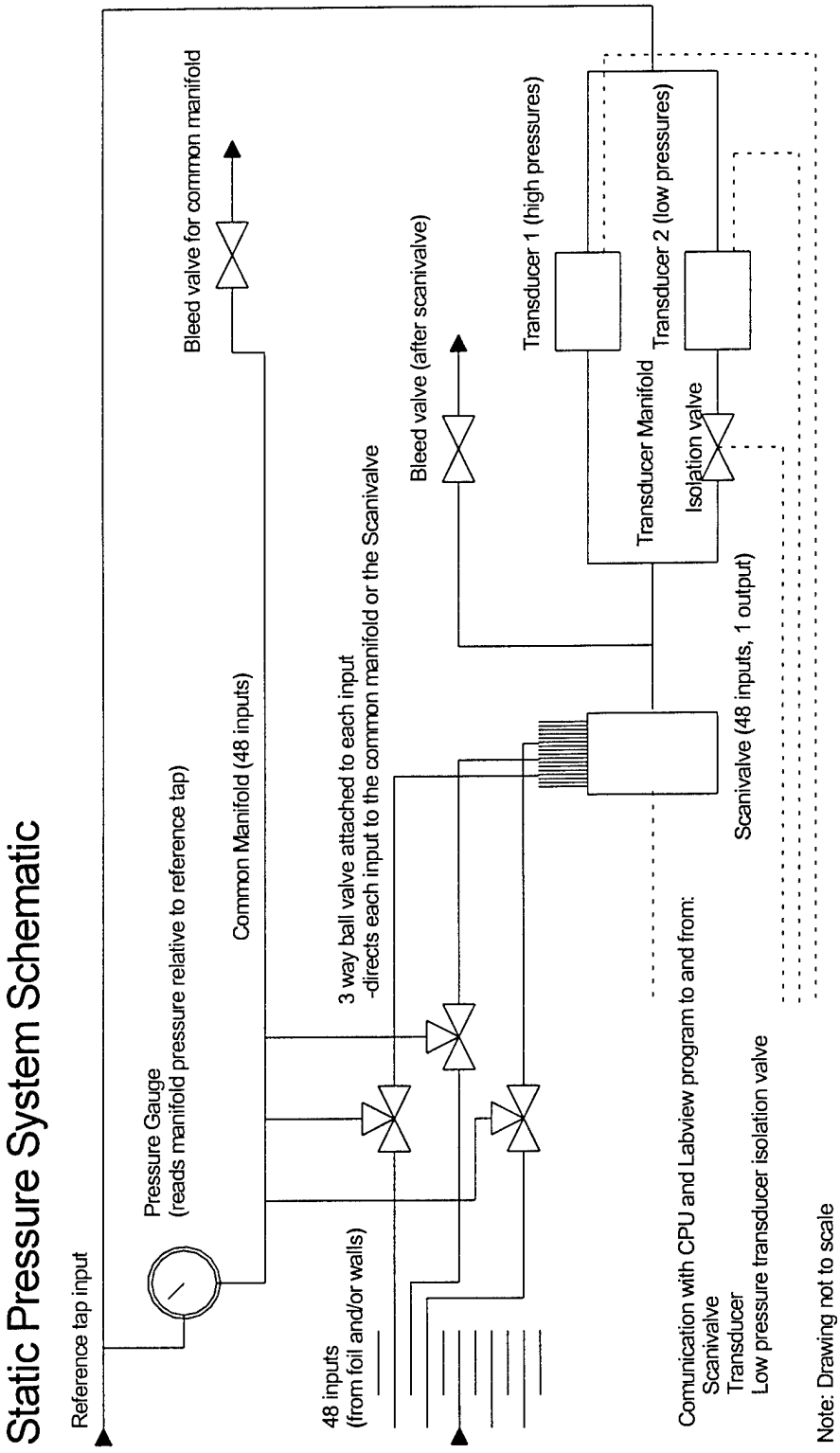

Appendix D: Transducer Specifications

Setra Transducer

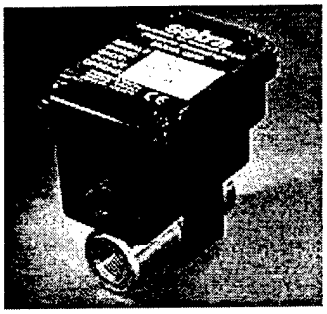

Model 230 Specifications	
Electrical Output Voltage	0 to 5 VDC 0 to 10 VDC
Electrical Output Current	4 to 20 mA
Accuracy (RSS Method)	±0.25% Full Scale
Type of Pressure	Differential (can be wet both sides)
Pressure Ranges	Unidirectional: 0 to 1, 2, 5, 10, 25, 50, 100 psid Bi-directional: 0 to ±0.5, ±1, ±2.5, ±5, ±10, ±25, ±50 psid
Thermal Effects	Thermal Compensation °F (°C): 30 to 150 (-1 to 65) %FS/100°F(100°C)max.zero: ±2.0 (±3.6) %FS/100°F(100°C)max.span: ±2.0 (±3.6)
Media	Gases or liquids compatible with 300 series and 17-4PH stainless steel, and Viton® "O" ring. (Hydrogen not recommended for use with 17-4 PH stainless steel.) *Viton® is a registered trademark of DuPont Dow Elastomers

(From www.setra.com)

Rosemount Transducer

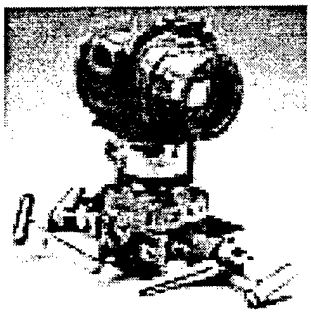

3051- MODEL 3051C DIFFERENTIAL PRESSURE TRANSMITTER

- Superior performance: 0.075% accuracy, 100:1 rangeability
- Differential pressure: calibrated spans from 0.1 inH 2 O to 2000 psi (0,25 mbar to 138 bar)
- SST, Hastelloy C ® , Monel ® , Tantalum (CD, CG only), or gold-plated Monel process isolators
- Compact, rugged, and lightweight design for easy installation
- Compound Range allows negative calibrations

(From www.rosemount.com)

Appendix E: Labview Code

Attached are Labview printouts of the Labview programs developed for use with the static pressure system on the Hifoil project. Both the user interface and the block diagram for each program have been included. The programs have been attached in the following order:

1.	Static Pressure Menu.vi	Menu progam
2.	Pressure Taps (Mod 6a).vi	Scanivalve controlled data acquisition
3.	Pressure Taps (Mod 6b).vi	User monitored, Scanivalve controlled
4.	Pressure Taps (Mod 6c).vi	User controlled data acquisition
5.	Calibration (mod 3).vi	Transducer calibration program
6.	Static Pressure Sampling.vi	Real time data sampling program

Static Pressure Menu.vi
C:\HIFOIL\Static Press Taps\Phase III\VIs\Static Pressure Menu.vi
Last modified on 11/5/2001 at 11:51 AM
Printed on 11/5/2001 at 11:53 AM

Connector Pane

Static Pressure Menu.vi

Front Panel

Standard DAQ (Scanivalve)	Monitored DAQ (Scanivalve)	Manual DAQ (no Scanivalve)	Calibration	Sample Pressure Taps	Bleed	Quit

Static Pressure Menu.vi
C:\HIFOIL\Static Press Taps\Phase III\VIs\Static Pressure Menu.vi
Last modified on 11/5/2001 at 11:51 AM
Printed on 11/5/2001 at 11:53 AM

Block Diagram

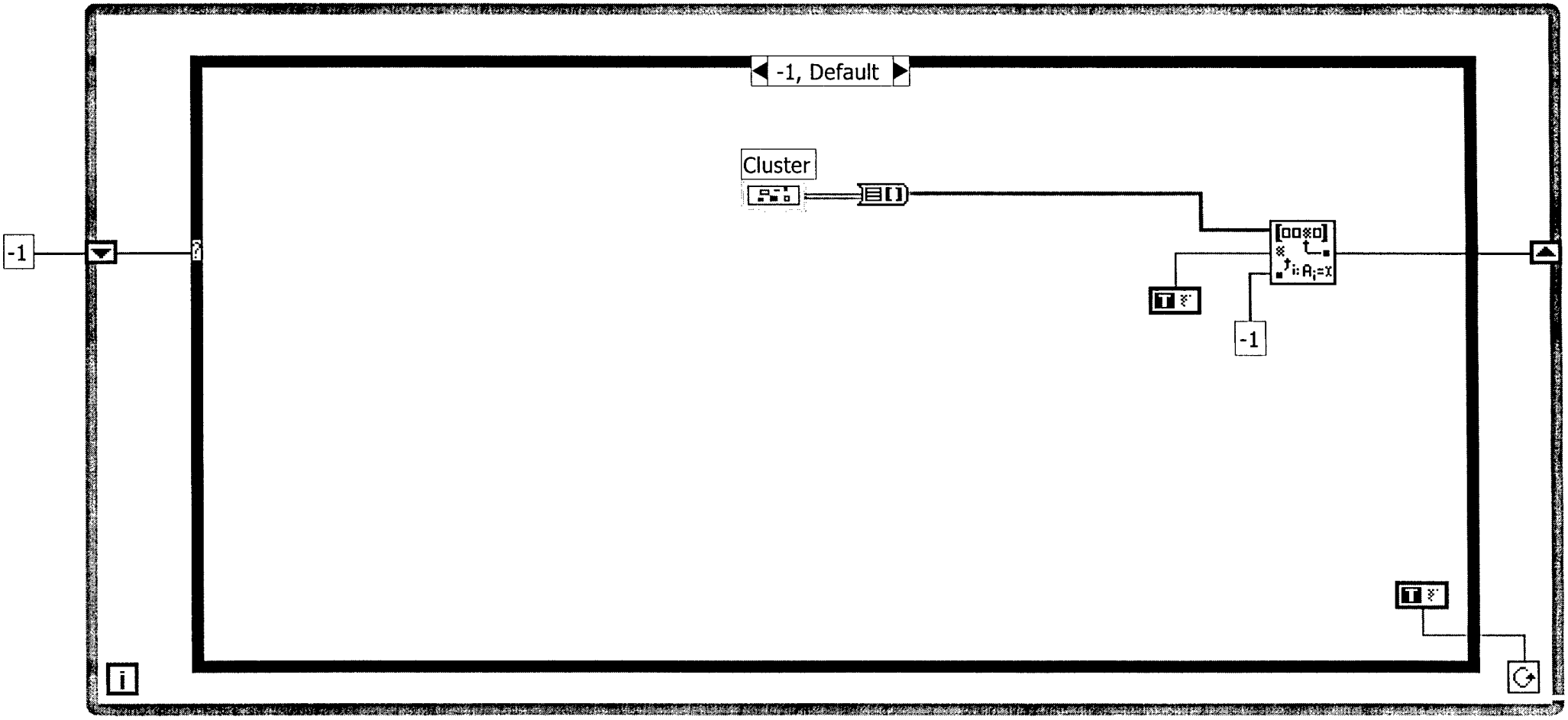

Static Pressure Menu.vi
C:\HIFOIL\Static Press Taps\Phase III\VIs\Static Pressure Menu.vi
Last modified on 11/5/2001 at 11:51 AM
Printed on 11/5/2001 at 11:53 AM

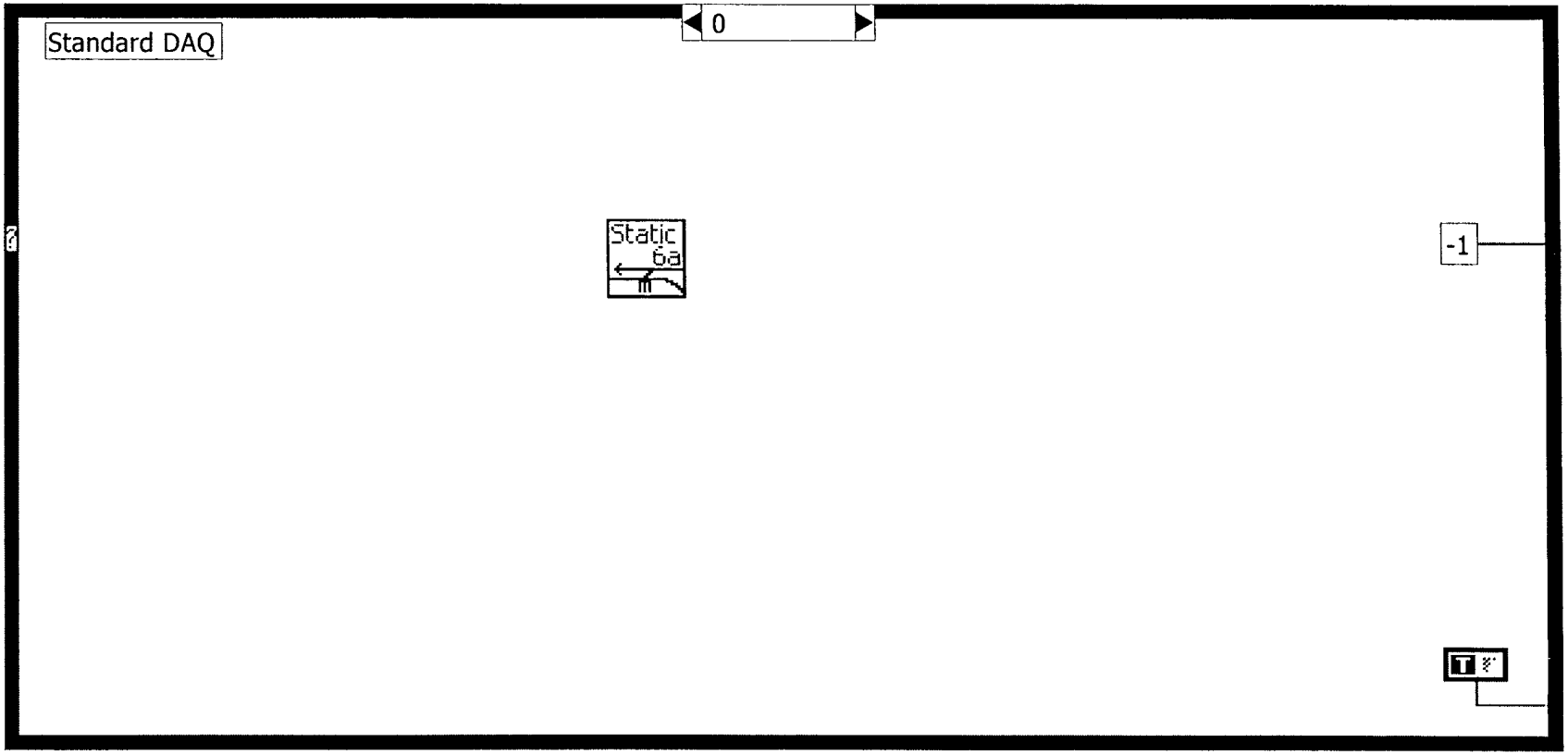

Static Pressure Menu.vi
C:\HIFOIL\Static Press Taps\Phase III\VIs\Static Pressure Menu.vi
Last modified on 11/5/2001 at 11:51 AM
Printed on 11/5/2001 at 11:53 AM

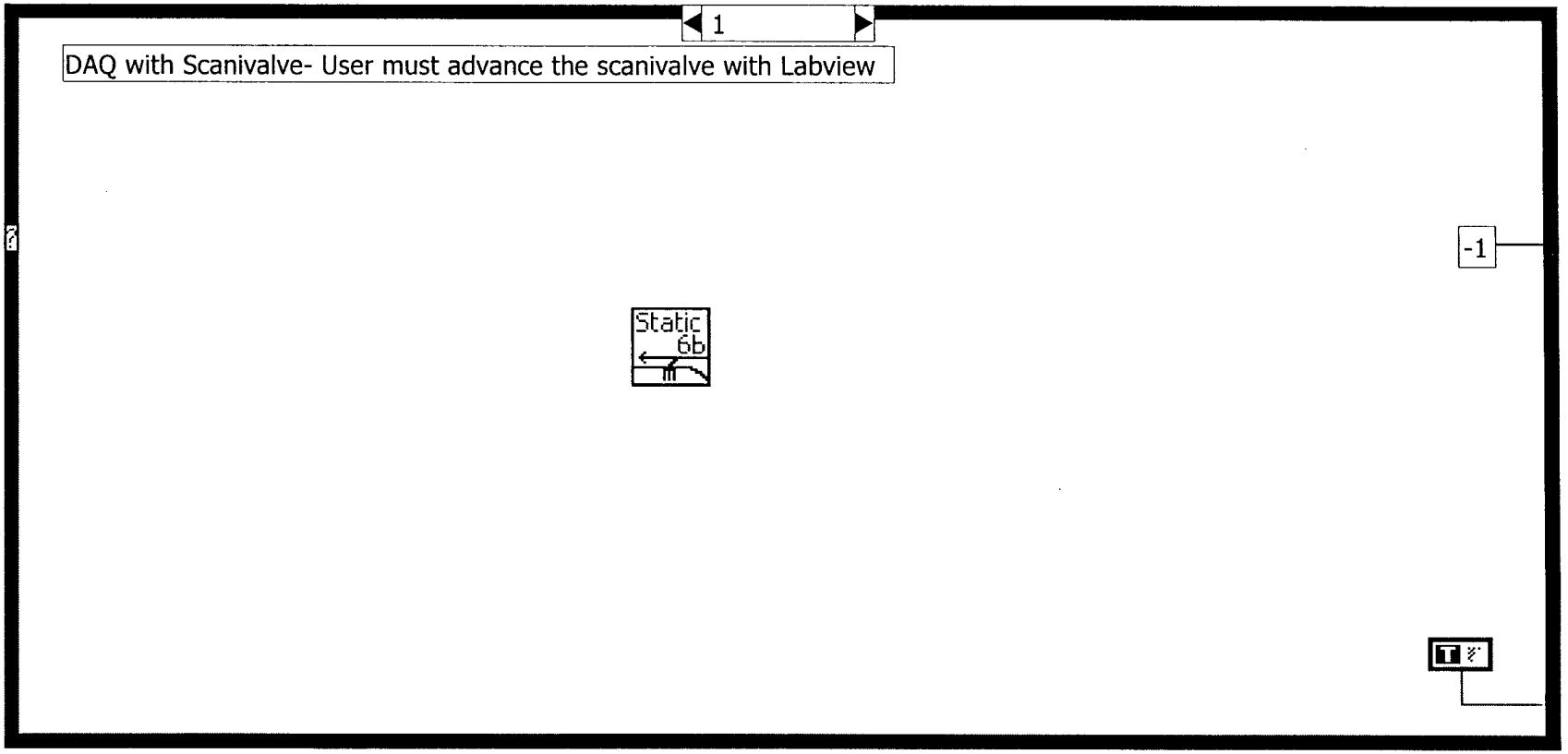

Static Pressure Menu.vi
C:\HIFOIL\Static Press Taps\Phase III\VIs\Static Pressure Menu.vi
Last modified on 11/5/2001 at 11:51 AM
Printed on 11/5/2001 at 11:53 AM

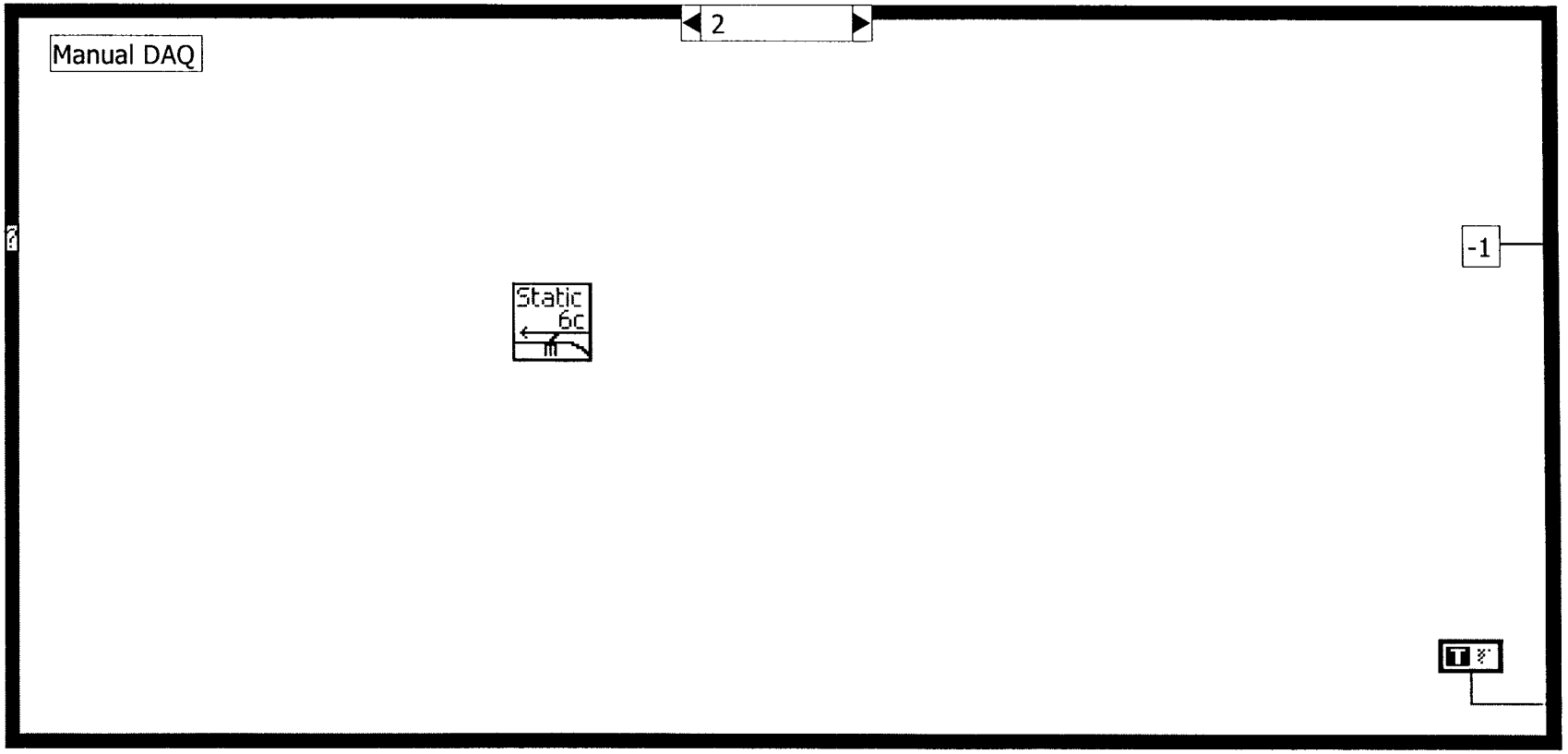

Static Pressure Menu.vi
C:\HIFOIL\Static Press Taps\Phase III\VIs\Static Pressure Menu.vi
Last modified on 11/5/2001 at 11:51 AM
Printed on 11/5/2001 at 11:53 AM

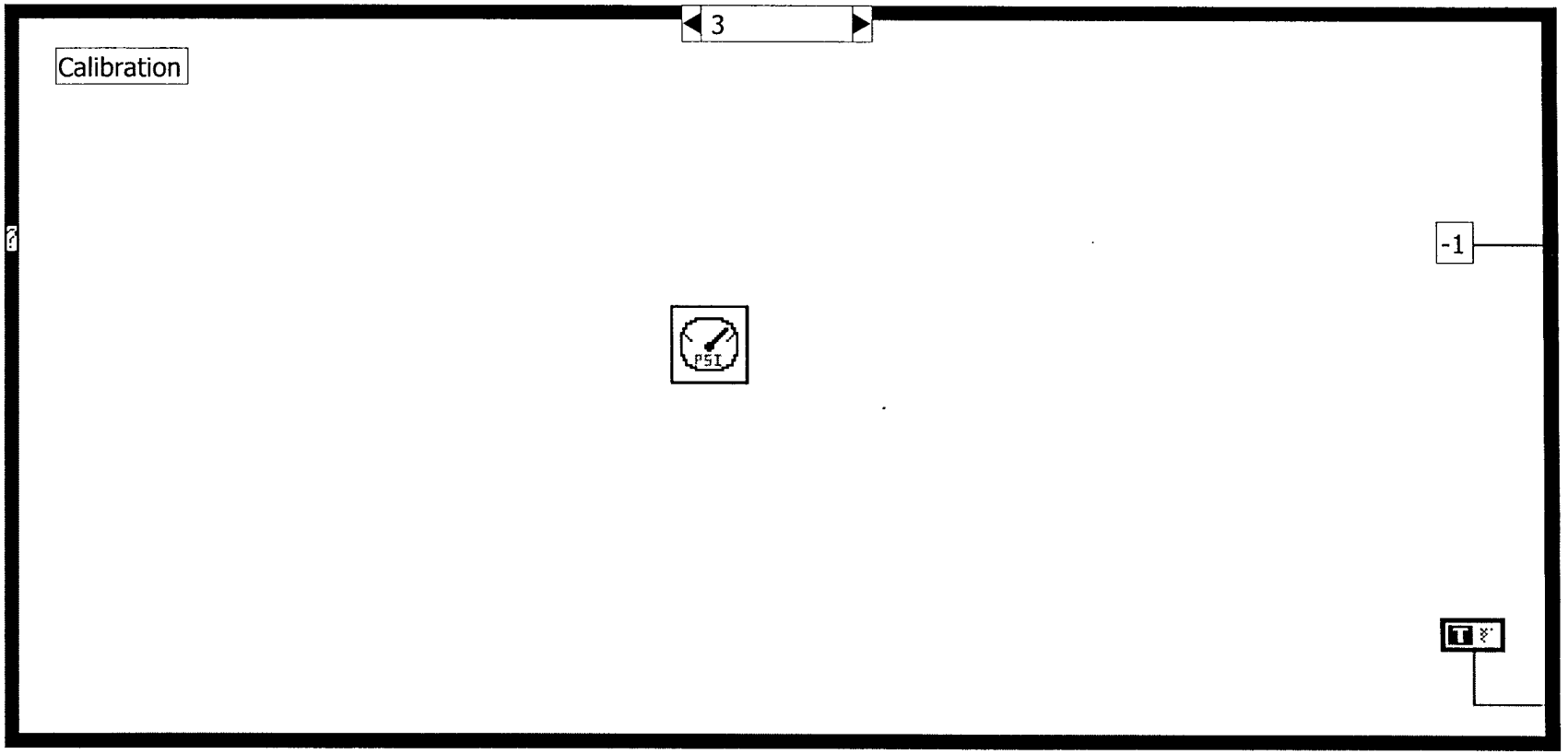

Static Pressure Menu.vi
C:\HIFOIL\Static Press Taps\Phase III\VIs\Static Pressure Menu.vi
Last modified on 11/5/2001 at 11:51 AM
Printed on 11/5/2001 at 11:53 AM

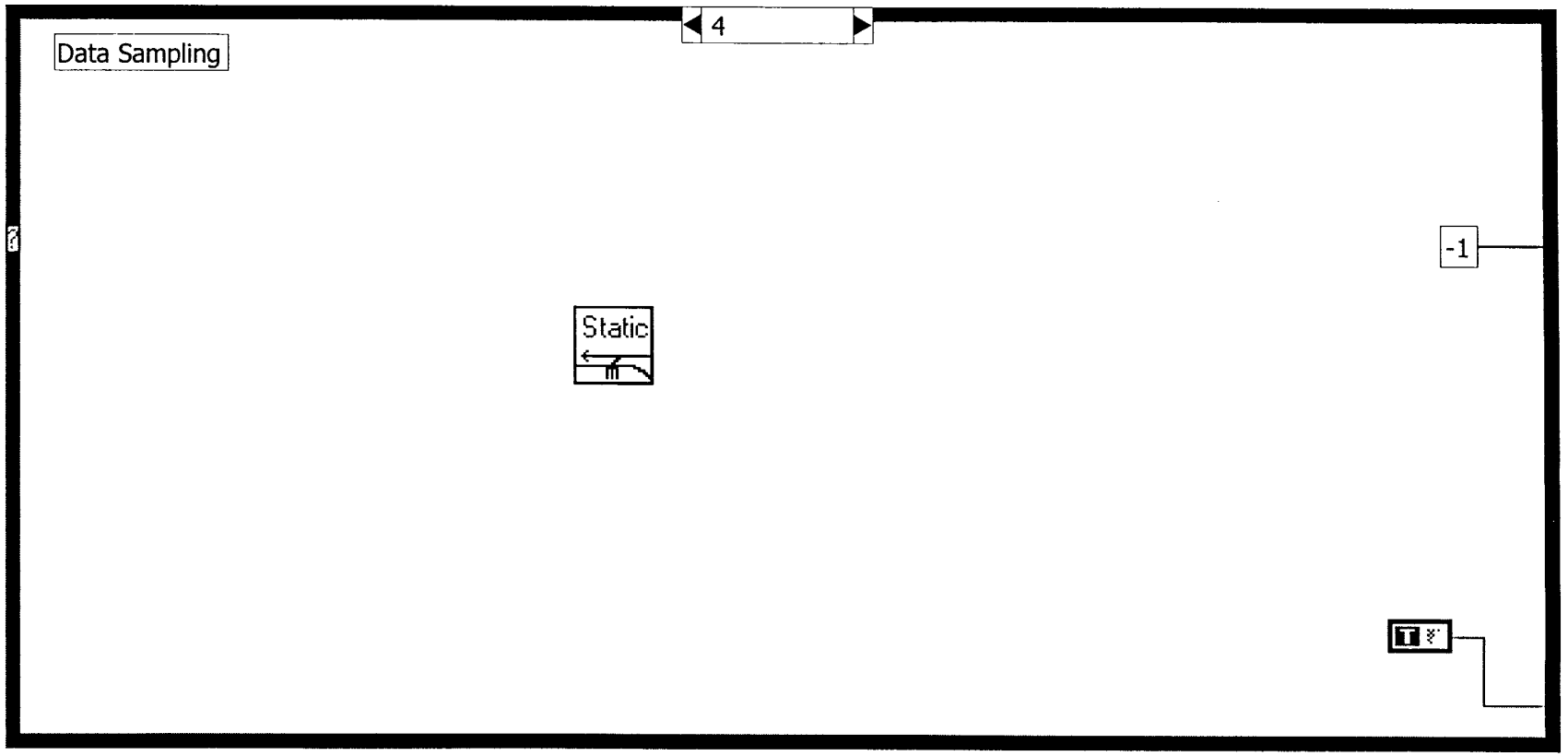

Static Pressure Menu.vi
C:\HIFOIL\Static Press Taps\Phase III\VIs\Static Pressure Menu.vi
Last modified on 11/5/2001 at 11:51 AM
Printed on 11/5/2001 at 11:53 AM

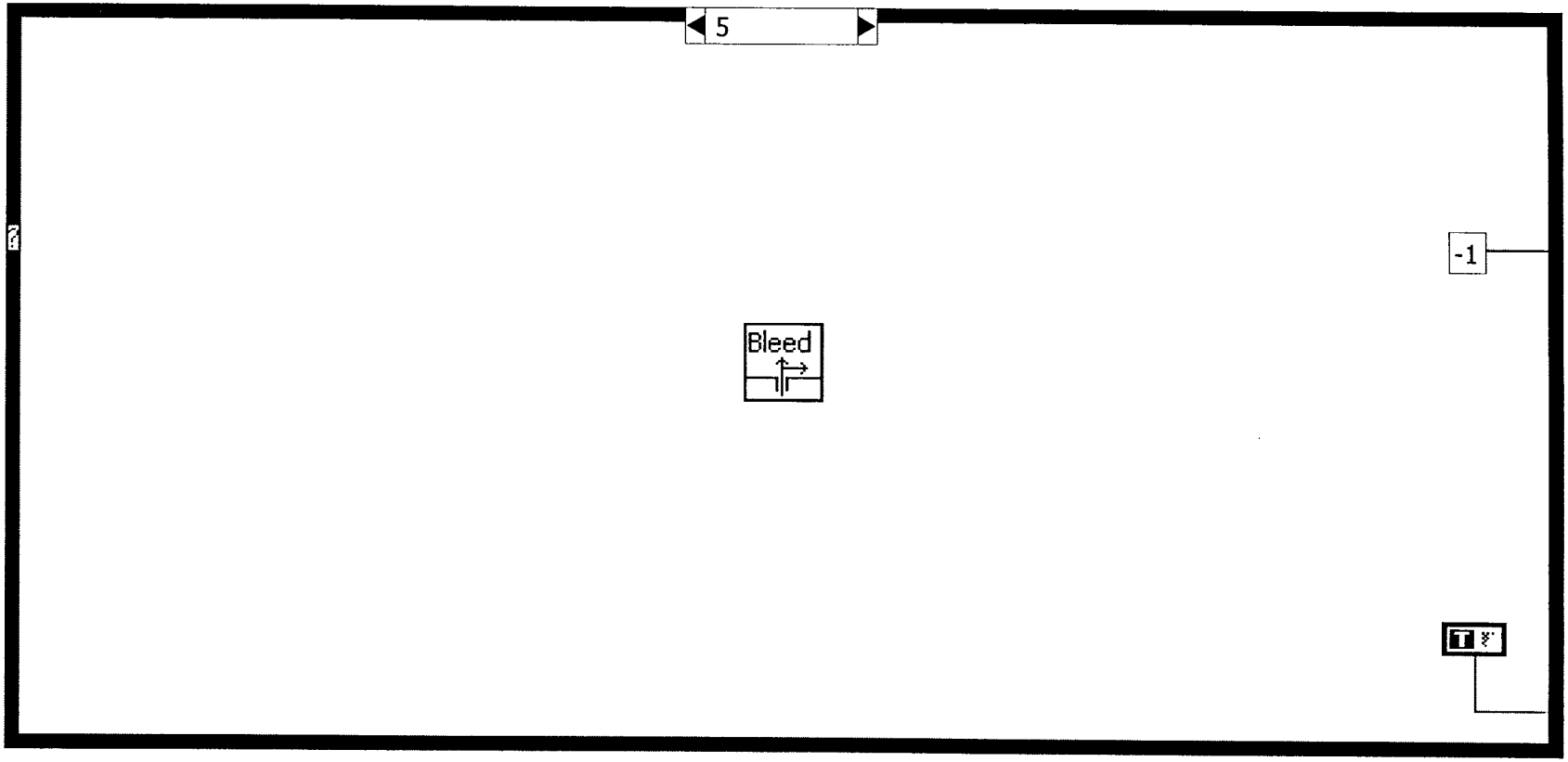

Static Pressure Menu.vi
C:\HIFOIL\Static Press Taps\Phase III\VIs\Static Pressure Menu.vi
Last modified on 11/5/2001 at 11:51 AM
Printed on 11/5/2001 at 11:53 AM

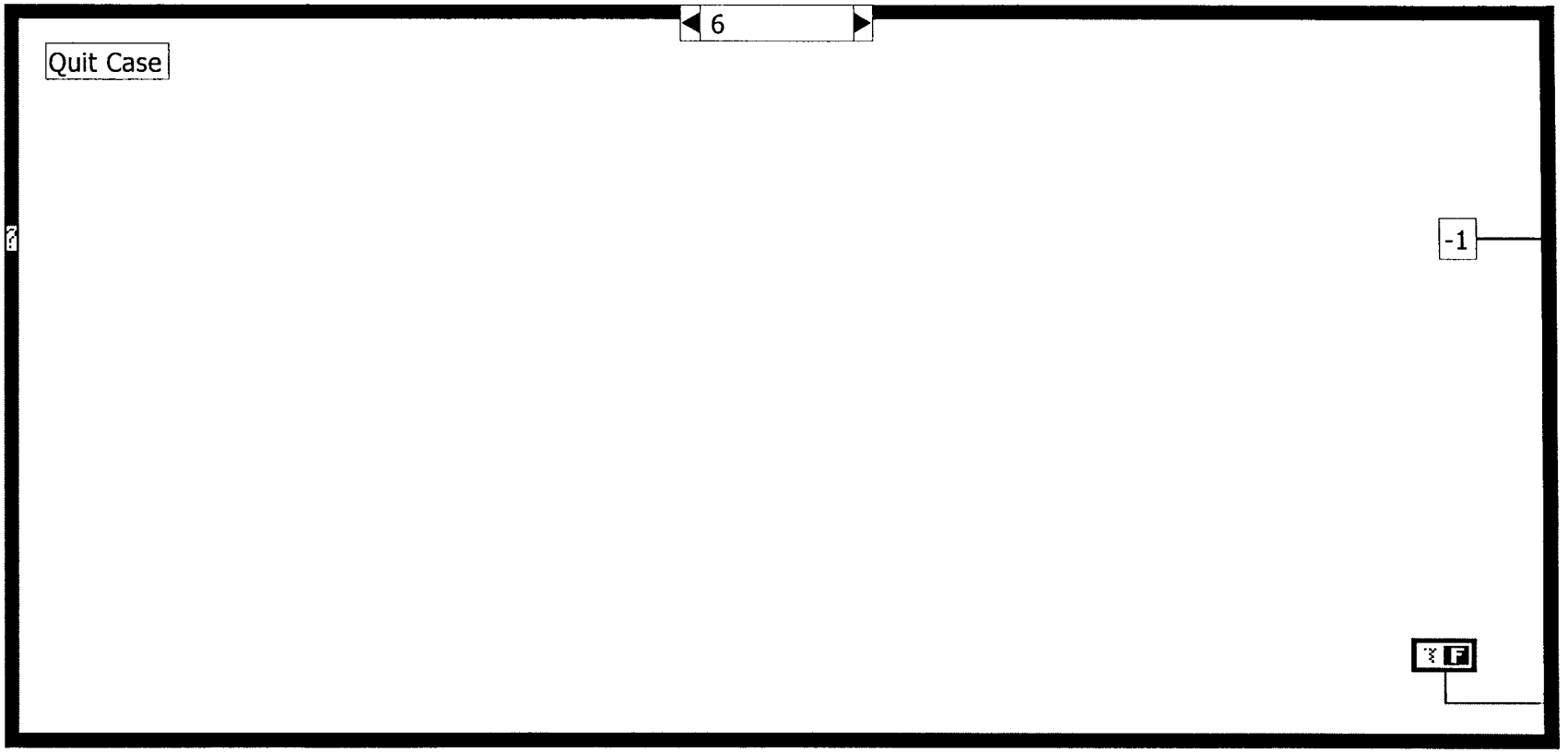

ressure Taps (Mod 6a).vi
C:\HIFOIL\Static Press Taps\Phase III\VIs\Pressure Taps (Mod 6a).vi
ast modified on 11/5/2001 at 11:53 AM
rinted on 11/5/2001 at 12:03 PM

Connector Pane

Pressure Taps (Mod 6a).vi

ront Panel

Static Pressure Taps- DAQ System

Data Aquisition

Number of Samples: 15000.00
Number of Channels: 30.00
Take Data
Current Channel: 1
Taking Data
Epsilon value: 1.00
Scan Rate (scans/s): 1000.00
Low Pressure Limit (psi): 0.09
Stop all DAQ
Done
Error

High Pressure Transducer (+/- 36 psi)

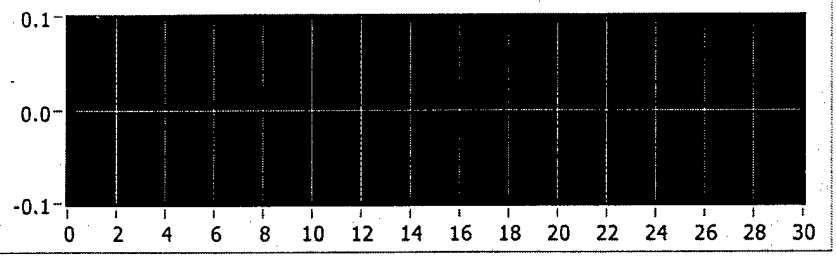

Low Pressure Transducer (+/- 1 psi)

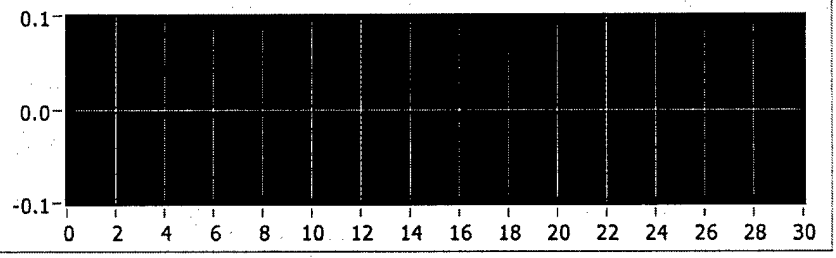

Output Data

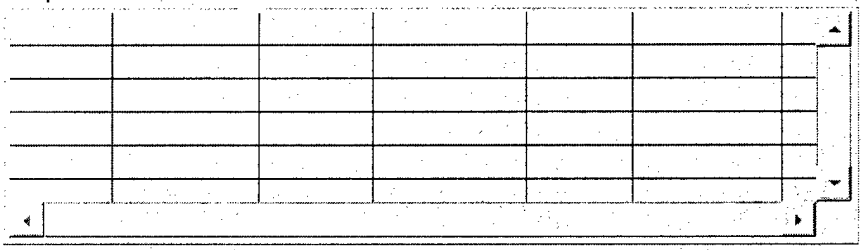

Ready to Save
Save Data

Ranges:
A- 100, 2.5
B- 100, 10
C- 100, 25
D- 700, 10
E- 700, 25

Complete this information before saving data

File Name (.txt): *.txt
Date (DDMMMYYYY): *2001
Time (24 hr):
Flow Speed (m/s):
Transducer Range:
Tunnel Pressure (psi):
Water Temp (Celcius):
Comments:
New File Path: C:\HIFOIL\Static Press Taps\

ressure Taps (Mod 6a).vi
C:\HIFOIL\Static Press Taps\Phase III\VIs\Pressure Taps (Mod 6a).vi
ast modified on 11/5/2001 at 11:53 AM
rinted on 11/5/2001 at 12:04 PM

Block Diagram

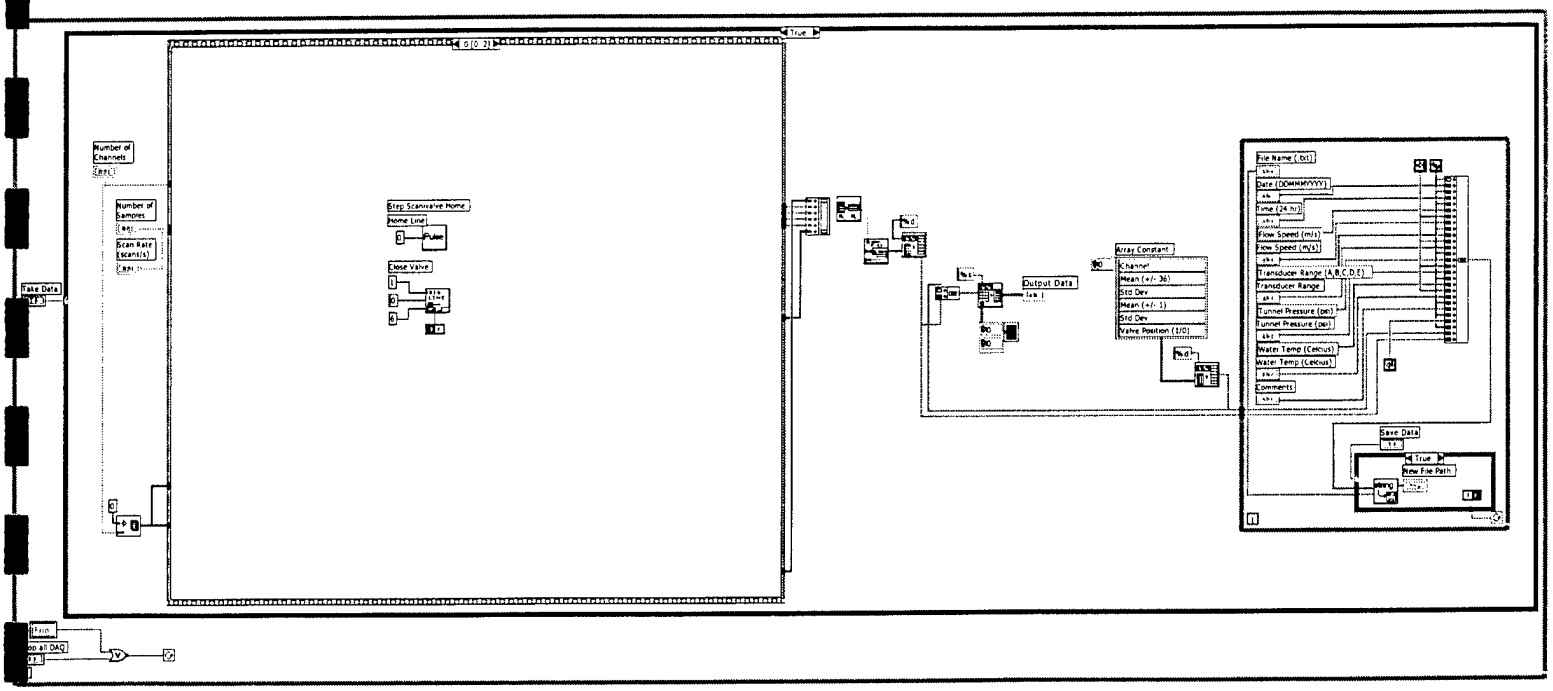

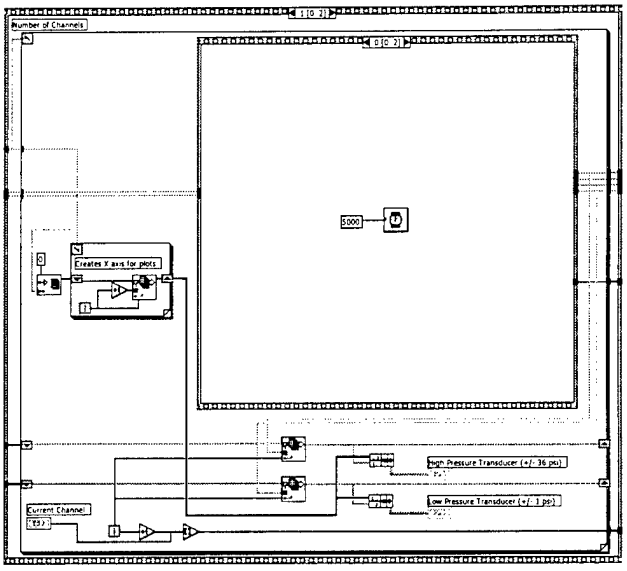

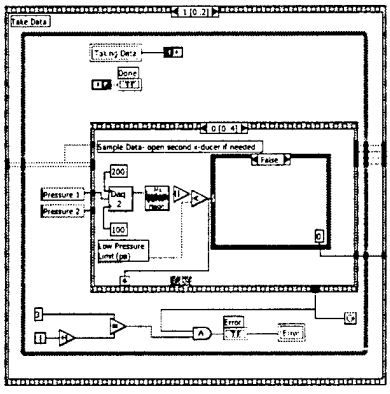

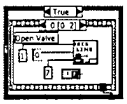

ressure Taps (Mod 6a).vi
C:\HIFOIL\Static Press Taps\Phase III\VIs\Pressure Taps (Mod 6a).vi
Last modified on 11/5/2001 at 11:53 AM
Printed on 11/5/2001 at 12:04 PM

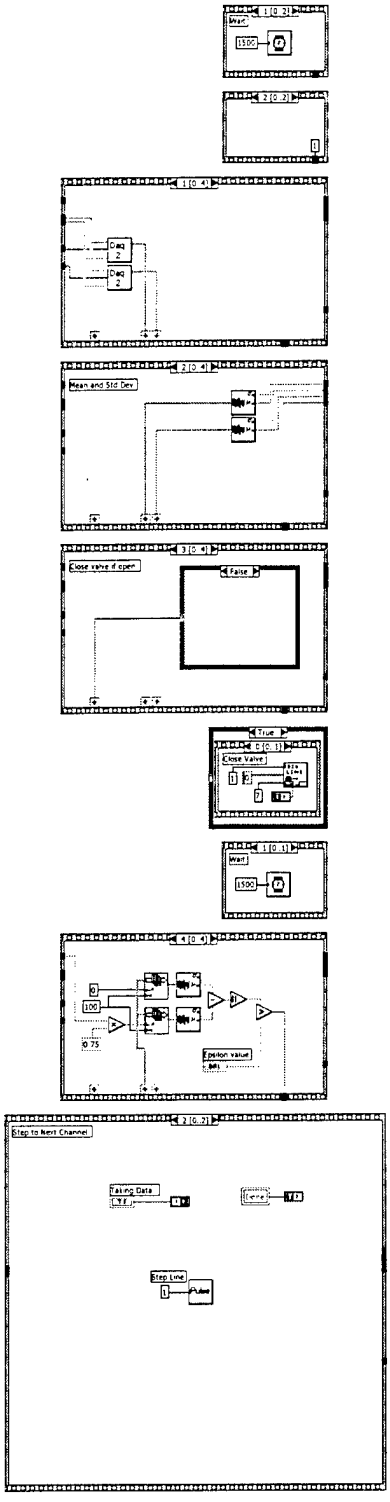

ressure Taps (Mod 6a).vi
C:\HIFOIL\Static Press Taps\Phase III\VIs\Pressure Taps (Mod 6a).vi
ast modified on 11/5/2001 at 11:53 AM
rinted on 11/5/2001 at 12:04 PM

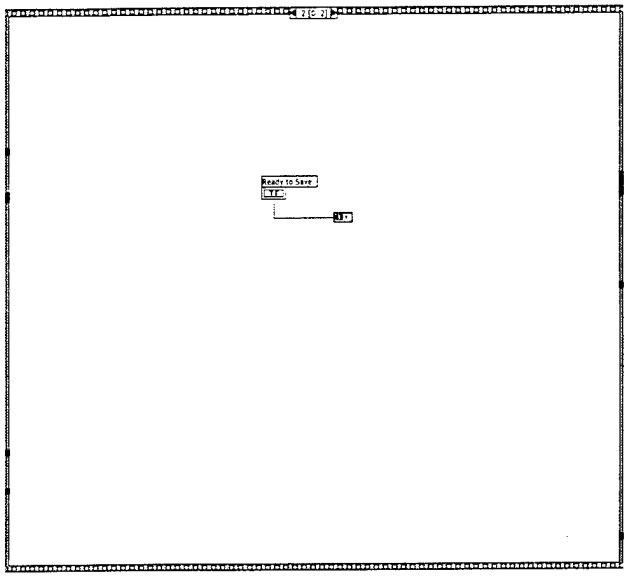

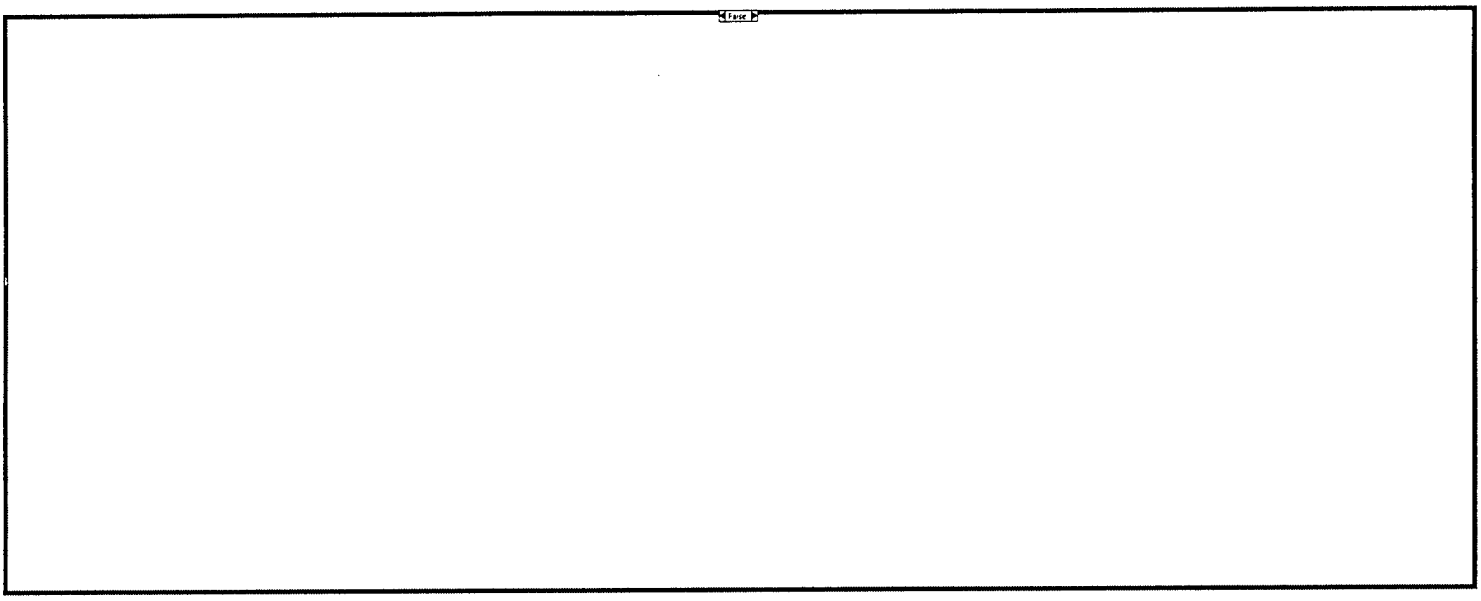

ressure Taps (Mod 6b).vi
C:\HIFOIL\Static Press Taps\Phase III\VIs\Pressure Taps (Mod 6b).vi
ast modified on 11/5/2001 at 11:54 AM
rinted on 11/5/2001 at 11:54 AM

Connector Pane

Pressure Taps (Mod 6b).vi

ront Panel

Static Pressure Taps- DAQ System

Data Aquisition

Number of Samples: 10000.00
Number of Channels: 30.00
Begin DAQ
Scan Rate (scans/s): 1000.00
Low Pressure Limit (psi): 0.36
Stop all DAQ

Current Channel: 1
Next Channel: 2
Channel Feedback
Step Scanivalve
Take Data Point
Ready
Working

Epsilon: 1.00
Error

+/- 36 psi

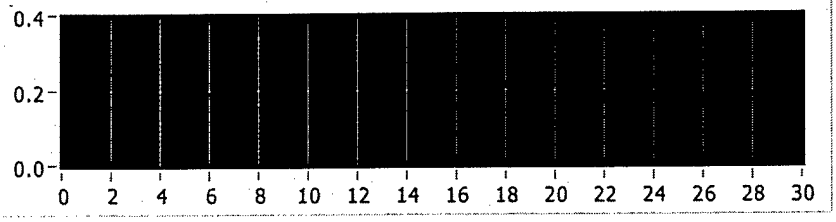

+/- 1 psi

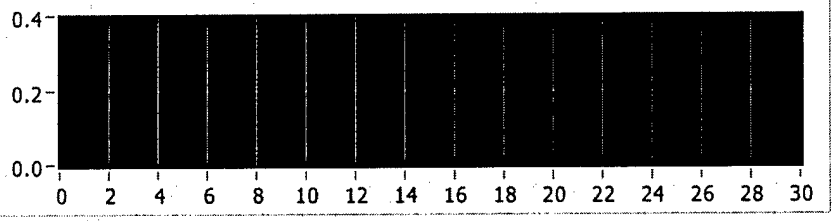

Output Data

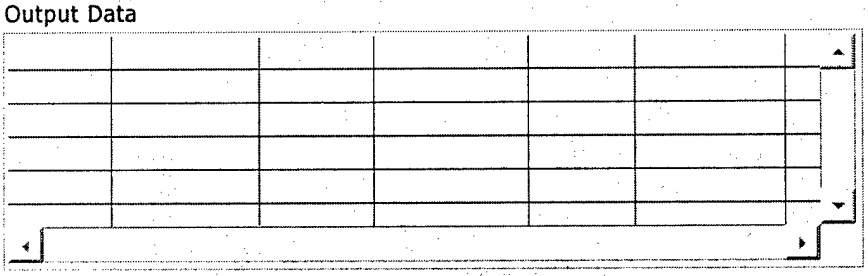

Save Data

Complete this information before saving data

File Name (.txt): *.txt
Date (DDMMMYYYY): *2001
Time (24 hr)
Flow Speed (m/s)
Transducer Range
Tunnel Pressure (psi)
Water Temp (Celcius)
Comments
New File Path: C:\HIFOIL\Static Press Taps\

ressure Taps (Mod 6b).vi
C:\HIFOIL\Static Press Taps\Phase III\VIs\Pressure Taps (Mod 6b).vi
ast modified on 11/5/2001 at 11:54 AM
rinted on 11/5/2001 at 11:54 AM

Block Diagram

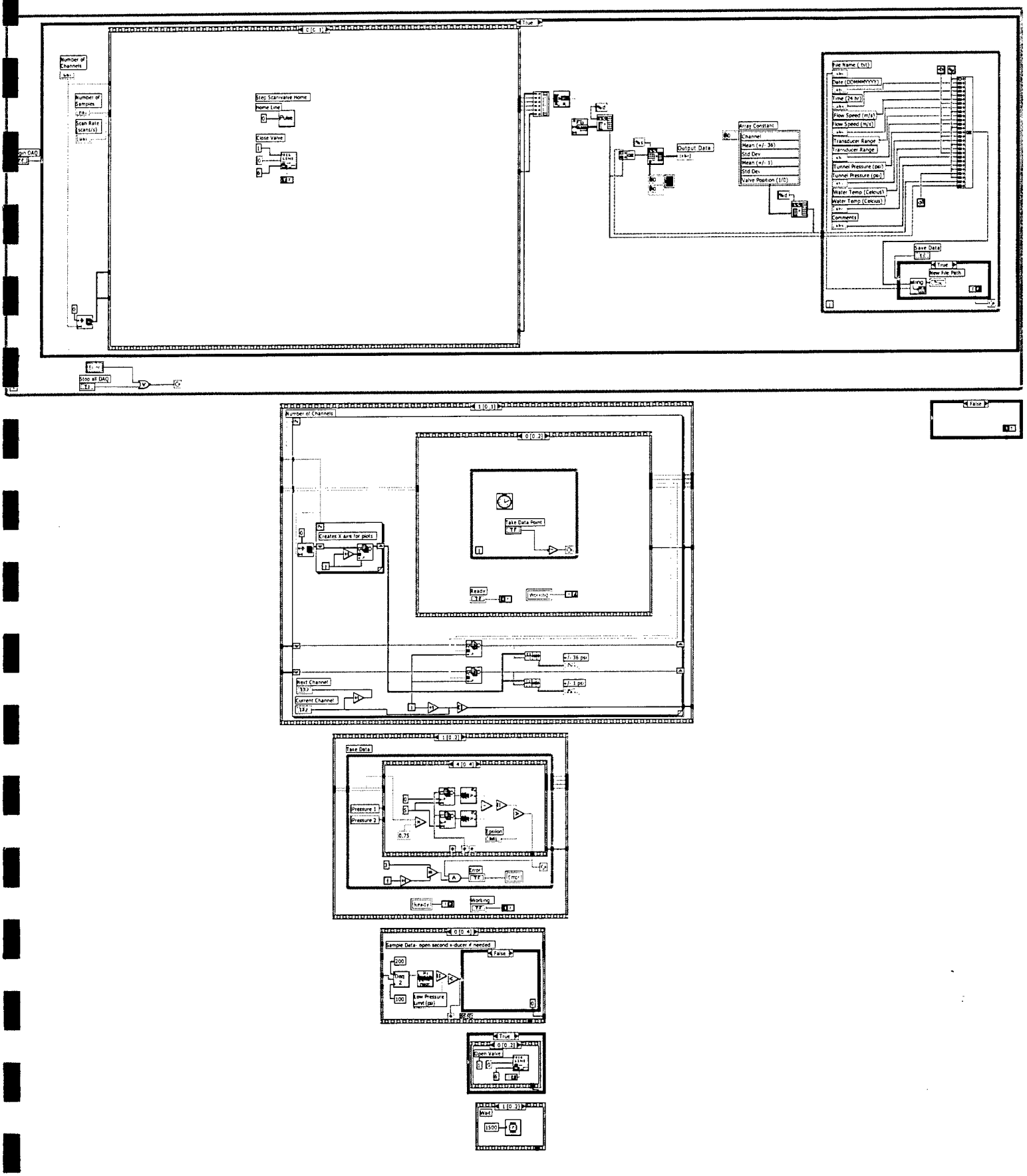

ressure Taps (Mod 6b).vi
C:\HIFOIL\Static Press Taps\Phase III\VIs\Pressure Taps (Mod 6b).vi
ast modified on 11/5/2001 at 11:54 AM
rinted on 11/5/2001 at 11:54 AM

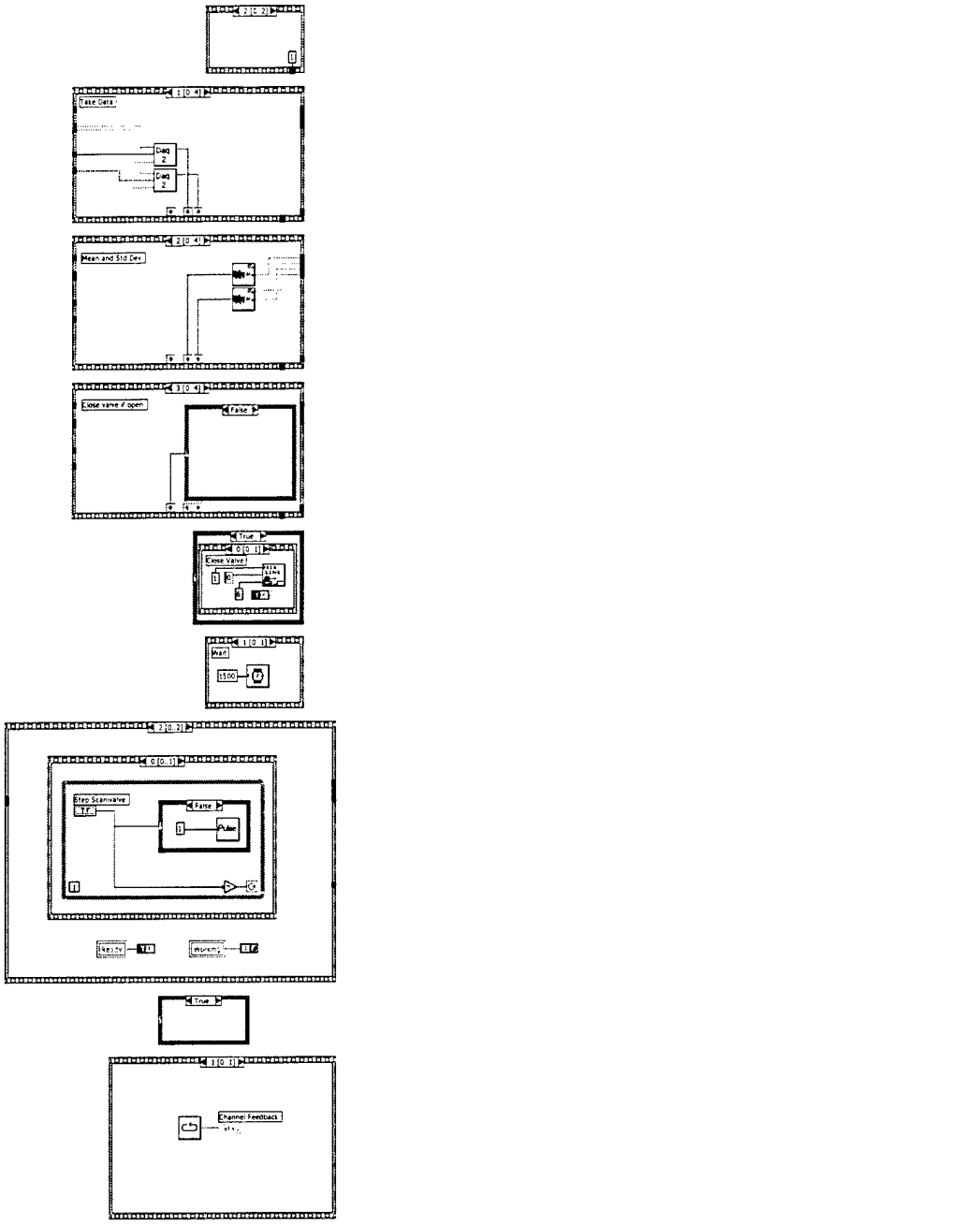

ressure Taps (Mod 6c).vi
C:\HIFOIL\Static Press Taps\Phase III\VIs\Pressure Taps (Mod 6c).vi
ast modified on 11/5/2001 at 11:55 AM
rinted on 11/5/2001 at 11:55 AM

Connector Pane

Pressure Taps (Mod 6c).vi

ront Panel

Static Pressure Taps- DAQ System

Data Aquisition

Number of Samples: 10000.00
Number of Channels: 30.00
Begin DAQ
Scan Rate (scans/s): 1000.00
Low Pressure Limit (psi): 0.09
Stop all DAQ

Current Channel: 1
Take Data Point
Next Channel: 2
Ready
Working

Epsilon: 1.00
Error

+/- 36 psi

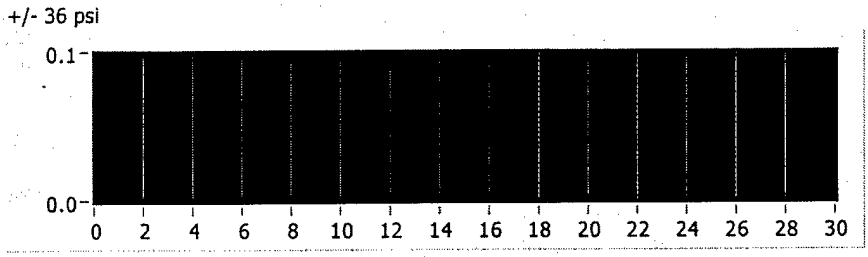

+/- 1 psi

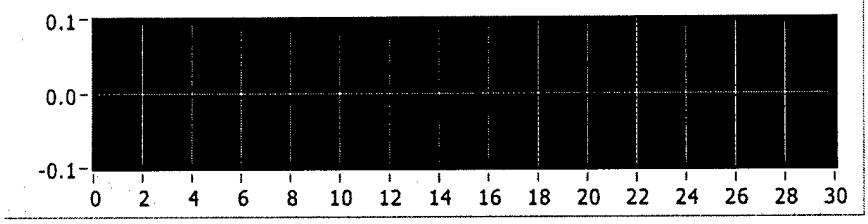

Output Data

Save Data

Complete this information before saving data

File Name (.txt): *.txt
Date (DDMMMYYYY): *2001
Time (24 hr):
Flow Speed (m/s):
Transducer Range:
Tunnel Pressure (psi):
Water Temp (Celcius):
Comments:
New File Path: C:\HIFOIL\Static Press Taps\

ressure Taps (Mod 6c).vi
C:\HIFOIL\Static Press Taps\Phase III\VIs\Pressure Taps (Mod 6c).vi
ast modified on 11/5/2001 at 11:55 AM
rinted on 11/5/2001 at 11:55 AM

Block Diagram

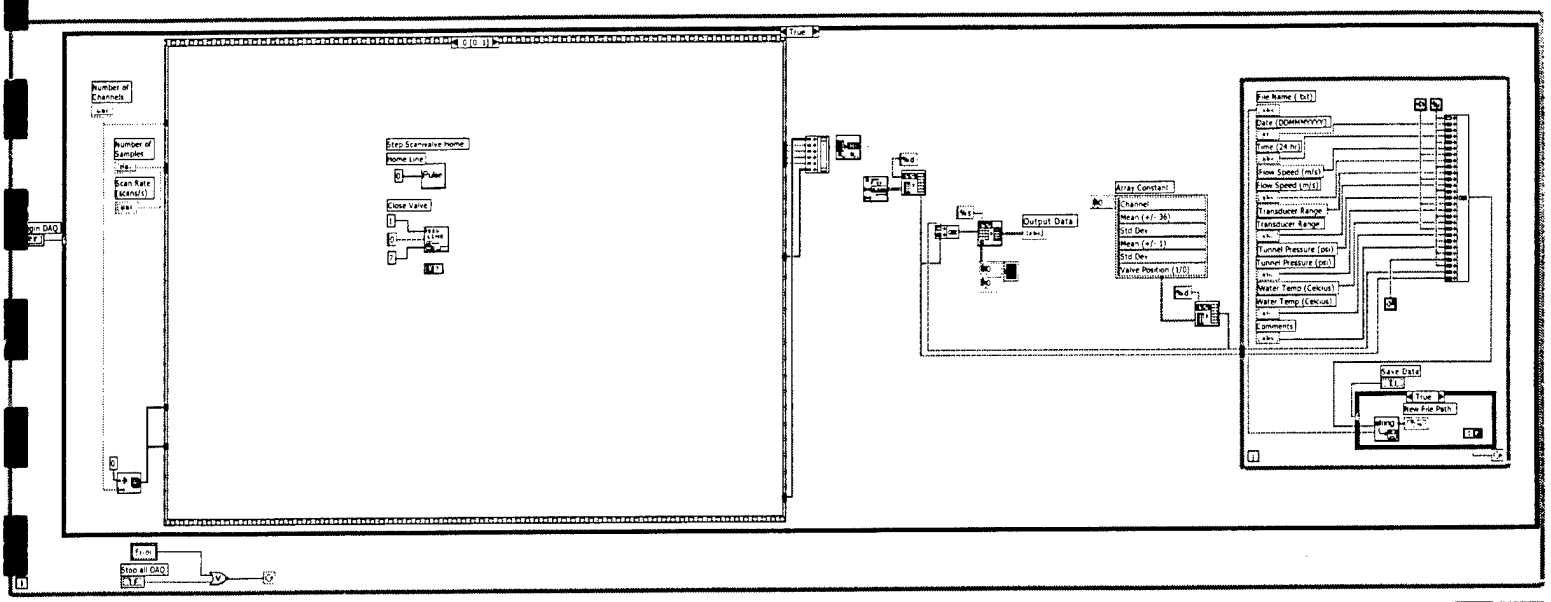

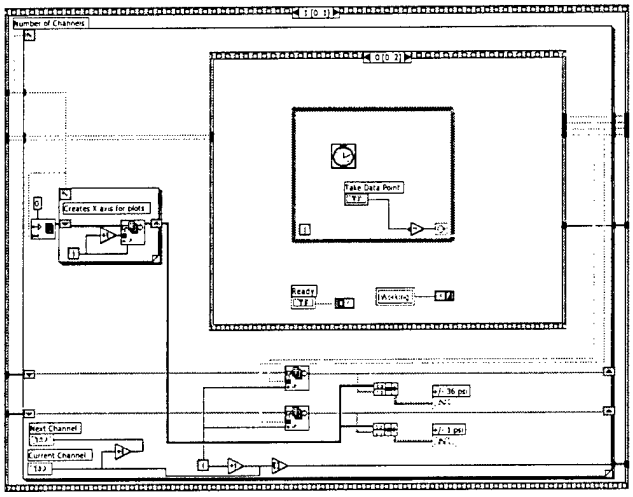

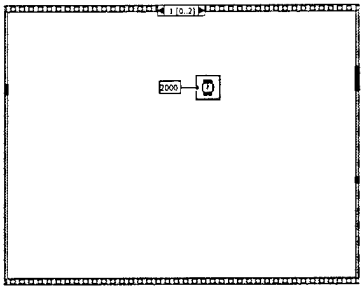

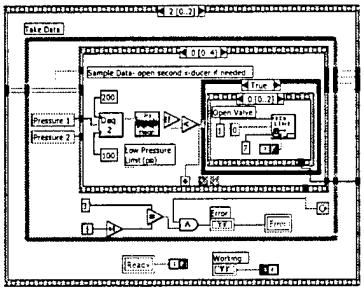

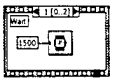

ressure Taps (Mod 6c).vi
C:\HIFOIL\Static Press Taps\Phase III\VIs\Pressure Taps (Mod 6c).vi
ast modified on 11/5/2001 at 11:55 AM
rinted on 11/5/2001 at 11:55 AM

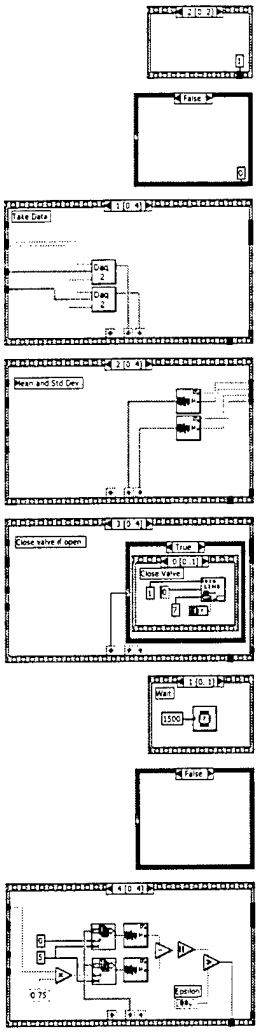

alibration (mod 3).vi
C:\HIFOIL\Static Press Taps\Phase III\VIs\Calibration (mod 3).vi
ast modified on 11/5/2001 at 12:00 PM
rinted on 11/5/2001 at 12:01 PM

Connector Pane

Calibration (mod 3).vi

alibration (mod 3).vi
C:\HIFOIL\Static Press Taps\Phase III\VIs\Calibration (mod 3).vi
ast modified on 11/5/2001 at 12:00 PM
rinted on 11/5/2001 at 12:01 PM

Front Panel

Transducer Calibration

Transducer Name: 1

Samples: 3000.00

Scan Rate: 1000.00

DAQ Channel
0- Transducer 1
1- Transducer 2
0

Output Data

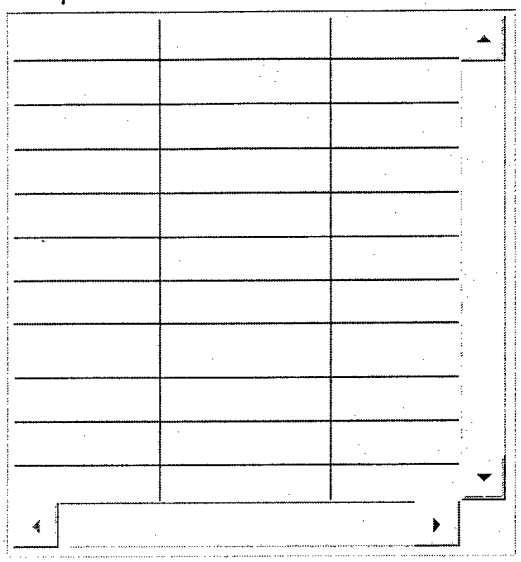

Slope (psi/volt): 0.00

Intercept: 0.0000

Save Calibration File

Calibration File Name: cRange*-*Aug.txt

New File Path: C:\HIFOIL\Static Press Taps\

Input indicated pressure and push button to record each individual data point.

11 total data points:
-5 with pressure on positive port
-1 with no pressure applied
-5 with pressure on negative port

Stop Calibration

Working

Calibration Complete

		Pressure (psi)	Mean Volts	Std Dev	Done
Positive	Point 1	0.00	0.00	0.00	
	Point 2	0.00	0.00	0.00	
	Point 3	0.00	0.00	0.00	
	Point 4	0.00	0.00	0.00	
	Point 5	0.00	0.00	0.00	
Zero Point	Point 6	0.00	0.00	0.00	
Negative	Point 7	0.00	0.00	0.00	
	Point 8	0.00	0.00	0.00	
	Point 9	0.00	0.00	0.00	
	Point 10	0.00	0.00	0.00	
	Point 11	0.00	0.00	0.00	

When all 11 points have been taken, the data can be viewed in the chart on the left and then saved to disk.

alibration (mod 3).vi
C:\HIFOIL\Static Press Taps\Phase III\VIs\Calibration (mod 3).vi
ast modified on 11/5/2001 at 12:00 PM
rinted on 11/5/2001 at 12:01 PM

Block Diagram

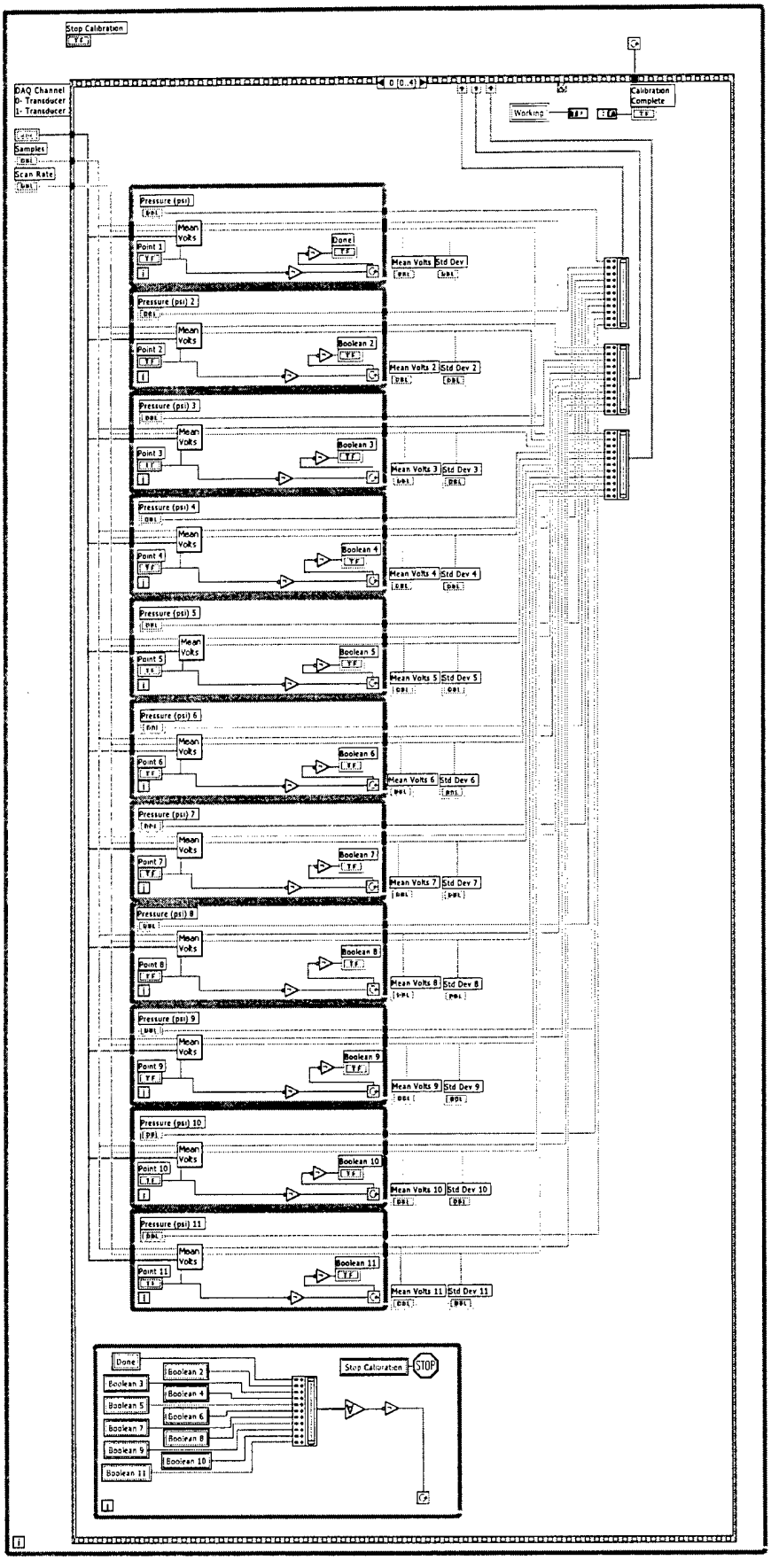

alibration (mod 3).vi
C:\HIFOIL\Static Press Taps\Phase III\VIs\Calibration (mod 3).vi
ast modified on 11/5/2001 at 12:00 PM
rinted on 11/5/2001 at 12:01 PM

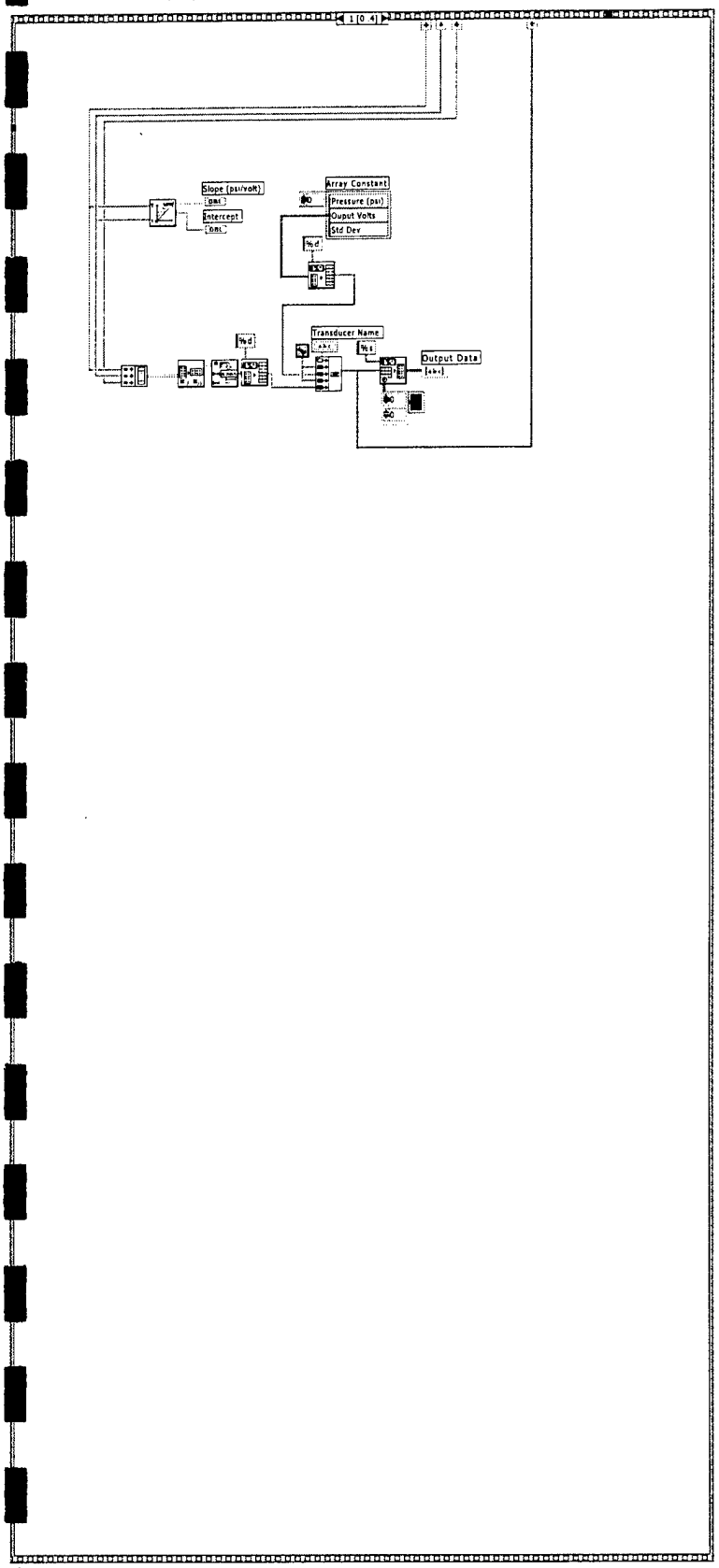

alibration (mod 3).vi
C:\HIFOIL\Static Press Taps\Phase III\VIs\Calibration (mod 3).vi
ast modified on 11/5/2001 at 12:00 PM
rinted on 11/5/2001 at 12:01 PM

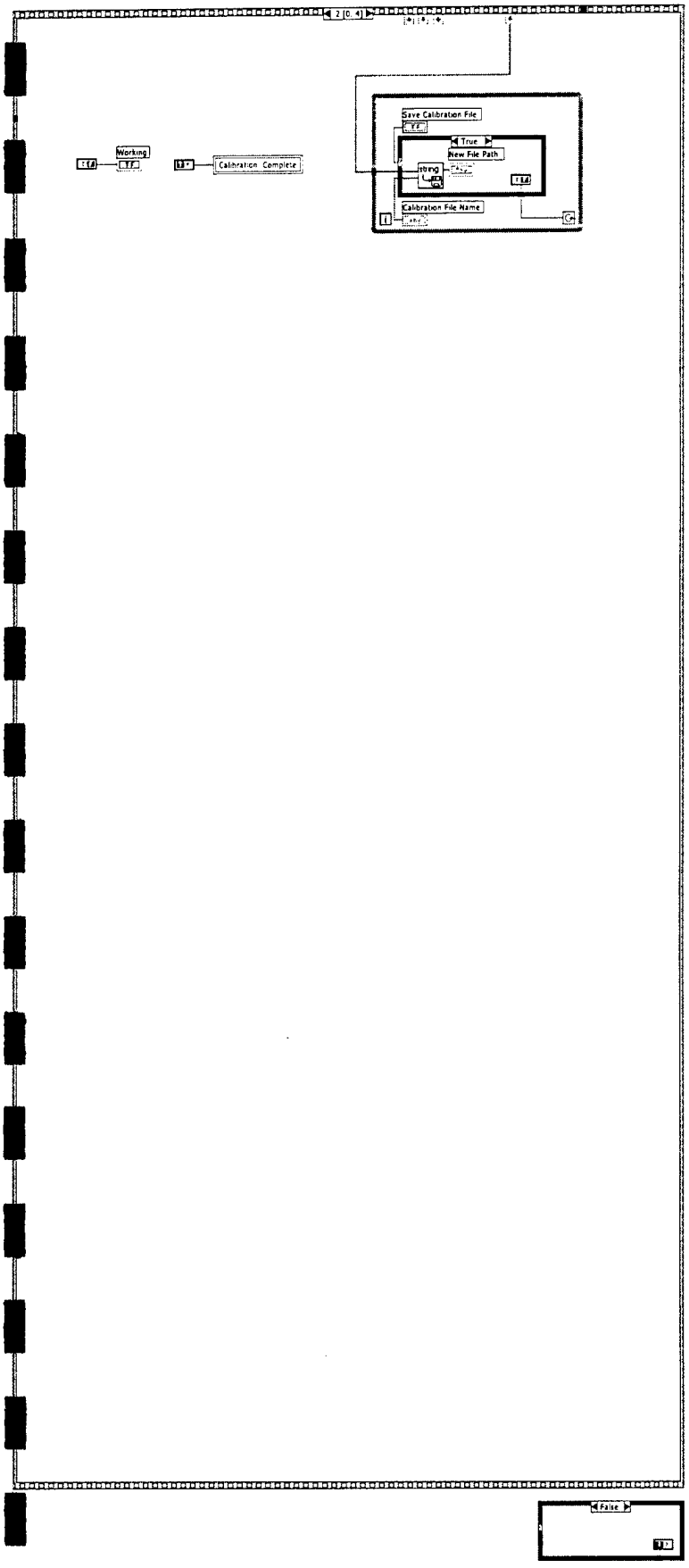

alibration (mod 3).vi
C:\HIFOIL\Static Press Taps\Phase III\VIs\Calibration (mod 3).vi
ast modified on 11/5/2001 at 12:00 PM
rinted on 11/5/2001 at 12:01 PM

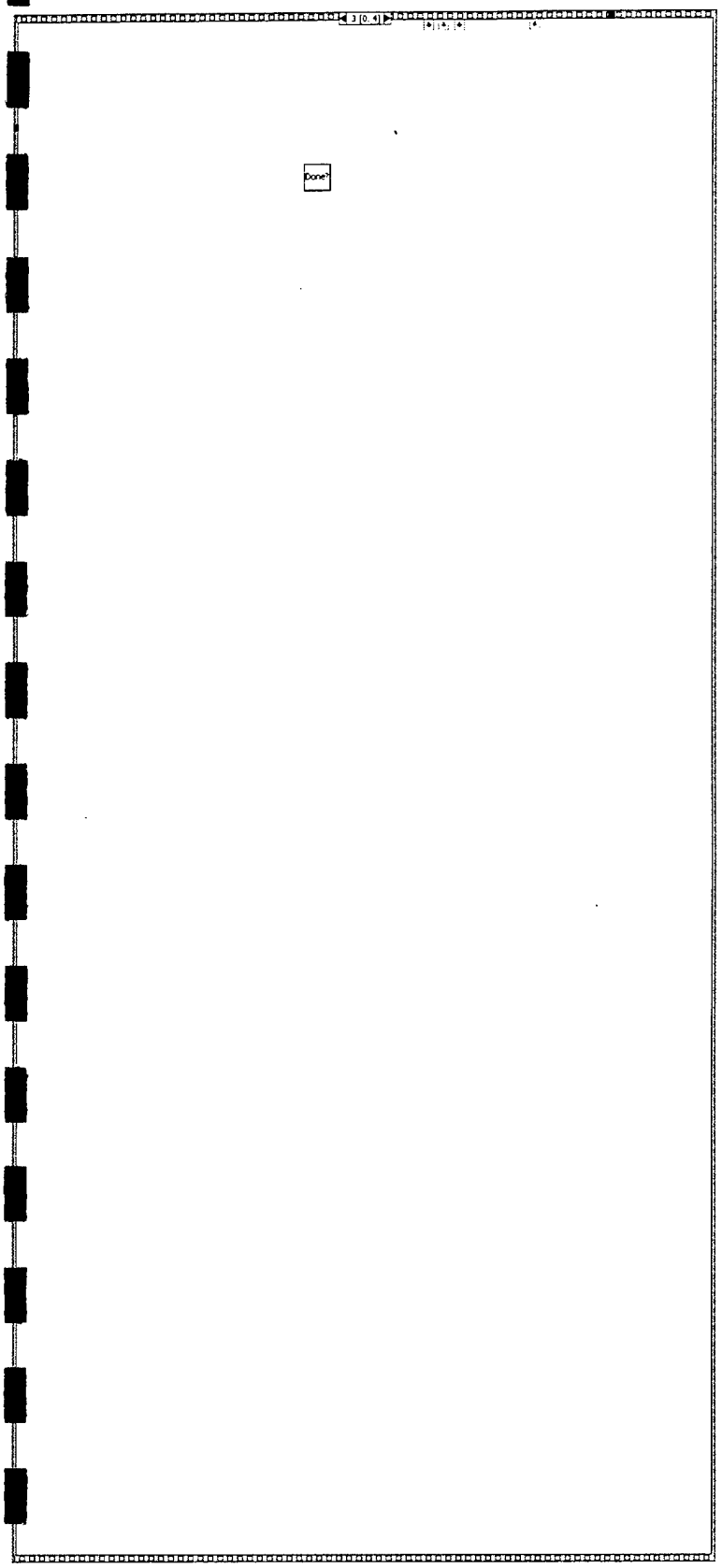

alibration (mod 3).vi
C:\HIFOIL\Static Press Taps\Phase III\VIs\Calibration (mod 3).vi
ast modified on 11/5/2001 at 12:00 PM
rinted on 11/5/2001 at 12:01 PM

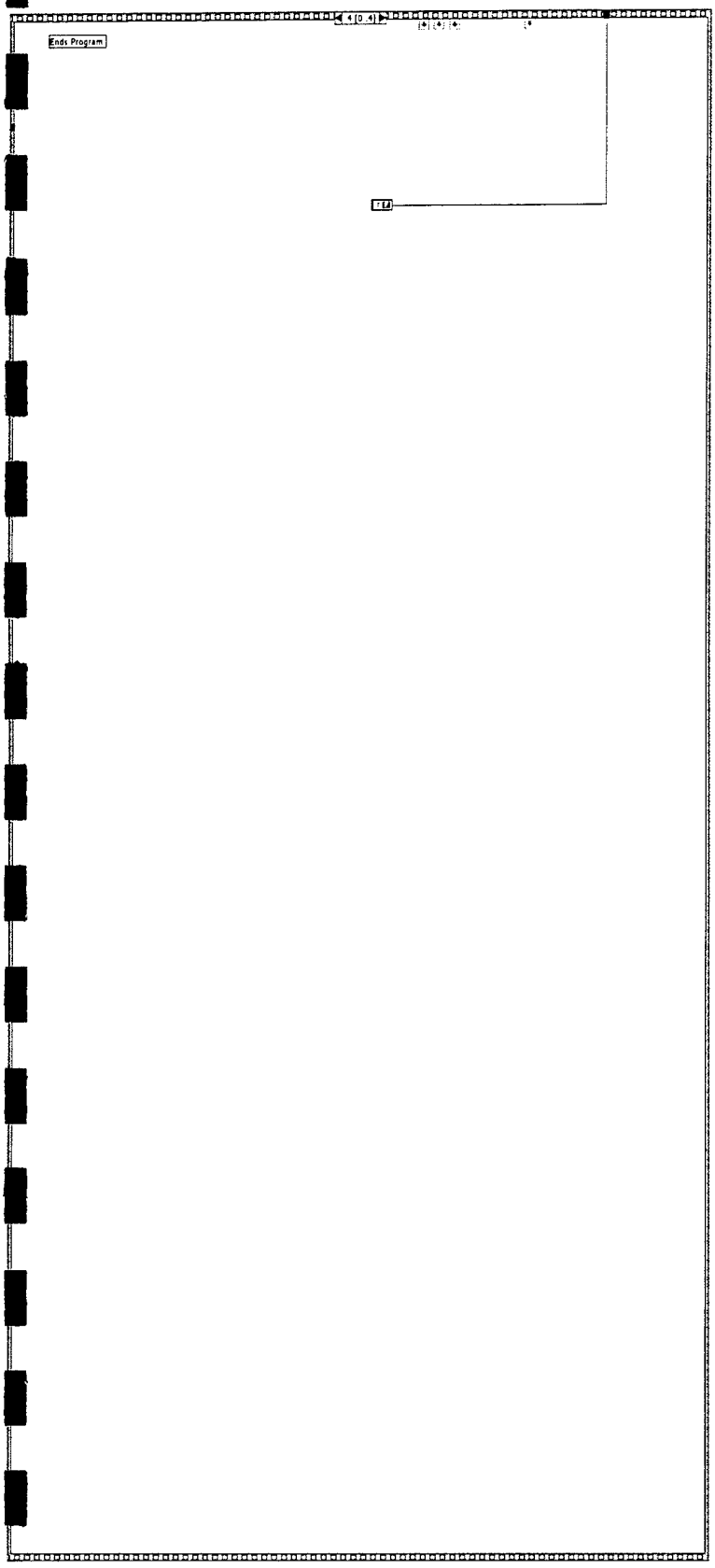

tatic Pressure Sampling.vi
C:\HIFOIL\Static Press Taps\Phase III\VIs\Static Pressure Sampling.vi
ast modified on 11/5/2001 at 11:55 AM
rinted on 11/5/2001 at 11:56 AM

Connector Pane

Static Pressure Sampling.vi

ront Panel

Static Pressure Taps- DAQ System

Data Sampling

Take Sample Data

Stop Sampling

Valve

Down- Close
Up- Open

Home

Step

Transducer Output (psi)

30
25
20
15
10
5
0
-5

0 1 2 3 4 5 6 7 8 9 10

Numerical Output

Stop all DAQ

Channel:
+/-36 psi - Pressure 1
+/-1 psi - Pressure 2

Pressure 1, Pressure 2

tatic Pressure Sampling.vi
C:\HIFOIL\Static Press Taps\Phase III\VIs\Static Pressure Sampling.vi
ast modified on 11/5/2001 at 11:55 AM
rinted on 11/5/2001 at 11:56 AM

Block Diagram

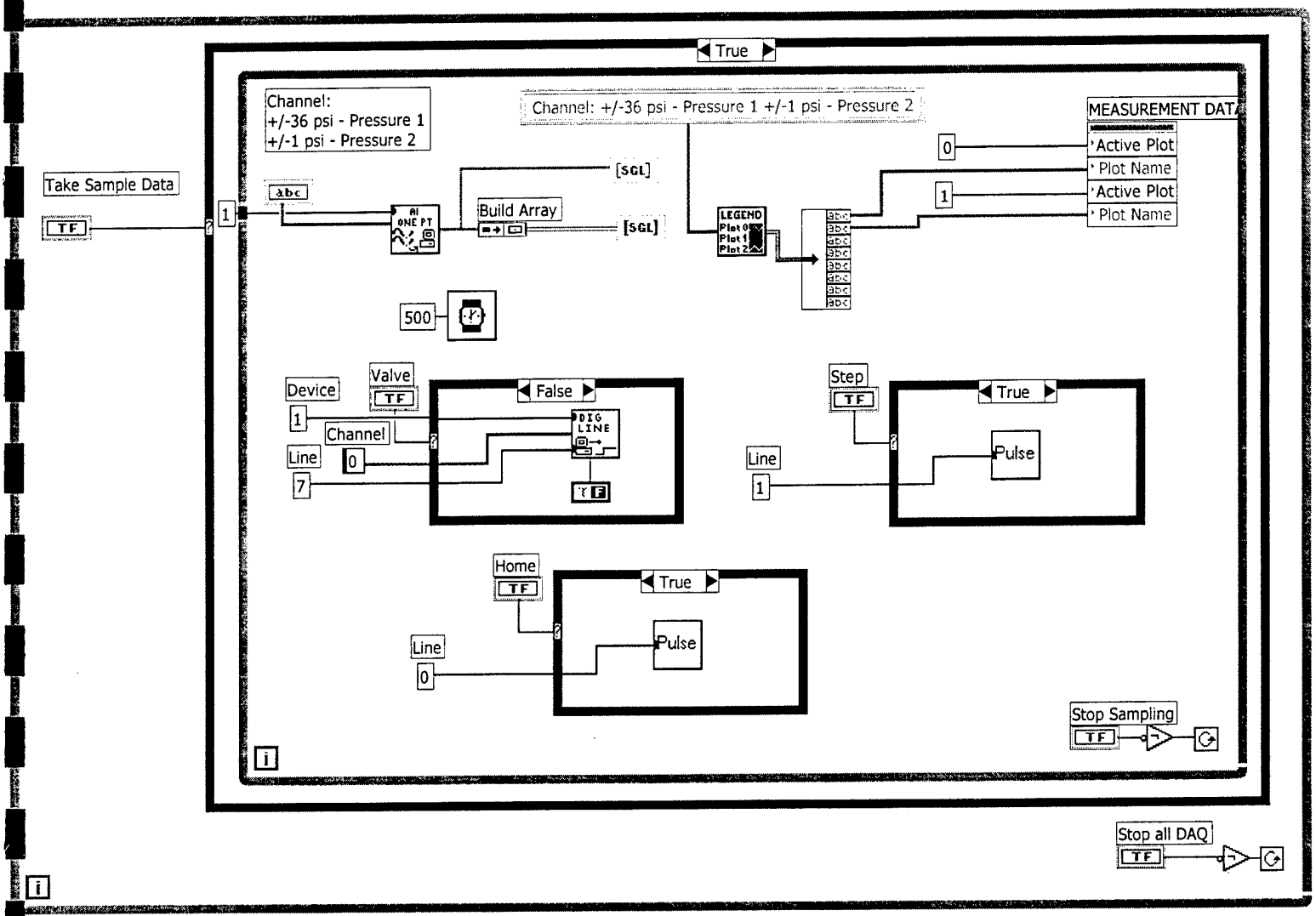

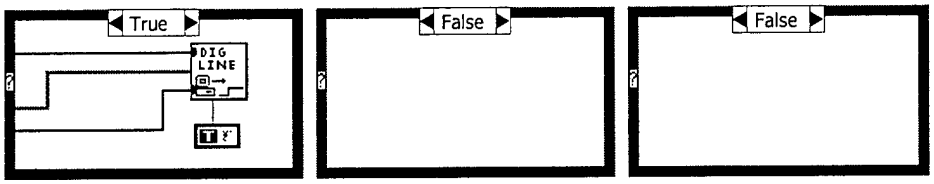

tatic Pressure Sampling.vi
C:\HIFOIL\Static Press Taps\Phase III\VIs\Static Pressure Sampling.vi
ast modified on 11/5/2001 at 11:55 AM
rinted on 11/5/2001 at 11:56 AM

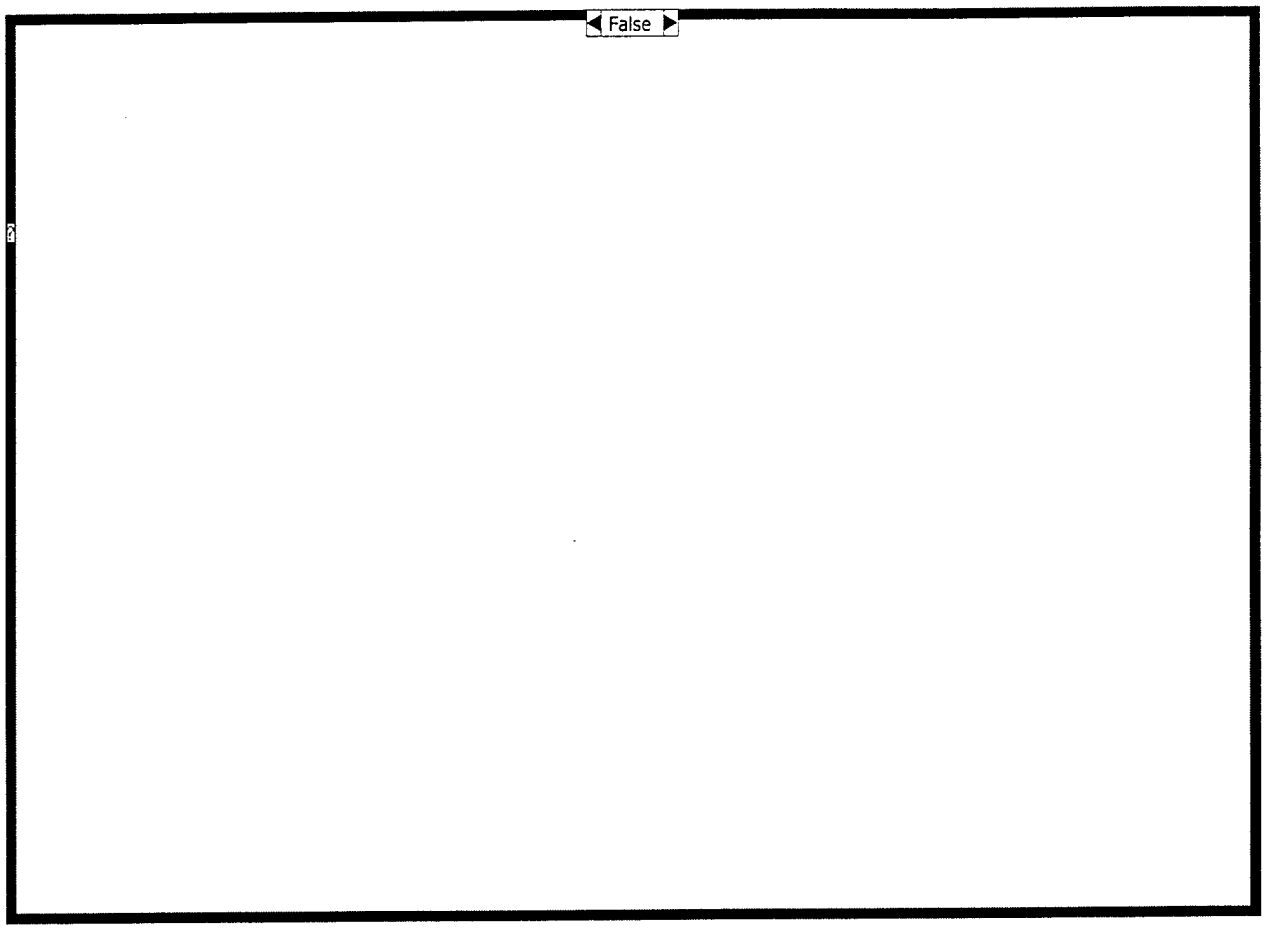

Appendix F: Matlab Code

Attached is a printout of the Matlab m-file entitled SPprocessing.m. This program was developed to process, correct and plot the static pressure data collected during the Hifoil project. All data contained in this document was processed using this code. This program used a log file entitled SP_log.txt to keep track of the entire set of static pressure data files. This log file is located in appendix G

```
%add needed file paths
addpath('C:\JHamel\Hifoil\Phase III\SP Post Processing Fall 2001');
addpath('C:\JHamel\Hifoil\Phase III\SP Post Processing Fall 2001\Data');
addpath('C:\JHamel\Hifoil\Phase III\SP Post Processing Fall 2001\Data\No
Flow Data');
%addpath('C:\HIFOIL\Static Press Taps\SP Post Processing Fall 2001');
%addpath('C:\HIFOIL\Static Press Taps\SP Post Processing Fall 2001
\Data');
%addpath('C:\HIFOIL\Static Press Taps\SP Post Processing Fall 2001\Data
\No Flow Data');

%file path for resulting data files
rpath='C:\JHamel\Hifoil\Phase III\SP Post Processing Fall 2001\Results
\';
%rpath='C:\HIFOIL\Static Press Taps\SP Post Processing Fall 2001\Results
\';

%specify number format
format long g

%set dx/c step size for all calcs
s=0.005; %0.0001;

%read log file
[infile,U,aoa,te,err1,err2,rho,nu,Re,noflow,outfile1,outfile2,runid,ff,o
ld,cal,T]=textread('SP_Log.txt','%s %f %d %d %f %f %f %f %f %s %s %s %s
%f %d %d %f','headerlines',1);

%read x/c and tap data
[xc0,yc0,xcn1,ycn1,xcp1,ycp1,hd,bcp0,bcp02,bcpn1,bcpp1]=textread
('x_c.txt','%f %f %f %f %f %f %f %f %f %f %f','headerlines',2);

%create output file for cld data
cldfile1=strcat(rpath,'cld0.txt');
fid1=fopen(cldfile1,'w');
fprintf(fid1,'Variables="Re_C"\r\n');
fprintf(fid1,'"TE"\r\n');
fprintf(fid1,'"AOA"\r\n');
fprintf(fid1,'"C_L"\r\n');
fprintf(fid1,'"err-C_L"\r\n');
fprintf(fid1,'"C_D"\r\n');
fprintf(fid1,'"err-C_D"\r\n');
fprintf(fid1,'Zone\r\n');
fprintf(fid1,'T="TE 0 AOA 0^o"\r\n');

cldfile2=strcat(rpath,'cld0m.txt');
fid2=fopen(cldfile2,'w');
fprintf(fid2,'Variables="Re_C"\r\n');
fprintf(fid2,'"TE"\r\n');
fprintf(fid2,'"AOA"\r\n');
fprintf(fid2,'"C_L"\r\n');
fprintf(fid2,'"err-C_L"\r\n');
fprintf(fid2,'"C_D"\r\n');
fprintf(fid2,'"err-C_D"\r\n');
fprintf(fid2,'Zone\r\n');
fprintf(fid2,'T="TE 2 AOA 0^o"\r\n');

cldfile3=strcat(rpath,'cldn1.txt');
fid3=fopen(cldfile3,'w');
fprintf(fid3,'Variables="Re_C"\r\n');
fprintf(fid3,'"TE"\r\n');
```

```
fprintf(fid3,'"AOA"\r\n');
fprintf(fid3,'"C_L"\r\n');
fprintf(fid3,'"err-C_L"\r\n');
fprintf(fid3,'"C_D"\r\n');
fprintf(fid3,'"err-C_D"\r\n');
fprintf(fid3,'Zone\r\n');
fprintf(fid3,'T="TE 0 AOA -1^o"\r\n');

cldfile4=strcat(rpath,'cldp1.txt');
fid4=fopen(cldfile4,'w');
fprintf(fid4,'Variables="Re_C"\r\n');
fprintf(fid4,'"TE"\r\n');
fprintf(fid4,'"AOA"\r\n');
fprintf(fid4,'"C_L"\r\n');
fprintf(fid4,'"err-C_L"\r\n');
fprintf(fid4,'"C_D"\r\n');
fprintf(fid4,'"err-C_D"\r\n');
fprintf(fid4,'Zone\r\n');
fprintf(fid4,'T="TE 0 AOA +1^o"\r\n');

deltafile=strcat(rpath,'delta.plt');
fid5=fopen(deltafile,'w');
fprintf(fid5,'Variables="i"\r\n');
fprintf(fid5,'"U"\r\n');
fprintf(fid5,'"AOA"\r\n');
fprintf(fid5,'"TE"\r\n');
fprintf(fid5,'"T"\r\n');
fprintf(fid5,'"Re_C"\r\n');
fprintf(fid5,'"Calibration"\r\n');
fprintf(fid5,'"dC_P"\r\n');
fprintf(fid5,'"dP"\r\n');

errfile=strcat(rpath,'err.txt');
fid6=fopen(errfile,'w');
fprintf(fid6,'Variables="i"\r\n');
fprintf(fid6,'"U"\r\n');
fprintf(fid6,'"AOA"\r\n');
fprintf(fid6,'"TE"\r\n');
fprintf(fid6,'"Re_C"\r\n');
fprintf(fid6,'"Max C_P"\r\n');
fprintf(fid6,'"Max P"\r\n');
fprintf(fid6,'"Max C_P-err"\r\n');
fprintf(fid6,'"Max P-err"\r\n');

clear cldfile1 cldfile2 cldfile3 cldfile4 deltafile errfile

%main computation loop
[d1,d2]=size(infile);
for i=1:d1
   clear infilei noflowi outfile1i outfile2i runidi tap td1 std1 td2
std2 valve ntap ntd1 nstd1 ntd2 nstd2
   clear nvalve offset1 offset2 cp1 cp2 tau Rd he cperr1 cperr2 cpstd1
cpstd2 eb1 eb2 discrete cp eb
   %load data file
   infilei=char(infile(i));
   noflowi=char(noflow(i));
   outfile1i=strcat(rpath,char(outfile1(i)));
   outfile2i=strcat(rpath,char(outfile2(i)));
   runidi=char(runid(i));

   if old(i)==1
```

```
      [tap,td1,std1,td2,std2,valve]=textread(infilei,'%f %f %f %f %f %
d','headerlines',10);
   else
      [tap,td1,std1,td2,std2,valve]=textread(infilei,'%f %f %f %f %f %
f','headerlines',11);
   end
   %correct pressures with noflow file
   if old(i)==1
      [ntap,ntd1,nstd1,ntd2,nstd2,nvalve]=textread(noflowi,'%f %f %f %f
%f %d','headerlines',10);
   else
      [ntap,ntd1,nstd1,ntd2,nstd2,nvalve]=textread(noflowi,'%f %f %f %f
%f %f','headerlines',11);
   end
   offset1=mean(ntd1);
   offset2=mean(ntd2);
   td1=td1-offset1;
   td2=td2-offset2;
   %convert pressures to Cp
   cp1=(td1*(101327/14.7))/(0.5*rho(i)*U(i)^2);
   cp2=(td2*(101327/14.7))/(0.5*rho(i)*U(i)^2);
   %hole error calculations
   tau=0.5*rho(i)*U(i)^2*0.002;
   Rd=(sqrt(tau/rho(i))*hd)/nu(i);
   if Rd<=385
      he=(tau*0.000157*Rd.^1.604)/(0.5*rho(i)*U(i)^2);
   else
      he=(tau*0.269*Rd.^0.353)/(0.5*rho(i)*U(i)^2);
   end
   %compute error bars
   cperr1=(err1(i)*(101327/14.7))/(0.5*rho(i)*U(i)^2);
   cperr2=(err2(i)*(101327/14.7))/(0.5*rho(i)*U(i)^2);
   cpstd1=(std1*(101327/14.7))/(0.5*rho(i)*U(i)^2);
   cpstd2=(std2*(101327/14.7))/(0.5*rho(i)*U(i)^2);
   eb1=sqrt(cpstd1.^2+cperr1^2+he.^2);
   eb2=sqrt(cpstd2.^2+cperr2^2+he.^2);
   for j=1:30
      if valve(j)==0
         cp2(j)=0;
         eb2(j)=0;
         cp(j)=cp1(j);
         eb(j)=eb1(j);
      else
         cp(j)=cp2(j);
         eb(j)=eb2(j);
      end
   end

   %fudge factor correction
   %cp=cp+ff(i);

   if aoa(i)==0
      if te(i)==0
         dcp=-cp-bcp0';
      else
         dcp=-cp-bcp02';
      end
   elseif aoa(i)==-1
      dcp=-cp-bcpn1';
   else
      dcp=-cp-bcpp1';
```

```
    end
    cpcorr=mean(dcp);
    cpc=cp+cpcorr;
    dpcorr=cpcorr*0.5*rho(i)*U(i)^2*14.7/101327;

    dout=[i;U(i);aoa(i);te(i);T(i);Re(i);cal(i);cpcorr';dpcorr'];
    fprintf(fid5,'%i %4.2f %d %d %5.2f %8.1f %d %6.5f %6.5f\r\n',dout);

    %output discrete Cp points
    discrete=[cp1';eb1';cp2';eb2';valve']';

    %write Cp data file
    cpdata=[xc0';yc0';-cp;-cpc;eb];
    fid=fopen(outfile1i,'w');
    fprintf(fid,'Variables="x/c"\r\n');
    fprintf(fid,'"y/c"\r\n');
    fprintf(fid,'"-Cp"\r\n');
    fprintf(fid,'"-Cp corr"\r\n');
    fprintf(fid,'"Err"\r\n');
    fprintf(fid,'Zone\r\n');
    fprintf(fid,'T="');
    fprintf(fid,runidi);
    fprintf(fid,'"\r\n');
    fprintf(fid,'%5.4f %5.4f %6.5f %6.5f %6.5f \r\n',cpdata);
    fclose(fid);

    maxerr=max(eb);
    maxerrp=maxerr*0.5*rho(i)*U(i)^2*14.7/101327;
    maxcp=max(cp);
    maxp=maxcp*0.5*rho(i)*U(i)^2*14.7/101327;

    errout=[i;U(i);aoa(i);te(i);Re(i);maxcp';maxp';maxerr';maxerrp'];
    fprintf(fid6,'%i %4.2f %d %d %8.1f %6.4f %6.4f %6.4f %6.4f\r
\n',errout);

    %decide AoA of data file, spline Cp data, compute CL
    if aoa(i)==0
       %0 degrees AoA
       xt=xc0(1):s:xc0(17);
       xb=xc0(30):s:xc0(18);
       yc=0:s:0.08002;
       xct=xc0([1:17]);
       xcb=xc0([18:30]);
       cpt=cp([1:17]);
       errt=eb([1:17]);
       cpt_high=cpt-errt;
       cpt_low=cpt+errt;
       cpb=cp([18:30]);
       errb=eb([18:30]);
       cpb_high=cpb+errb;
       cpb_low=cpb-errb;
       %spline data
       fcpt=interp1(xct,cpt,xt,'spline');
       fcpt_high=interp1(xct,cpt_high,xt,'spline');
       fcpt_low=interp1(xct,cpt_low,xt,'spline');
       fcpb=interp1(xcb,cpb,xb,'linear');
       fcpb_high=interp1(xcb,cpb_high,xb,'linear');
       fcpb_low=interp1(xcb,cpb_low,xb,'linear');
       %calculate CL and error bars
       cl=s*(-trapz(fcpt)+trapz(fcpb));
       cl_high=s*(-trapz(fcpt_high)+trapz(fcpb_high));
```

```
    cl_low=s*(-trapz(fcpt_low)+trapz(fcpb_low));
    elh=cl_high-cl;
    ell=cl-cl_low;
    ecl=(elh+ell)/2;
    %drag coefficient calculations
    %create variables
    ycf=yc0([1:10,25:30]);
    ycr=yc0([11:17]);
    cpf=cp([1:10,25:30]);
    errf=eb([1:10,25:30]);
    cpf_high=cpf+errf;
    cpf_low=cpf-errf;
    cpr=cp([11:17]);
    errr=eb([11:17]);
    cpr_high=cpr-errr;
    cpr_low=cpr+errr;
    %spline data
    fcpf=interp1(ycf,cpf,yc,'spline');
    fcpf_high=interp1(ycf,cpf_high,yc,'spline');
    fcpf_low=interp1(ycf,cpf_low,yc,'spline');
    fcpr=interp1(ycr,cpr,yc,'spline');
    fcpr_high=interp1(ycr,cpr_high,yc,'spline');
    fcpr_low=interp1(ycr,cpr_low,yc,'spline');
    %calculated Cd and error bars
    cd=s*(trapz(cpf)-trapz(cpr));
    cd_high=s*(trapz(cpf_high)-trapz(cpr_high));
    cd_low=s*(trapz(cpf_low)-trapz(cpr_low));
    edh=cd_high-cd;
    edl=cd-cd_low;
    ecd=(edh+edl)/2;
    cldoutput=[te(i)',aoa(i)',cl',ecl',cd',ecd'];
elseif aoa(i)==-1
    %-1 degrees AoA
    xt=xcn1(2):s:xcn1(17);
    xb=xcn1(1):s:xcn1(18);
    yc=0.00274:s:0.09900;
    %lift coefficient calculations
    %create variables
    xct=xcn1([2:17]);
    xcb=xcn1([18:30,1]);
    cpt=cp([2:17]);
    errt=eb([2:17]);
    cpt_high=cpt-errt;
    cpt_low=cpt+errt;
    cpb=cp([18:30,1]);
    errb=eb([18:30,1]);
    cpb_high=cpb+errb;
    cpb_low=cpb-errb;
    %spline data
    fcpt=interp1(xct,cpt,xt,'linear');
    fcpt_high=interp1(xct,cpt_high,xt,'linear');
    fcpt_low=interp1(xct,cpt_low,xt,'linear');
    fcpb=interp1(xcb,cpb,xb,'linear');
    fcpb_high=interp1(xcb,cpb_high,xb,'linear');
    fcpb_low=interp1(xcb,cpb_low,xb,'linear');
    %calculate CL and error bars
    cl=s*(-trapz(fcpt)+trapz(fcpb));
    cl_high=s*(-trapz(fcpt_high)+trapz(fcpb_high));
    cl_low=s*(-trapz(fcpt_low)+trapz(fcpb_low));
    elh=cl_high-cl;
    ell=cl-cl_low;
```

```
    ecl=(elh+ell)/2;
    %drag coefficient calculations
    %create variables
    ycf=ycn1([1:10,27:30]);
    ycr=ycn1([11:26]);
    cpf=cp([1:10,27:30]);
    errf=eb([1:10,27:30]);
    cpf_high=cpf+errf;
    cpf_low=cpf-errf;
    cpr=cp([11:26]);
    errr=eb([11:26]);
    cpr_high=cpr-errr;
    cpr_low=cpr+errr;
    %spline data
    fcpf=interp1(ycf,cpf,yc,'spline');
    fcpf_high=interp1(ycf,cpf_high,yc,'spline');
    fcpf_low=interp1(ycf,cpf_low,yc,'spline');
    fcpr=interp1(ycr,cpr,yc,'spline');
    fcpr_high=interp1(ycr,cpr_high,yc,'spline');
    fcpr_low=interp1(ycr,cpr_low,yc,'spline');
    %calculated Cd and error bars
    cd=s*(trapz(cpf)-trapz(cpr));
    cd_high=s*(trapz(cpf_high)-trapz(cpr_high));
    cd_low=s*(trapz(cpf_low)-trapz(cpr_low));
    edh=cd_high-cd;
    edl=cd-cd_low;
    ecd=(edh+edl)/2;
    cldoutput=[te(i)',aoa(i)',cl',ecl',cd',ecd'];
else
    %+1 degrees AoA
    xt=xcp1(1):s:xcp1(17);
    xb=xcp1(30):s:xcp1(18);
    yc=-0.03490:s:0.06406;
    %lift coefficient calculations
    %create variables
    xct=xcp1([1:17]);
    xcb=xcp1([18:30]);
    cpt=cp([1:17]);
    errt=eb([1:17]);
    cpt_high=cpt-errt;
    cpt_low=cpt+errt;
    cpb=cp([18:30]);
    errb=eb([18:30]);
    cpb_high=cpb+errb;
    cpb_low=cpb-errb;
    %spline data
    fcpt=interp1(xct,cpt,xt,'linear');
    fcpt_high=interp1(xct,cpt_high,xt,'linear');
    fcpt_low=interp1(xct,cpt_low,xt,'linear');
    fcpb=interp1(xcb,cpb,xb,'linear');
    fcpb_high=interp1(xcb,cpb_high,xb,'linear');
    fcpb_low=interp1(xcb,cpb_low,xb,'linear');
    %calculate CL and error bars
    cl=s*(-trapz(fcpt)+trapz(fcpb));
    cl_high=s*(-trapz(fcpt_high)+trapz(fcpb_high));
    cl_low=s*(-trapz(fcpt_low)+trapz(fcpb_low));
    elh=cl_high-cl;
    ell=cl-cl_low;
    ecl=(elh+ell)/2;
    %drag coefficient calculations
    %create variables
```

```
      ycf=ycp1([1:9,18:30]);
      ycr=ycp1([10:17]);
      cpf=cp([1:9,18:30]);
      errf=eb([1:9,18:30]);
      cpf_high=cpf+errf;
      cpf_low=cpf-errf;
      cpr=cp([10:17]);
      errr=eb([10:17]);
      cpr_high=cpr-errr;
      cpr_low=cpr+errr;
      %spline data
      fcpf=interp1(ycf,cpf,yc,'spline');
      fcpf_high=interp1(ycf,cpf_high,yc,'spline');
      fcpf_low=interp1(ycf,cpf_low,yc,'spline');
      fcpr=interp1(ycr,cpr,yc,'spline');
      fcpr_high=interp1(ycr,cpr_high,yc,'spline');
      fcpr_low=interp1(ycr,cpr_low,yc,'spline');
      %calculated Cd and error bars
      cd=s*(trapz(cpf)-trapz(cpr));
      cd_high=s*(trapz(cpf_high)-trapz(cpr_high));
      cd_low=s*(trapz(cpf_low)-trapz(cpr_low));
      edh=cd_high-cd;
      edl=cd-cd_low;
      ecd=(edh+edl)/2;
      cldoutput=[te(i)',aoa(i)',cl',ecl',cd',ecd'];
   end

   if aoa(i)==0
      if te(i)==0
         cldout=[Re(i),cldoutput];
         fprintf(fid1,'%8i %i %i %6.5f %6.5f %6.5f %6.5f \r\n',cldout);
      else
         cldout=[Re(i),cldoutput];
         fprintf(fid2,'%8i %i %i %6.5f %6.5f %6.5f %6.5f \r\n',cldout);
      end
   elseif aoa(i)==-1
      cldout=[Re(i),cldoutput];
      fprintf(fid3,'%8i %i %i %6.5f %6.5f %6.5f %6.5f \r\n',cldout);
   else
      cldout=[Re(i),cldoutput];
      fprintf(fid4,'%8i %i %i %6.5f %6.5f %6.5f %6.5f \r\n',cldout);
   end

   %hold on
   %plot(xt,-fcpt,xb,-fcpb)

   %clear unused variables
   clear Rd cd_high cd_low cl_high cl_low cpb_high cpb_low cperr1 cperr2
cpf cpf_high
   clear cpf_low cpr cpr_high cpr_low cpstd1 cpstd2 cpt_high cpt_low edh
edl elh ell
   clear errb errf errr errt fcpb_high fcpb_low fcpf fcpf_high fcpf_low
fcpr
   clear fcpr_high fcpr_low fcpt_high fcpt_low he noflowi nstd1 nstd2
ntap ntd1 ntd2 nvalve
   clear offset1 offset2 std1 std2 tau td1 td2 valve ycf ycr
   clear fid cpdata m cldoutput cldout

   %NOTES:
   %Re,U,aoa,infile,infilei,noflow,nu,outfile,outfilei,rho,d1,hd- data
   %cp,cp1,cp2,eb,eb1,eb2,cl,ecl,cd,ecd- results
```

```
   %s,xc0,yc0,xcn1,ycn1,xcp1,ycp1,xc,yc,xct,xcb,cpt,cpb,fcpt,fcpb-
useful variable/data vectors

end %main for loop
fclose(fid1);
fclose(fid2);
fclose(fid3);
fclose(fid4);
fclose(fid5);
fclose(fid6);
```

Appendix G: Data Log File

This appendix contains a print out of the log file used to keep track of all data associated with each individual static pressure data file, such as flow speed, angle of attack, trailing edge configuration and water temperature. This log file was used by the Matlab computer code to aid in the data regression used to analyze the data presented in this document. The Matlab computer code can be found in appendix F.

Static Pressure Log

Chord 2.1195 Span Rate 1000

Run	File Name	Date	Time	U (m/s)	AoA	TE #	Transducer Info Range	#1 Err (psi)	#2 Err (psi))	Temp (°F)	Density	Viscosity	Re_c	Duration (s)	Samples	No Flow File Name			Ouput File Name 1	runid	Phase II end date run # string	Old file?	16-Mar Calibration
001	SP-15-28Feb.txt	28-Feb	1643	15.00	0	0	F	0.054113	0.050000	79.7	996.80	8.7213E-07	3.6697E+07	9	900	SP-0-none.txt	1500	0	SP001_001500.plt	001-TE0-AOA0-U15	001	1	1
002	SP-9-28Feb.txt	28-Feb	1741	9.00	0	0	F	0.054113	0.050000	79.7	996.80	8.7213E-07	2.2018E+07	9	900	SP-0-none.txt	900	0	SP002_00900.plt	002-TE0-AOA0-U9	002	1	1
003	SP-12-02Mar.txt	2-Mar	1254	12.00	0	0	F	0.054113	0.050000	82.6	996.32	8.4132E-07	3.0432E+07	9	900	SP-0-02Mar-1.txt	1200	0	SP003_001200.plt	003-TE0-AOA0-U12	003	1	1
004	SP-6-02Mar.txt	2-Mar	1347	6.00	0	0	F	0.054113	0.050000	82.6	996.32	8.4132E-07	1.5216E+07	9	900	SP-0-02Mar-1.txt	600	0	SP004_00600.plt	004-TE0-AOA0-U6	004	1	1
005	SP-18.3-02Mar.txt	2-Mar	1726	18.30	0	0	F	0.054113	0.050000	86.1	995.61	8.0308E-07	4.8619E+07	9	900	SP-0-02Mar-1.txt	1830	0	SP005_001830.plt	005-TE0-AOA0-U18.3	005	1	1
006	SP-3n1-09Mar-1.txt	9-Mar	938	3.00	-1	0	F	0.054113	0.050000	92.1	994.55	7.4905E-07	8.5452E+06	9	900	SP-0n1-09Mar-1.txt	300	n1	SP006_0n1300.plt	006-TE0-AOAn1-U3	006	1	1
007	SP-3n1-09Mar-2.txt	9-Mar	1040	3.00	-1	0	F	0.054113	0.050000	92.0	994.55	7.4905E-07	8.5452E+06	9	900	SP-0n1-09Mar-1.txt	300	n1	SP007_0n1300.plt	007-TE0-AOAn1-U3	007	1	1
008	SP-3n1-09Mar-4.txt	9-Mar	1339	3.00	-1	0	F	0.054113	0.050000	91.6	994.73	7.5695E-07	8.4560E+06	9	900	SP-0n1-09Mar-2.txt	300	n1	SP008_0n1300.plt	008-TE0-AOAn1-U3	008	1	1
009	SP-18.3n1-09Mar-1.txt	9-Mar	1459	18.30	-1	0	F	0.054113	0.050000	92.9	994.55	7.4905E-07	5.2126E+07	9	900	SP-0n1-09Mar-2.txt	1830	n1	SP009_0n11830.plt	009-TE0-AOAn1-U18.3	009	1	1
010	SP-18.3n1-09Mar-2.txt	9-Mar	1532	18.30	-1	0	F	0.054113	0.050000	93.9	994.38	7.4116E-07	5.2681E+07	9	900	SP-0n1-09Mar-2.txt	1830	n1	SP010_0n11830.plt	010-TE0-AOAn1-U18.3	010	1	1
011	SP-18.3n1-09Mar-3.txt	9-Mar	1604	18.30	-1	0	F	0.054113	0.050000	95.0	994.03	7.2536E-07	5.3828E+07	9	900	SP-0n1-09Mar-2.txt	1830	n1	SP011_0n11830.plt	011-TE0-AOAn1-U18.3	011	1	1
012	SP-12n1-09Mar.txt	9-Mar	1745	12.00	-1	0	F	0.054113	0.050000	97.4	993.67	7.0957E-07	3.6083E+07	9	900	SP-0n1-09Mar-1.txt	1200	n1	SP012_0n11200.plt	012-TE0-AOAn1-U12	012	1	1
013	SP-6n1-09Mar.txt	9-Mar	1824	6.00	-1	0	F	0.054113	0.050000	97.3	993.67	7.0957E-07	1.8041E+07	9	900	SP-0n1-09Mar-1.txt	600	n1	SP013_0n1600.plt	013-TE0-AOAn1-U6	013	1	1
014	SP-18.3p1-14Mar.txt	14-Mar	1733	18.30	1	0	F	0.054113	0.050000	100.9	993.14	6.8588E-07	5.6927E+07	9	900	SP-0p1-14Mar.txt	1830	p1	SP014_0p11830.plt	014-TE0-AOAp1-U18.3	014	1	1
015	SP-3p1-15Mar-1.txt	15-Mar	833	3.00	1	0	F	0.054113	0.050000	100.1	993.14	6.8588E-07	9.3322E+06	9	900	SP-0p1-15Mar.txt	300	p1	SP015_0p1300.plt	015-TE0-AOAp1-U3	015	1	1
016	SP-3p1-15Mar-2.txt	15-Mar	905	3.00	1	0	F	0.054113	0.050000	100.0	993.14	6.8588E-07	9.3322E+06	9	900	SP-0p1-15Mar.txt	300	p1	SP016_0p1300.plt	016-TE0-AOAp1-U3	016	1	1
017	SP-6p1-15Mar-1.txt	15-Mar	1030	6.00	1	0	F	0.054113	0.050000	99.8	993.32	6.9378E-07	1.8452E+07	9	900	SP-0p1-15Mar.txt	600	p1	SP017_0p1600.plt	017-TE0-AOAp1-U6	017	1	1
018	SP-6p1-15Mar-2.txt	15-Mar	1102	6.00	1	0	F	0.054113	0.050000	99.7	993.32	6.9378E-07	1.8452E+07	9	900	SP-0p1-15Mar.txt	600	p1	SP018_0p1600.plt	018-TE0-AOAp1-U6	018	1	1
019	SP-12p1-15Mar.txt	15-Mar	1342	12.00	1	0	F	0.054113	0.050000	102.2	992.68	6.7366E-07	3.8006E+07	9	900	SP-0p1-15Mar.txt	1200	p1	SP019_0p11200.plt	019-TE0-AOAp1-U12	019	1	1
020	SP-6-16Mar.txt	16-Mar	1100	6.00	0	0	F	0.054113	0.050000	98.7	993.50	7.0167E-07	1.8244E+07	9	900	SP-0-16Mar.txt	600	0	SP020_00600.plt	020-TE0-AOA0-U6	020	1	1
021	SP-12-16Mar.txt	16-Mar	1208	12.00	0	0	F	0.054113	0.050000	98.7	993.50	7.0167E-07	3.6489E+07	9	900	SP-0-16Mar.txt	1200	0	SP021_001200.plt	021-TE0-AOA0-U12	021	1	1
022	SP-3m2-17Aug-1.txt	17-Aug	1445	3.00	0	2	C	0.005415	0.001810	83.2	996.14	8.3176E-07	7.6955E+06	10	10000	SP-0m2-17Aug.txt	300	0	SP022_20300.plt	022-TE2-AOA0-U3	022	0	2
023	SP-12m2-20Aug-1.txt	20-Aug	856	12.00	0	2	E	0.037883	0.001810	83.1	996.14	8.3176E-07	3.0782E+07	15	15000	SP-0m2-20Aug.txt	1200	0	SP023_201200.plt	023-TE2-AOA0-U12	023	0	3
024	SP-12m2-20Aug-2.txt	20-Aug	900	12.00	0	2	E	0.037883	0.001810	83.4	996.14	8.3176E-07	3.0782E+07	15	15000	SP-0m2-20Aug.txt	1200	0	SP024_201200.plt	024-TE2-AOA0-U12	024	0	3
025	SP-12m2-20Aug-3.txt	20-Aug	954	12.00	0	2	E	0.037883	0.001810	83.9	996.14	8.3176E-07	3.0782E+07	15	15000	SP-0m2-20Aug.txt	1200	0	SP025_201200.plt	025-TE2-AOA0-U12	025	0	3
026	SP-18.3m2-20Aug-1.txt	20-Aug	1029	18.30	0	2	E	0.037883	0.001810	85.0	995.79	8.1264E-07	4.8047E+07	15	15000	SP-0m2-20Aug.txt	1830	0	SP026_201830.plt	026-TE2-AOA0-U18.3	026	0	3
027	SP-18.3m2-20Aug-2.txt	20-Aug	1051	18.30	0	2	E	0.037883	0.001810	85.7	995.79	8.1264E-07	4.8047E+07	15	15000	SP-0m2-20Aug.txt	1830	0	SP027_201830.plt	027-TE2-AOA0-U18.3	027	0	3
028	SP-18.3m2-20Aug-3.txt	20-Aug	1121	18.30	0	2	E	0.037883	0.001810	86.9	995.61	8.0308E-07	4.8619E+07	15	15000	SP-0m2-20Aug.txt	1830	0	SP028_201830.plt	028-TE2-AOA0-U18.3	028	0	3
029	SP-6m2-20Aug-1.txt	20-Aug	1222	6.00	0	2	C	0.005415	0.001810	87.0	995.44	7.9352E-07	1.6133E+07	15	15000	SP-0m2-20Aug.txt	600	0	SP029_20600.plt	029-TE2-AOA0-U6	029	0	4
030	SP-6m2-20Aug-2.txt	20-Aug	1245	6.00	0	2	C	0.005415	0.001810	87.0	995.44	7.9352E-07	1.6133E+07	15	15000	SP-0m2-20Aug.txt	600	0	SP030_20600.plt	030-TE2-AOA0-U6	030	0	4
031	SP-6m2-20Aug-3.txt	20-Aug	1307	6.00	0	2	C	0.005415	0.001810	87.0	995.44	7.9352E-07	1.6133E+07	15	15000	SP-0m2-20Aug.txt	600	0	SP031_20600.plt	031-TE2-AOA0-U6	031	0	4
032	SP-3m2-20Aug-1.txt	20-Aug	1440	3.00	0	2	C	0.005415	0.001810	86.9	995.61	8.0308E-07	7.9703E+06	15	15000	SP-0m2-20Aug.txt	300	0	SP032_20300.plt	032-TE2-AOA0-U3	032	0	5
033	SP-3m2-20Aug-2.txt	20-Aug	1508	3.00	0	2	C	0.005415	0.001810	86.9	995.61	8.0308E-07	7.9703E+06	15	15000	SP-0m2-20Aug.txt	300	0	SP033_20300.plt	033-TE2-AOA0-U3	033	0	5
034	SP-2.25m2-21Aug-2.txt	21-Aug	1344	2.25	0	2	B	0.005415	0.000722	85.5	995.79	8.1264E-07	5.9074E+06	15	15000	SP-0-none.txt	225	0	SP034_20225.plt	034-TE2-AOA0-U2.25	034	0	6
035	SP-1.5m2-21Aug-2.txt	21-Aug	1904	1.50	0	2	B	0.005415	0.000722	85.3	995.79	8.1264E-07	3.9383E+06	15	15000	SP-0-none.txt	150	0	SP035_20150.plt	035-TE2-AOA0-U1.5	035	0	6
036	SP-6m2-23Aug-1.txt	23-Aug	1300	6.00	0	2	C	0.005415	0.001810	89.7	995.08	7.7441E-07	1.6531E+07	15	15000	SP-0-none.txt	600	0	SP036_20600.plt	036-TE2-AOA0-U6	036	0	7
037	SP-12m2-23Aug-1.txt	23-Aug	1429	12.00	0	2	E	0.037883	0.001810	90.0	994.91	7.6485E-07	3.3475E+07	15	15000	SP-0-none.txt	1200	0	SP037_201200.plt	037-TE2-AOA0-U12	037	0	8
038	SP-12m2-23Aug-2.txt	23-Aug	1450	12.00	0	2	E	0.037883	0.001810	90.0	994.91	7.6485E-07	3.3475E+07	15	15000	SP-0-none.txt	1200	0	SP038_201200.plt	038-TE2-AOA0-U12	038	0	8
039	SP-18.3-27Aug-1.txt	27-Aug	1026	18.30	0	0	E	0.037883	0.001810	88.0	995.26	7.8396E-07	4.9804E+07	15	15000	SP-0-27Aug.txt	1830	0	SP039_001830.plt	039-TE0-AOA0-U18.3	039	0	9
040	SP-18.3-27Aug-2.txt	27-Aug	1045	18.30	0	0	E	0.037883	0.001810	88.7	995.26	7.8396E-07	4.9804E+07	15	15000	SP-0-27Aug.txt	1830	0	SP040_001830.plt	040-TE0-AOA0-U18.3	040	0	9
041	SP-12-27Aug-1.txt	27-Aug	1240	12.00	0	0	E	0.037883	0.001810	91.7	994.73	7.5695E-07	3.3824E+07	15	15000	SP-0-27Aug.txt	1200	0	SP041_001200.plt	041-TE0-AOA0-U12	041	0	9
042	SP-12-27Aug-2.txt	27-Aug	1315	12.00	0	0	E	0.037883	0.001810	92.0	994.55	7.4905E-07	3.4181E+07	15	15000	SP-0-27Aug.txt	1200	0	SP042_001200.plt	042-TE0-AOA0-U12	042	0	9
043	SP-6-27Aug-1.txt	27-Aug	1413	6.00	0	0	C	0.005415	0.001810	92.1	994.55	7.4905E-07	1.7090E+07	15	15000	SP-0-27Aug.txt	600	0	SP043_00600.plt	043-TE0-AOA0-U6	043	0	10
044	SP-6-27Aug-2.txt	27-Aug	1432	6.00	0	0	C	0.005415	0.001810	92.1	994.55	7.4905E-07	1.7090E+07	15	15000	SP-0-27Aug.txt	600	0	SP044_00600.plt	044-TE0-AOA0-U6	044	0	10
045	SP-6-27Aug-3.txt	27-Aug	1500	6.00	0	0	C	0.005415	0.001810	92.1	994.55	7.4905E-07	1.7090E+07	15	15000	SP-0-27Aug.txt	600	0	SP045_00600.plt	045-TE0-AOA0-U6	045	0	10
046	SP-3-27Aug-1.txt	27-Aug	1614	3.00	0	0	C	0.005415	0.001810	92.0	994.55	7.4905E-07	8.5452E+06	15	15000	SP-0-27Aug.txt	300	0	SP046_00300.plt	046-TE0-AOA0-U3	046	0	11
047	SP-3-27Aug-2.txt	27-Aug	1634	3.00	0	0	C	0.005415	0.001810	92.0	994.55	7.4905E-07	8.5452E+06	15	15000	SP-0-27Aug.txt	300	0	SP047_00300.plt	047-TE0-AOA0-U3	047	0	11
048	SP-3-27Aug-3.txt	27-Aug	1655	3.00	0	0	C	0.005415	0.001810	92.0	994.55	7.4905E-07	8.5452E+06	15	15000	SP-0-27Aug.txt	300	0	SP048_00300.plt	048-TE0-AOA0-U3	048	0	11
049	SP-3-27Aug-4.txt	27-Aug	1715	3.00	0	0	C	0.005415	0.001810	92.0	994.55	7.4905E-07	8.5452E+06	15	15000	SP-0-27Aug.txt	300	0	SP049_00300.plt	049-TE0-AOA0-U3	049	0	11
050	SP-1.5-27Aug-1.txt	27-Aug	1830	1.50	0	0	B	0.005415	0.000722	92.0	994.55	7.4905E-07	4.2726E+06	15	15000	SP-0-27Aug.txt	150	0	SP050_00150.plt	050-TE0-AOA0-U1.5	050	0	12
051	SP-1.5-27Aug-2.txt	27-Aug	1856	1.50	0	0	B	0.005415	0.000722	92.0	994.55	7.4905E-07	4.2726E+06	15	15000	SP-0-27Aug.txt	150	0	SP051_00150.plt	051-TE0-AOA0-U1.5	051	0	12
052	SP-1.5-27Aug-3.txt	27-Aug	1917	1.50	0	0	B	0.005415	0.000722	92.0	994.55	7.4905E-07	4.2726E+06	15	15000	SP-0-27Aug.txt	150	0	SP052_00150.plt	052-TE0-AOA0-U1.5	052	0	12